U.PORTO
FEUP FACULDADE DE ENGENHARIA
UNIVERSIDADE DO PORTO

ANALYSIS AND DESIGN OF CONCRETE CULVERTS – COMPARISON BETWEEN SHELL AND FRAME MODELS

NUNO JOSÉ CORREIA DE MAGALHÃES DE OLIVEIRA OSÓRIO

Thesis submited for the partial fulfillment of the requirements for the degree of

MASTER IN CIVIL ENGINEERING — SPECIALIZATION IN STRUCTURES

Supervisor: Professor Doctor José Miguel de Freitas Castro

Co-supervisor: Engineer Miran Cemalovic

MARCH 2023

MESTRADO INTEGRADO EM ENGENHARIA CIVIL 2022/2023

DEPARTAMENTO DE ENGENHARIA CIVIL

Tel. +351-22-508 1901

Fax +351-22-508 1446

✉ miec@fe.up.pt

Editado por

FACULDADE DE ENGENHARIA DA UNIVERSIDADE DO PORTO

Rua Dr. Roberto Frias

4200-465 PORTO

Portugal

Tel. +351-22-508 1400

Fax +351-22-508 1440

✉ feup@fe.up.pt

http://www.fe.up.pt

To my loved ones

"No such thing as a life that's better than yours (love yourz)"

Jermaine Lamarr Cole

Acknowledgements

To my supervisor at FEUP, Professor Miguel Castro, for his efforts in making this internship, and overall experience, possible, and for the help provided throughout this work;

To my tutor at *Sweco*, Engineer Miran Cemalovic, for all the help, guidance, shared knowledge and patience;

From here, I will carry the acknowledgements in Portuguese:

À minha Mãe e ao meu Pai. Sem eles nada disto seria possivel. Obrigado pela vida, pelo carinho, pela educação, pelo esforço diário, por fazerem de mim a pessoa que eu sou;

Ao meu irmão e à minha irmã, João e Beatriz, por toda a amizade e camaradagem, por me fazerem crescer e por crescerem comigo;

À Leonor, por todo o apoio, motivação e amizade, desde o primeiro dia;

A todos os meus amigos que me acompanharam neste percurso;

Por fim, uma palavra extra de agradecimento à Leonor e à Beatriz pela ajuda crucial na realização deste trabalho.

Abstract

The use of software as a tool for analysis in the field of Civil Engineering is a growing practice. Some of the most commonly used softwares involve the finite element method, since it is an accurate approach in the analysis and design of structures. This method involves discretizing the structure into smaller elements, enabling calculation of the structural response to external loads. However, the choice of element type and structural system can significantly impact the analysis.

In this work, a comparison of two Concrete Box Culvert designs is performed using SOFISTIK, a finite element software. The software offers different element types, each with its own modelling. To better understand the performance of these elements, we compare two structures: one modeled as a Frame using one-dimensional beam elements and the other modeled as a Shell using two-dimensional shell elements.

The comparison is conducted through evaluating different results provided by SOFISTIK, such as displacement, stresses, and reinforcement. The aim of this study is to provide insights into the behaviour of different element types and to aid in the selection of the most appropriate structure for a given situation. Ultimately, this investigation is conducted with the purpose of contributing to the development of more accurate and efficient structural designs, leading to safer and more sustainable construction practices.

KEY WORDS: Finite element, *Sofistik*, Frame structure, Shell structure

Resumo

A utilização de *software* como ferramenta de análise no campo da Engenharia Civil é uma prática cada vez mais recorrente. Alguns dos *softwares* mais frequentemente utilizados envolvem o método dos elementos finitos, dado que se trata de uma abordagem precisa na análise e conceção de estruturas. Este método envolve a discretização da estrutura em elementos mais pequenos, permitindo o cálculo da resposta estrutural a cargas externas. No entanto, a escolha do tipo de elemento e do sistema estrutural a utilizar pode ter um impacto significativo na análise.

Na presente dissertação, é realizada uma comparação entre dois projetos de *culverts* em caixa de betão através do SOFISTIK, um *software* de elementos finitos. Este *software* dispõe de diferentes tipos de elementos, cada um com a sua própria modelação. Para melhor compreender o desempenho destes elementos, são comparadas duas estruturas: uma modelada como um Portico, usando elementos de viga unidimensional e a outra modelada como Casca, usando elementos bidimensionais.

A comparação é realizada através da avaliação de diferentes resultados obtidos pelo SOFISTIK, tais como deslocamentos, tensões, e armaduras. O objetivo deste estudo é fornecer uma visão do comportamento de diferentes tipos de elementos e ajudar na seleção da estrutura mais apropriada para uma dada situação. Por fim, esta investigação é conduzida com o propósito de contribuir para o desenvolvimento de conceções estruturais mais precisas e eficientes, levando a práticas de construção mais seguras e sustentáveis.

PALAVRAS CHAVE: Elementos finitos, *Sofistik*, Estrutura tipo Pórtico, Estrutura tipo Cascas.

Contents

Acronyms, Abbreviations and Symbols

ACRONYMS

ACI	American Concrete Institute
AISC	American Institution of Steel Construction
ASE	Advanced Solution Engine
CDB	Central Data Base
EB	Euler-Bernoulli Beam Theory
EC	Eurocode
EN	European Norm
EQU FEA	Finite Element Analysis
FEM	Finite Element Method
IBC	International Building Code
KT	Kirchhof Theory
LC	Load Case
LM	Load Model
LRFD	Load and Resistance Factor Design
LSD	Limite State Design
MT	Mindlin Theory
SSD	Sofistik Structural Desktop
STR TB	Timoshenki Beam Theory
USL	Ultimate Limit State

ABBREVIATIONS

d.o.f	Degrees of Freedom

SYMBOLS

Latin Alphabet

A	Area
A_s, a_s	Cross-section area of reinforcement
a_{cc}	Coefficient that accounts for the long term effects in the compression resistance of Concrete
b	Overall width of a cross-section
D_C	Compression force in the concrete
d	displacement; / Effective depth of a cross-section
E	Elastic Modulus
F	Force
f_{bd}	Design bond strength of concrete
f_c	Compressive strength of concrete
f_{cd}	Design value of concrete compressive strength
$f_{cd,fat}$	Design value of concrete fatigue compressive strength
f_{ck}	Characteristic compressive cylinder strength of concrete at 28 days
f_{cm}	Mean compressive cylinder strength of concrete at 28 days
$f_{ctk,0.5}$	Lower fractile value of tensile strength of concrete
f_{ctm}	Mean tensile strength of concrete
f_t	Tensile strength of reinforcement
f_{tc}	Compressive strength of reinforcement
f_{td}	Design tensile strength of reinforcement
f_y	Yield strength of reinforcement
f_{yc}	Compressive yield strength of reinforcement
f_{yd}	Design strength of reinforcement
f_{yk}	Characteristic yield strength of reinforcement
G	Shear modulus
h	Overall depth of a cross-section
I	Inertia
K	Compression Modulus
k	Curvature
L	Length
M	Bending moment
m_{xx}, m_{yy}, m_{xy}	Moments
m_I, m_{II}	Principal bending moments
N_{xx}, N_{yy}, N_{xy}	Virtual panel forces
N_I, N_{II}	Principal panel forces
n_{xx}, n_{yy}, n_{xy}	Stresses
n_I, n_{II}	Principal normal forces
Q_ik	Characteristic value of a single axle load
u_i	Axial displacement at node i
V	Axial Force
Z_I	Tension force in the principal reinforcement direction
Z_{II}	Tension force in the cross reinforcement direction

Greek Alphabet

α	Slope / Angle of the main reinforcement.
β_Q	Adjustment factor of Load Model 2
γ	Self weight
γ_c	Partial factor for the ultimate limit state of concrete
γ_s	Partial factor for the ultimate limit state of steel
Θ	Independent variable
θ	angle
ε	Strain
μ	Poisson ratio
ρ	Density
ρ	Radius
σ	Internal axial stress
v_1	Vertical translation
ϕ	Rotation
ϕ_m	Angle between Principal bending moments
ϕ_N	Angle between Principal panel forces
ϕ_n	Angle between Principal normal forces

List of Figures

List of Tables

1

Introduction

The present dissertation is the result of the work conducted in a professional environment workspace, which aims to investigate the application of FEM to analyse a culvert structure. This study involves the design and analysis of the culvert structure using the software *SOFISTIK*.

The present work was carried out at *Sweco*, an engineering consultancy company located in Bergen, Norway. The primary objective of this project is to gain an understanding of the suitability of the culvert structure in diverse contexts, thereby facilitating the decision-making process regarding the selection of the appropriate type of structure - between frame or shell - for each specific situation.

The present chapter provides a brief contextualisation of the project, accompanied by a description of the company and sector, the defined objectives and the adopted methodology.

1.1 Context and objectives of the project

Over the last few decades, the construction industry has undergone a rapid evolution driven by increasing demand for complex and sustainable infrastructure.

This industry faces a variety of challenges, such as increasing demand for infrastructure and buildings to support a growing population and urbanization. This demand puts pressure on construction companies to complete projects quickly and efficiently, while also maintaining high-quality standards. The other main challenge for this industry is related to environmental concerns. Increasingly strict regulations on emissions, waste disposal, and sustainable building practices require companies to adopt new technologies and practices to minimize their environmental impact. For this purpose, nowadays, engineers prioritize the design and analysis of structures through software tools, in order to ensure that all the necessary requirements are met before proceeding to the construction phase. As such, designing and constructing civil engineering structures has become a high-stakes and challenging task.

Culverts are one of the most common structures in transportation infrastructure, widely used to facilitate the safe and efficient flow of water, vehicles, and pedestrians. They provide a cost-effective solution for passage under elements such as highways, railways, and even natural barriers like mountains.

One of the main challenges faced by engineers in the design of culverts is the selection of the appropriate structural model. In recent years, frame and shell models have emerged as the two most popular and reliable types of models for culvert analysis and design. Despite their wide use, there is still much debate and uncertainty around the best approach to take when designing culverts, and which model is the most effective and efficient for a given set of circumstances.

The objective of this project is to analyse and compare the performance of frame and shell models for the design of concrete culverts, with the aim of contributing to a better understanding of the applicability and suitability of each model for different construction scenarios. Through a comprehensive review of the literature, empirical analyses, and practical experiments, the intention is to explore the benefits and limitations of each model and provide insights into the factors that engineers should consider when selecting a suitable structural model for a particular culvert design project.

1.2 COMPANY BACKGROUND AND MOTIVATION

Sweco is an architecture and engineering consultancy, specialising in planning and designing buildings and community infrastructures. It is one of the largest consultancies in Europe, with a workforce of over 20,000 employees established in 14 countries, carrying out projects in 70 countries around the world. The company provides services to various sectors, including transportation, energy, and water, and has a strong reputation for delivering innovative and sustainable solutions.

Sweco's operations in Norway are particularly noteworthy, with a long history of delivering complex infrastructure projects in the challenging Norwegian landscape, characterized by its mountainous terrain. The company has been involved in the design and construction of several significant infrastructure projects in this country, such as tunnels, bridges, roads and culverts. Culverts are essential components of many infrastructure projects, and their design plays a crucial role in ensuring the long-term viability of these projects.

The frame and shell models for culvert design each have their advantages and limitations, which led *Sweco* to engage in a project that would support the decision-making process regarding the selection of the appropriate model to employ in specific scenarios.

By comparing the results of the application of the two models, *Sweco* aimed to identify the strengths and weaknesses of each approach and develop a reference for future culvert design projects. This reference would help *Sweco* engineers and designers make more informed decisions about which model to use in different conditions, ensuring that the most suitable and efficient design is selected for each project.

1.3 STRUCTURE OF THE DISSERTATION

This dissertation is divided into 5 chapters that provide a detailed description of the project's framework and methodology.

Chapter 1 contextualizes the project and the environment in which it was developed, lays out the work objectives and outlines the methodology and structure considered.

In Chapter 2 a literature review is presented, that covers the theoretical foundations of the research. Here is defined what is a culvert structure and why it is so commonly used. A short overview of what is Finite Element Analysis and the theories behind it. And finally the design process of Frame and Shell models

Chapter 3 details the application of the introduced methodology to the software *SOFISTIK*. A brief description of how to interact with the software is exposed as the difficulties encountered with handling the Finite Element modelling. It is also detailed the conditions and considerations taken in each model analysed regarding the software.

In Chapter 4 is where the parametric study is described, with the specific modelling considerations listed and the assumptions presented for each case. Also, the results obtained are analysed and discussed in this chapter.

Lastly, in Chapter 5 the conclusions are summarised, along with recommendations for analysis and proposals for future improvements.

2

Theoretical background

The presented chapter's purpose is to provid context and theoretical background for the subjects covered by this work of investigation. This study aims to analyse the behaviour of a concrete box culvert when designed as a Frame and as a Shell, with a Finite Element Analysis software. Therefore, an introduction to the Culvert structure is provided initially. The analysis is performed to compare two distinct finite elements provided by the software. Hence, a description of the theory of the Finite Element Analysis is presented. This method resorts to small, individual elements to represent the *Finite Element Structure*. There are various different types of elements that can be used, with each element modelling in different manners. Therefore, it is important to distinguish the different possible scenarios and understand the process behind the analysis of these elements. Finally, the Frame and Shell models are described, along with a description of their structural systems and methods of design. In this section, the formulation for designing both models is also included.

2.1 What is a Culvert

As the present thesis focuses on box culverts, it is imperative to provide a comprehensive definition of this structure and examine its features, benefits, and drawbacks. Therefore, the following section is dedicated to this discussion.

2.1.1 Introduction to Culverts

A culvert is an underground structure that is specifically designed to enable the passage over or through it. It may be placed under highways or railways to facilitate the smooth flow of traffic, or it can be utilized to allow the passage of animals or watercourses. Additionally, culverts can function as tunnels, providing a means of passage through natural elements such as mountains.

Regarding its geometry, the size of this structure can range from small box culverts to large arch culverts. They can also vary in their design, by having a simple or multi-span construction. In other words, a culvert with a single span or opening may be constructed to support solely its own weight and additional loads that it can be subjected to, such as the weight of the soil above it. Conversely, a multi-span culvert has more than one opening and is designed to withstand the additional stresses and loads that result from having multiple spans (Patel et al., 2019).

This structure is primary designed to allow passage, serving either as an hydraulic conduit to convey water from one side of a road to the other or as a traffic load bearing structure for permanent or temporary periods, such as during road construction (Balkham et al., 2010). They can be employed on a variety of settings, including residential areas, commercial areas, and rural areas. They are particularly beneficial in regions with steep terrain or prone to flooding, where they can help manage water flow and prevent damage to roads and infrastructure.

Overall, culverts are an essential component of modern infrastructure, helping to manage water flow and facilitate safe and efficient transportation. As such, they are a key consideration in civil engineering projects and must be carefully designed and constructed to ensure their long-term effectiveness and safety.

2.1.2 Types of Culverts

The design of this structure can vary depending on its intended purpose and the environment in which they will be installed. The three main types of culverts are pipe, arch and box culverts.

Firstly, pipe culverts are the most common type of culvert and are suitable for small to medium-sized drainage applications. They have a circular or semi-circular shape and can be constructed using materials such as concrete, steel, or plastic (Moore, 2001). Arch culverts, on the other hand, have a semi-circular shape and are capable of spanning larger distances than pipe culverts. They are frequently used to convey water under highways and railroads (Sezen et al., 2008).

Finally, box culverts have a rectangular shape and are typically composed of reinforced concrete. They can handle heavy loads and are suitable for larger drainage applications. They are often employed for animal crossings beneath highways or other large infrastructure projects (Patel, Jamle, 2019).

Other types of culverts include bridge culverts, which function as both a bridge and a culvert, and conveyor culverts, which are used to convey materials such as coal and other ores.

In summary, the type of culvert used is determined by the specific project requirements and the environment context in which it will be installed.

2.1.3 Advantages and Disadvantages

Culverts can be constructed from various materials, including high-density polyethylene (HPDE), steel, aluminum and concrete, with the latter being the most commonly used one. Concrete culverts are a popular choice due to their durability, longevity, and resistance to corrosion and erosion

(Awwad et al., 2000). They are able to withstand the effects of harsh environmental conditions and can last for many years with minimal maintenance.

When the span and width are short, culverts are often preferred options compared to bridges, mainly due to their cost-effectiveness. One of the main benefits of culvert and frame bridges is that there are no mechanical parts such as bearings and expansion joints, which may be very costly to maintain over time. Also, they require less engineering and materials than bridges, which makes them easier and less expensive to construct. Concrete culverts have the added advantage of being able to be built in areas where space is limited, which allows for greater flexibility in design and placement (Balkham et al., 2010).

The use of culverts can be specially beneficial when they are constructed with concrete. This material is characterized by its durability and strength. It is well-suited to handle the demands of heavy loads and frequent use, making it a reliable and long-lasting solution for transportation and utility infrastructure. Additionally, concrete is particularly resistant to corrosion and erosion, reducing the need for maintenance over time, which makes it an ideal material for infrastructure projects where long-term functionality is crucial. Furthermore, depending on the specific project requirements, precast concrete components can be used to expedite the installation process and reduce costs, making concrete culverts a preferred solution for cases when the time for the completion of the project is short (Kattimani, Shreedhar, 2013).

On the other hand, one of the main drawbacks of using concrete culverts instead of bridges is their limited capacity for vehicular and pedestrian traffic. Since they are typically designed for water flow, their ability to handle heavier trucks and trailers is more shortened.

Moreover, culverts are not always environmentally friendly, as they can disrupt or block the natural flow of water, potentially harming fish and other aquatic life. In addition, during large floods, concrete culverts can be easily damaged or over topped, leading to significant damage to the surrounding area. Furthermore, culverts are typically less visually appealing than bridges and may not offer the same aesthetic value to the area.

To conclude, concrete culverts are an important component of transportation and utility infrastructure, providing a clear path for vehicles, pedestrians, and other users to cross over or through streams, rivers, and other bodies of water. Despite the drawbacks associated with their application, the durability, strength, and resistance to corrosion compensate for these limitations and make them a valuable asset.

2.2 Finite Element Analysis

Finite element analysis (FEA), also known as Finite Element Method (FEM) is a numerical technique that obtains approximated solutions based on provided data, such as varying shapes or applied loads. Due to its versatility, it has gained a lot of popularity among users of various fields, such as Engineering and Science (Roylance, 2001). One of the main benefits of this method is that it provides a quick and reliable tool to mathematically model and numerically solve extremely complicated problems, both static and dynamic, using only a computer. When using the finite element method, a large number of complex systems of algebraic equations need to be assembled and solved. The computer provides the necessary resources to accomplish this task through general-purpose FEA programs. Regarding the field of Civil Engineering, FEM is broadly applied in the analysis of structural elements such as beams, frames, plates, shells, foundations and others (Cook et al., 2001). The ability to predict the performance of a design is particularly valuable, since it allows for safer and more cost-efficient designs. Thus, the use of the finite element method contributes considerably to the efficiency and accuracy of the daily work of a Civil Engineer.

The main objective of FEM is to numerically solve problems of field variables, which are physical quantities that posses a value for each point in space and time. To achieve this goal, it is necessary to first determine the field distribution of one or more variables, for example, the distribution of stresses in a paving slab. This distribution might be described by differential or integral equations, which must be previously defined in order to formulate the finite element problem (Szabó, Babuska, 2021).

The process of discretization is a fundamental concept in FEA, as complex systems often have an infinite number of unknowns, making analysis impractical. The finite element procedure is used to reduce the unknowns to a finite number by dividing the region into subsystems, or elements, each of which can be analysed independently. Within each element, the unknown field variables are expressed in terms of assumed approximating functions, such as interpolation functions or shape functions. This process is called discretization, and it allows the continuous model in the analysis to be approximated using information at a finite number of discrete locations (Segerlind, 1984). In other words, the finite element procedure involves dividing the structure into small, manageable elements, and then approximating the behaviour of each element using a simplified model that considers a finite number of variables. By doing so, it becomes possible to analyse the structure more efficiently and accurately, while still accounting for the complex behaviour of the system as a whole (Roylance, 2001).

In the domain of structural analysis, the discretization process involves dividing the structure into individual finite elements connected between each other by nodes. These elements may be visualized as small pieces of the structure and may assume various forms, ranging from one-dimensional to three-dimensional. Examples of such elements include one-dimensional beam elements or two-dimensional plate elements (Cook et al., 2001). Different elements produce different outcomes and, therefore, it is essential to consider the behaviour of each different finite element, as well as the specific problem being analysed, such as the geometry, boundary conditions and loading conditions. For instance, a one-dimensional element may be sufficient to model a slender beam, whereas a two-dimensional element may be required to model a thin plate subjected to bending. Conversely, a complex structure like a bridge may need a three-dimensional element to model its behavior accurately.

The process of assembling all finite elements into a structure, such as a body or region, is known as a finite element structure. This structure closely resembles the actual body being analysed. The elements are arranged in a specific order to create a mesh, which will be represented by a system of algebraic equations to be solved for unknowns at the nodes. The mesh is designed to fill the entire volume of the solid structure while ensuring that there is no geometrical overlap between the elements. The reason behind this rule is to avoid redundancy in the analysis. If two finite elements overlap, they will represent the same portion of the structure, and the program will analyse it twice, leading to unnecessary calculations and potentially causing errors. Also, filling the entire volume of the solid ensures that no part of it is left without analysis (Segerlind, 1984).

The system of algebraic equations, assuming a quasi-static loading, can be represented as:

$$\{f\} = [k]\{d\} \tag{2.1}$$

where *{f}* is a vector of the forces at the nodes, *{d}* is the displacement vector, and *[k]* will be a matrix. This matrix is unique to each finite element and describes its nodal behaviour when the forces *{f}* are applied. By taking each of these individual matrices and combining them into a unique matrix, the global stiffness matrix *[k]* is obtained. Just like the element stiffness matrix represents the behaviour of the element, the global stiffness matrix will represent the behaviour of the Finite Element structure.

In this case, the field variable will be the displacement at nodes that result from the applied load. The geometry and the displacements of each element are completely described by the geometric positions and displacements of the element nodal points. The element nodal coordinates prior to any displacements are known, and the nodal displacements are the unknowns to be calculated. The basic step is to interpolate the element geometry and the element displacements by using the nodal values. In other words, the approximating functions are defined in terms of field variables of these nodes. Thus, in the *FEA* the unknowns are the field variables of the nodal points. The actual variation in the region spanned by an element is more complicated to reach, but *FEA* provides an approximate solution (Szabó, Babuska, 2021).

It is also important to mention that the FEM used in the context of this work is only considering linear problems, which means that the properties of the materials constituting the structure are maintained constant, when the structure is subjected to loading. Linearity also requires the deformations to be small enough in order to the equilibrium equations be written using the original geometry instead of the deformed shape. That is, nonlinear behaviour such as the yielding of steel or crumbling of concrete are to be excluded (Bathe, 2008).

2.3 One-dimensional elements

One of the structural systems investigated in this project is the Frame model. This system, when modeled using FEM, is defined by the utilization of one-dimensional components. For example, a continuous beam that spans two or more supports can be replicated by employing one beam element for each span between the supports. The accuracy of the analysis increases with the number of elements employed (Cook et al., 2001).

One-dimensional elements include a straight bar loaded axially, a straight beam loaded laterally, between other examples. In frames, there are two main types of elements: Bar elements, carrying only axial loading, and Beam elements, which carry shear forces, in the normal direction, and moment. (Parke, Hewson, 2022).

2.3.1 Bar element

The bar element is characterized as an uniform prismatic bar, with length L, elastic modulus E and cross-sectional area A. It is usually represented as a simple line and has a node at each end (Cook et al., 2001). These nodes are allowed to displace only in the axial direction, with axial displacements at nodes taking the value of u_1 at node 1 and u_2 at node 2.

The internal axial stress, which follows Hooke's law, with the following expression $\sigma = E * \varepsilon$, can be related to nodal forces by free-body diagrams, in which applied force F is equal to the area of the cross-section times the axial stress:

$$F_1 + A * \sigma = 0 \tag{2.2}$$

The extension of the element is the subtraction of the displacement in node 1 from the displacement in node 2, divided by the total length of the element.

$$\varepsilon = \frac{u_2 - u_1}{L} \tag{2.3}$$

Therefore, an equilibrium state of the node is represented by the following formula:

$$F_1 + A * E * \frac{u_2 - u_1}{L} = 0 \tag{2.4}$$

Since there are two forces, F_1 and F_2, each one applied to each node, and applying the same steps to F_2, we obtain the following equation:

$$[k] * \{d\} = \{F\} \Leftrightarrow \begin{bmatrix} k & -k \\ -k & k \end{bmatrix} * \begin{Bmatrix} u_1 \\ u_2 \end{Bmatrix} = \begin{Bmatrix} F_1 \\ F_2 \end{Bmatrix} \tag{2.5}$$

where [k] is the element stiffness matrix, d is the displacement vector and F is the force vector applied to the element.

In this equation, $A * E/L = k$ is regarded as k, the stiffness of a linear spring, because it is assumed that, just like the spring, the bar element has displacements exclusively in the axial direction.

In the case of a structure composed by two bar elements connected, with the stiffness of each element being k_1 and k_2, the structure's stiffness matrix is:

$$\begin{bmatrix} k_1 & -k_1 & 0 \\ -k_1 & k_1+k_2 & k_2 \\ 0 & -k_2 & k_1 \end{bmatrix} * \begin{Bmatrix} u_1 \\ u_2 \\ u_3 \end{Bmatrix} = \begin{Bmatrix} F_1 \\ F_2 \\ F_3 \end{Bmatrix} \Leftrightarrow \begin{bmatrix} K \end{bmatrix} * \begin{Bmatrix} D \end{Bmatrix} = \begin{Bmatrix} F \end{Bmatrix} \tag{2.6}$$

This matrix [K] is called the global stiffness matrix. It results from the sum of the individual matrices of each bar, where the nodes shared between two bars are influenced by both of them. One example of this is the possibility to check that the force F2 will have an influence on the behaviour of the 3 nodes of the structure composed by the two bars.

2.3.2 Beam element

A beam is defined as a structure whose length, L, is much larger than its cross-section dimensions and whose axis is defined along the length. Its cross-section is normal to this axis and assumed to be constant along it (Murty, 1984). Similar to a bar element, a beam is represented as a line with a node at each end. However, in the latter case, each node has two degrees of freedom (d.o.f), namely, transversal translation, along the y-axis, and rotation, over the z-axis. This d.o.f will take the notation of v and ϕ, with the index number with respect to the corresponding node. The rotation's vector representation point along the z axis, normal to the xy plane (Cook et al., 2001)(Faroudja et al., 2017).

To analyse this element, the axial displacements are restricted and only bending deformations are considered, assuming that transverse shear deformation can be ignored. This is the general case of beam theory, also known as Euler-Bernoulli beam theory. The referenced theory is extensively used to analyse complex structures since it provides designers with a simple tool to work with. Beam models are used in the modeling stage because they allow a clear perspective of the behaviour of the whole structure (Wang et al., 2000). It is also a valuable way to validate computational solutions.

2.3.3 Beam theories

In the design of concrete frame structures, it is crucial to know the behaviour of beams under different loading conditions, as it enables accurate prediction of the mechanics of these elements. This understanding is fundamental for ensuring a correct, safe, and optimal design and use of the structure (Carrera, Giunta, 2010). The classical beam theories, such as the Euler-Bernoulli (EB) and Timoshenko (TB) theories, provide the foundation for comprehending the bending and deflection behaviour of beams. These theories form the basis of classical one-dimension models for the bending analysis of beam structures made of isotropic materials. These models simplify the complex, three-dimensional structures into one-dimensional problems through the expression of ordinary differential equations in terms of a single span-wise variable along the axis of the beam (Bauchau, Craig, 2009).

It is worth mentioning that, while these theories are widely used in the analysis of beams, they are only accurate for slender elements, where the mechanics are governed by global bending. As the beam becomes less slender, its mechanics become increasingly three-dimensional and the classical models yield less accurate results (Carrera, Giunta, 2010). The EB beam theory, also called Classical Beam Theory, assumes that the cross-section maintains its shape as the beams bend. It neglects the transverse shear strain, resulting in an infinitely rigid beam in the transverse direction. This theory is usually applied to beams with simple shapes and small deflections. On the other hand, the TB beam theory takes into account shear deformations and rotational effects in beams, making it a more appropriate choice for beams with complex shapes and larger deflections, or when the vibration of the beam is studied (Cook et al., 2001).

The choice of beam theory to be employed in the design process depends on the specific requirements of the structure, namely the type and magnitude of loads, the beam shape, and the desired level of accuracy. In general, the Euler-Bernoulli theory is employed for more conservative results, while the Timoshenko theory provides more accurate results, making it more suitable for more thicker beams. (Liu, Teng, 2002).

Euler-Bernoulli Beam Theory

Euler-Bernoulli Beam Theory is predicated on some assumptions. The first one, and most significant, states that the cross-section of the beam is infinitely rigid in its own plane. This implies that there are no deformations in the plane of the cross-section along the beam's length, while the beam still permits deformation along its length. As a result, the in-plane displacement can be characterized by two translations and one rotation (Carrera, Giunta, 2010).

However, this assumption is related only to the in-plane displacements of the cross-section. Hence, two additional assumptions must be made to account for the out-of-plane displacements. On one hand, during the deformation, the cross-section is assumed to remain plane. But on the other, the cross-section remains normal to the deformed axis of the beam (Murty, 1984). Figure 1 shows a simple representation of deformed and undeformed beams.

Figure 1: Undeformed (left) and deformed (right) beams

In a 3-dimensional Cartesian Coordinate system, the beam lies on the x, being this axis the center of the cross-section. The y-axis corresponds to the cross-section base and the z-axis corresponds to its height. This section is assumed to be symmetric according to the xz-plane, being in this plane that the bending takes place.

The bending and physical properties are constant along the beam's span. Thus, the deformation of the beam will also be constant, resulting in a constant curvature. This curvature can be defined as a semi-circle with the center in a point 0, at a distance of p from the axis of the beam (Carrera, Giunta, 2010).

After deformation, any plane perpendicular to the length of the beam will be an axis of symmetry of the beam. For the deformed cross-section to satisfy this symmetry requirement, it must remain plane and perpendicular to the deformed axis of the beam.

There are other assumptions that can be made to facilitate the interpretation of the behaviour of the beam. The out-of-plane displacement of this element is described by the Euler-Bernoulli Beam Equation, which relates the displacement of the beam to the applied force acting in the same direction (Murty, 1984)(Carrera, Giunta, 2010).

Deduction of the Euler-Bernoulli Beam Equation

Considering a cantilever with an applied force F in the loose end with the direction of the z-axis,this force will produce a displacement in the free end of the beam, and a curvature along its length. According to the beam theory, this curvature will be constant.

In a given point A(x,y), the slope angle will be α. And at a given point B(x+dx, y+dy) the angle will be α+dα. The angle in the centre of the semi-circle between A and B and radius ρ, will be dα.

The length of the semi-circle between A and B is denoted as *ds* and is obtained by multiplying the difference between the slopes of both points, dα, with the radius, ρ. The curvature, *k*, is the inverse of the radius:

$$k = \frac{1}{\rho} \tag{2.7}$$

Therefore, it is possible to make the following relation:

$$k = \frac{1}{\rho} = \frac{1}{\frac{ds}{d\alpha}} = \frac{d\alpha}{ds} \tag{2.8}$$

Since the beam curve very little, the curvature will consequently be very small. Therefore, the following assumption is made:

$$ds \approx dx \quad \Leftrightarrow \quad k \approx \frac{d\alpha}{dx} \tag{2.9}$$

Additionally, the tangent of the beam in each point, with slope α is:

$$tg(\alpha) = \frac{dy}{dx} \tag{2.10}$$

That is the change in transverse displacement per unit of length. But since the curvature has a very small value, it is possible to make the following approximation for the slope of the deflection curve:

$$tg(\alpha) = \frac{dy}{dx} \approx \alpha \tag{2.11}$$

Consequently, the curvature will be:

$$k = \frac{1}{\rho} = \frac{d^2y}{dx^2} \tag{2.12}$$

The bending moment (rotation imposed by the force) can be related to the curvature by the following equations:

$$M = \frac{EI}{\rho} \quad \Leftrightarrow \quad \frac{1}{\rho} = \frac{M}{EI} \tag{2.13}$$

Where E is the Young's Modulus and I is the Inertia of the cross-section. After matching both formulas of radius, ρ, the next equation is obtained:

$$\frac{d^2y}{dx^2} = \frac{M}{EI} \tag{2.14}$$

According to some basic formulations in mechanics of materials, the shear force and moment are obtained trough the following equations:

$$V(x) = \int F(x)dx \quad \text{and} \quad M(x) = \int V(x) + m1 \tag{2.15}$$

$$M(x) = \iint F(x) + mx1 + m2 \quad \Leftrightarrow \quad F(x) = \frac{d^2}{dx^2}M(x) \tag{2.16}$$

By relating the equations presented previously, the Euler-Bernoulli Beam Equation is formulated:

$$F(x) = \frac{d^2}{dx^2}(EI \cdot \frac{d^2y}{dx^2}) \tag{2.17}$$

If the properties of the beam do not vary along its length, then the previous equations can be simplified to

$$F(x) = EI \cdot \frac{d^4y}{dx^4} \tag{2.18}$$

The previous equation, denoted as the Euler-Bernoulli Beam equation, holds great significance in the field of structural engineering and FEA, as it is used as the governing equation of beam elements, describing its behavior under bending.

Timoshenko Beam Theory

Timoshenko's theory is another classic one-dimensional model for the bending analysis of beam structures. Transverse shear deformation and rotational bending effects are taken into account in this theory. This model is fit to describe the behaviour of beams in complex scenarios, for example, when beam vibration is studied (Cook et al., 2001).

This is a more complex theory and will not be considered for the scope of this work.

Beam Stiffness Matrix

A given beam element, modeled by either EB or TB, for example the one shown in Figure 6, which has 4 d.o.f, has a stiffness matrix with four rows and four columns, like the one presented in Equation 2.19.

$$\{f\} = [k]\{d\} \quad \Leftrightarrow \quad \begin{Bmatrix} F_1 \\ M_1 \\ F_2 \\ M_2 \end{Bmatrix} = \begin{bmatrix} k_{11} & k_{12} & k_{13} & k_{14} \\ k_{21} & k_{22} & k_{23} & k_{24} \\ k_{31} & k_{32} & k_{33} & k_{34} \\ k_{41} & k_{42} & k_{43} & k_{44} \end{bmatrix} = \begin{Bmatrix} v_1 \\ \phi_1 \\ v_2 \\ \phi_2 \end{Bmatrix} \tag{2.19}$$

The explanation of the stiffness matrix will be presented further in this chapter.

2.4 Two-dimensional elements

The Shell model is the second structural system compared in this project. Shells are one kind of surface elements present in FEA software, like membrane and plate elements.

Surface Elements are characterized by having one dimension, commonly referred to as the thickness, that is significantly smaller than the other two dimensions. This entails that the structure's behaviour is determined by the deformation of its surfaces rather than its volume. The average surface of the element and the thicknesses perpendicular to it define surface elements. Typically, the thickness is assumed to be constant across the element, which might be flat, curved, or a mix of the two. Surface elements are commonly used to simulate structures such as shells, roofs, and domes in engineering and architecture (Timoshenko, Woinowsky-Krieger, 1989). They may also be utilized to create complicated curved surfaces like airplane fuselages and ship hulls.

Because each of these elements has distinct properties, it is important to properly characterize them. This section will provide a review of different types of surface elements available in FEA software, as well as considerations regarding their behaviour.

2.4.1 Membrane element

The membrane element is characterized by its lack of flexural and transverse shear stiffness, which precludes it from experiencing bending moments. However, it does possess in-plane stiffness, allowing it to withstand loads that are contained within its plane. Such loads include axial forces in both directions (Nx and Ny) and shear force (Nxy) (Craveiro et al., 2021). Membrane elements have three d.o.f. per node out of which two d.o.f.s are in-plane translations and one d.o.f. corresponds to the out of plane rotation.

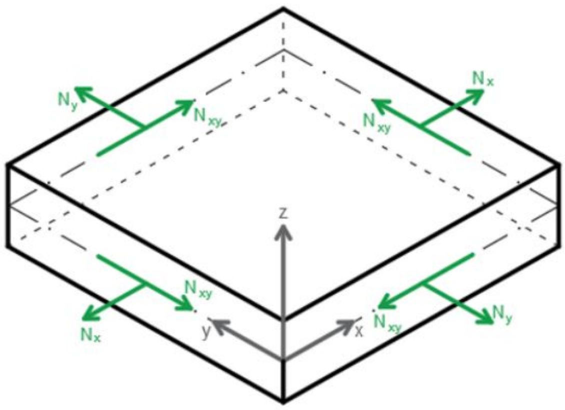

Figure 2: Membrane element (Craveiro et al., 2021)

In order to sustain out-of-plane loading, membranes rely on in-plane stresses. As a result of their unique properties, membranes as structural members are commonly employed in tension-dominated applications, such as tents, air-supported structures and membrane roofs.

2.4.2 Plate element

The plate element represents a flat surface which is subjected to loading that is normal to their plane, resisting it by means of bending. The response of plate elements to loading is described by bending moments in both directions (Mx and My), torsional moment (Mxy), and shear forces in both directions (Vx and Vy) outside the plane of the plate (Craveiro et al., 2021) (Cook, Young, 1998).

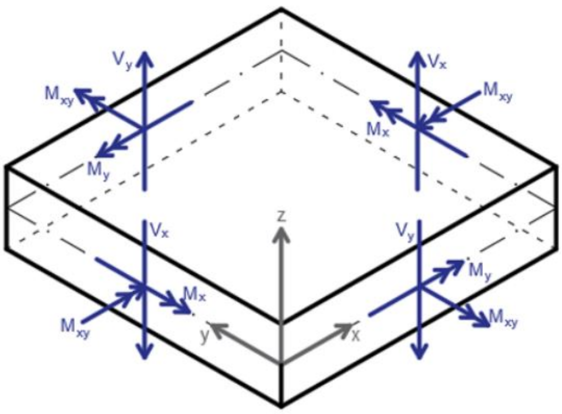

Figure 3: Plate element (Craveiro et al., 2021)

Plates as structural elements are intended to sustain out-of-plane loading through bending stresses. As such, they are commonly employed in structures like bridge decks, floor systems and roofing elements. In cases where a plate possesses an extremely thin profile, the bending stiffness will be nearly non-existing, rendering it incapable of resisting lateral loading. Instead, it can only resist membrane loading and therefore, is classified as a membrane (Skibeli, 2017). Plate elements have three degrees of freedom per node, two of which are in-plane rotations and the other is out-of-plane translation.

2.4.3 Shell element

The final surface element is the shell, which is an element that combines the properties of membrane and plate elements. As a result, shells exhibit both bending and in-plane stiffness, allowing them to resist forces from all directions (Cook, Young, 1998). By combining plate and membrane elements, it has 6 d.o.f per node, being all three in-plane translations and rotations along all axes.

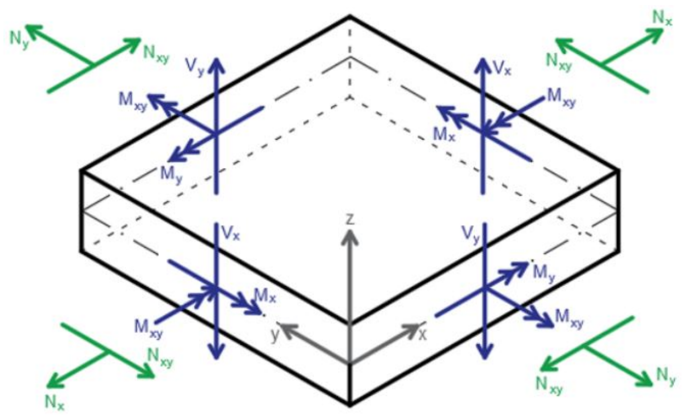

Figure 4: Shell element (Craveiro et al., 2021)

Shells as structural elements are utilized in a variety of applications where both bending and tension are predominant factors. They are commonly found in curved construction such as domes, egg-shaped structures, and similar geometries. In addition, they are frequently used in the design of roofs, tunnels, nuclear power plants towers, and other structures that incorporate curved, conical or cylindrical shapes (Gupta, 1984).

For the analysis of both plates and shells, it is usual to consider these structural elements as bodies with two surfaces separated by a thickness, denoted as *"t"*. The mid surface of these elements is located at the midpoint of the thickness, i.e. *t/2*, situated between the inner and outer surfaces. This mid surface is used as the *xy* plane, with *z=0*, serving as the reference plane for the analysis of the elements (Cook et al., 2001).

A shell is characterized by its curved surface. This surface possesses two principal radii of curvature at every point, normal to the shell. Each of these radii can be envisioned as the radius of a small arc drawn in the shell mid-surface. The arcs that correspond to the principal radii of curvature intersect at a right angle, with one being the largest and the other being the smallest of all the possible arcs in the mid-surface (Cook, Young, 1998).

Shells resist forces predominantly through membrane action due to their geometry, with bending occurring around borders and structural discontinuities (Gupta, 1984). This state of stress in x and y directions can be represented as the superposition of membrane stresses and bending stresses.

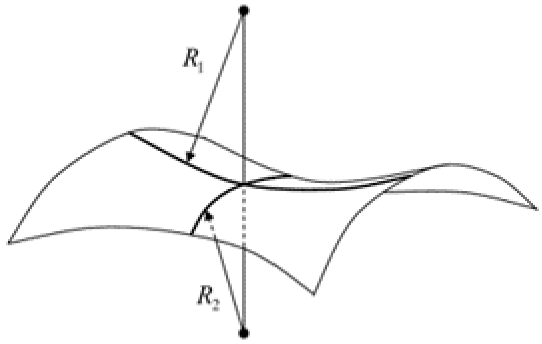

Figure 5: Radii of curvature of a shell

2.4.4 PLATE THEORY

Plate theories are mathematical models used to describe the response of plate elements to external loading. The two most important plate theories are the Kirchhoff theory and the Mindlin theory. The ensuing discussion will provide an overview of these two theories. It is important to note that, although they are called plate theories, they apply to both plates and shells (Timoshenko, Woinowsky-Krieger, 1989)(Wang et al., 2000).

Kirchhoff Theory

The Kirchhoff Theory (KT), also known as the classical thin plate theory, is based on the theory of beams. It presumes that the plate is thin and subjected to pure bending, where homogeneous plate deformation results in the mid-surface becoming a neutral surface. For this case of pure bending, this theory is based on the displacement field and defined by following equations:

$$u(x,y,z) = -z * \frac{\partial \omega_0}{\partial x} \tag{2.20}$$

$$v(x,y,z) = -z * \frac{\partial \omega_0}{\partial y} \tag{2.21}$$

$$\omega(x,y,z) = \omega_0(x,y) \tag{2.22}$$

where (u,v,ω) are the displacement components along the (x,y,z) coordinate directions, respectively, and ω_0 is the transverse deflection of a point on the mid-plane (z = 0) (Wang et al., 2000).

As a result of this displacement field, straight lines that were normal to the *xy-plane* before deformation will remain straight and normal to the mid-surface after deformation. This assumption is made in order to neglect the effects of transverse normal stress, as well as transverse shear stresses in the planes xz and yz. Moreover, the length of the normal lines is considered to remain constant. As a result, bending and in-plane stresses will be the only factors contributing to deformations. It is crucial to remember that these presumptions only hold true for materials that are homogeneous and isotropic.

Nonetheless, this theory has some limitations like the fact that it presupposes the plate to be thin and the stresses to be small, which is not the case in all applications. Furthermore, it is assumed that the plate is loaded only in the normal of its plane, which is also not accurate for most structures.

Mindlin Theory

The Mindlin Theory (MT), also referred to as the first order shear deformation plate theory, is based on the following displacement field equations:

$$u(x,y,z) = z\phi_x(x,y) \tag{2.23}$$

$$v(x,y,z) = z\phi_y(x,y) \tag{2.24}$$

$$\omega(x,y,z) = \omega_0(x,y) \tag{2.25}$$

where ϕ_x and $-\phi_y$ denote rotations about the y and x axes, respectively. MT is an extension of the KT that considers the influence of transverse shear deformation. In contrast to KT, MT acknowledges that transverse shear deformation remains constant in relation to the thickness coordinate (Wang et al., 2000). This modification is appropriate for relatively thicker plates, where transverse shear deformations are significant.

Parallelism with Beam Theories

Both these theories can be regarded as an extension of beam theories. The EB beam theory is related to the KT plate theory, while the TB theory for beams is related to MT plate theory.

Regarding the Kirchhoff model, it is based on assumptions that are closely related to those of the Euler-Bernoulli beam theory. Whereas beam theory deals with the kinematics of the beam' cross-section, KT deals with a set of material particles aligned in the normal direction to the mid-plane of the plate. In KT, this normal material line is assumed to be infinitely rigid along its length, i.e., no deformations occur in the normal direction of the plate's mid-surface. This assumption parallels the beam theory assumption that the cross-section of the beam is infinitely rigid in its own plane and, therefore, no deformations will occur in that plane. Similarly, the assumption that the lines normal to the plate's mid-surface remain normal after deformation parallels the assumption in beam theory that the cross-section of the beam remains normal to the deformed axis of the beam (Bauchau, Craig, 2009).

On the other hand, the Mindlin model is related to the Timoshenko Beam theory in the sense that both theories consider the effects of transverse shear stresses and rotations on the structure and both can be classified as first-order shear deformation theories.

Shells can be classified into two categories, thin and thick, based on the minimum length-to-thickness ratio. The behaviour of these shells differs in terms of shear deformation. Thin shells do not undergo shear deformation, and hence, KT can be applied. On the other hand, thick shells are assumed to experience shear deformation, and therefore MT can be applied. Under the KT, the shell's behaviour will be based on the concept of "membrane action" where the shell behaves like a thin, flexible membrane and is subjected to small stresses primarily in its plane. Thus, membrane actions dominate, and this is known as a membrane-dominated shell.

2.5 FINITE ELEMENT FORMULATION

2.5.1 SHAPE FUNCTIONS

The finite element method resorts to discretization to decompose the structure into a mesh of individual elements with a node at each end. Although the nodal values are known, it is important to understand what happens between the nodes defining the mesh, that is, the element. To determine the behaviour of the element, it is necessary to define a rule to which the element can obey: the shape function. This consists in an approximation polynomial that defines the range of a dependent variable in terms of generalized coefficients and independent variables/spatial coordinates(x,y,z). In other words, the shape function is a function that interpolates the behaviour of the element, describing the variation of displacement factor along its length. It characterizes the movement of the element in terms of pure bending and transverse displacement. The number of shape functions of a system will depend upon the number of nodes and the number of variables per node. Each degree of freedom generates its own shape function. Also, different shape functions generate different element matrices (Cook et al., 2001).

In terms of a generalized d.o.f a_i, an interpolation polynomial with dependent variable Θ and independent variable x can be written, according to Cook et al. (2001), in the following way:

$$\Theta = \sum_{i=0}^{n} a_i x^i \quad \text{and} \quad \Theta = [X] \cdot a \tag{2.26}$$

in which

$$[X] = [1 \quad x \quad x^2 \quad \cdots \quad x^n] \quad \text{and} \quad a = [a_0 \quad a_1 \quad a_2 \quad \cdots \quad a_n]^T \tag{2.27}$$

where n = 1 represents linear interpolation, n = 2 represents quadratic interpolation, and so on. The a_i can be expressed in terms of nodal values of Θ, which appear at known values of x. The relation between nodal values Θ_e and the a_i is symbolized as

$$\Theta_e = [A] \cdot a \tag{2.28}$$

where each row of $[A]$ is $[X]$ evaluated at the appropriate nodal location. From the three previous equations, it is possible to obtain:

$$\Theta = [N] \cdot \{\Theta_e\} \quad \text{where} \quad [N] = [X][A]^{-1} = [N_1 \quad N_2 \quad \cdots] \tag{2.29}$$

An individual N_i in matrix $[N]$ is called the shape function. Each N_i states the interpolated $\Theta = \Theta(x)$ when the corresponding Θ_i is unity and all the other Θ_i are zero.

In FEA, the assembly of elements causes element nodal values Θ_e to appear in D, the global vector of d.o.f. As a result, Θ_e of each element is calculated by solving the global equation $[K]\{D\} = \{R\}$

Consider the two-noded beam element, with 4 d.o.f, presented in Figure 6.

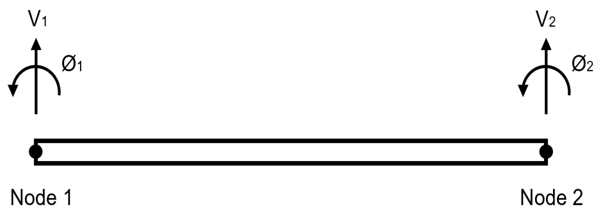

Figure 6: Beam element with 4 d.o.f.

A general Displacement Function for the element presented would be:

$$v = C_1 + C_2 \cdot x + C_3 \cdot x^2 + C_4 \cdot x^3 \tag{2.30}$$

This equation provides the displacement at any point x of the length of the element. As it is possible to verify, the function has four coefficients due to the fact that the bar has four degrees of freedom. The equation is expressed as the product of the shape function and the degree of freedom. To get the shape functions, it is necessary to apply boundary conditions and solve the Displacement Function with respect to the d.o.f:

$$\begin{aligned} x = 0 \rightarrow v(0) &= C_1 + C_2 \cdot 0 + C_3 \cdot 0^2 + C_4 \cdot 0^3 \\ \Leftrightarrow v(0) &= C_1 \rightarrow v_1 = C_1 \end{aligned} \tag{2.31}$$

The rotation of a node is given by the change in transverse displacement per unit length, (or the change in the Displacement Function with respect to x), that is:

$$\phi = \frac{dv}{dx} \Leftrightarrow \phi = C_2 + 2C_3 \cdot x + 3C_4 \cdot x^2 \tag{2.32}$$

By applying boundary conditions to the previous equation, the value of the rotation in node 1 is obtained:

$$x = 0 \rightarrow \phi(0) = C_2 \Leftrightarrow \phi_1 = C_2 \tag{2.33}$$

In node 2, x will take the value of the length of the element. Therefore $x = l$. Applying this boundary condition to the Displacement Function will produce the following solution:

$$\begin{aligned} &\rightarrow v(l) = C_1 + C_2 \cdot l + C_3 \cdot l^2 + C_4 \cdot l^3 \\ x = l &\Leftrightarrow v_2 = C_1 + C_2 \cdot l + C_3 \cdot l^2 + C_4 \cdot l^3 \qquad \Leftrightarrow \phi_2 = C_2 + 2C_3 \cdot l + 3C_4 \cdot l^2 \\ &\phi(l) = C_2 + 2C_3 \cdot l + 3C_4 \cdot l^2 \end{aligned} \tag{2.34}$$

By combining in a system the equations of v_1, ϕ_1, v_2, and ϕ_2 and rearranging them in order of the

C variables, the following system is obtained:

$$\begin{cases} v_1 = C_1 \\ \phi_1 = C_2 \\ v_2 = C_1 + C_2 \cdot l + C_3 \cdot l^2 + C_4 \cdot l^3 \\ \phi_2 = C_2 + 2C_3 \cdot l + 3C_4 \cdot l^2 \end{cases} \Leftrightarrow \begin{cases} C_1 = v_1 \\ C_2 = \phi_1 \\ C_3 = \frac{-3v_1}{l^3} + \frac{-2\phi_1}{l} + \frac{3v_2}{l^2} + \frac{-\phi_2}{l} \\ C_4 = \frac{2v_1}{l^3} + \frac{\phi_1}{l^2} + \frac{-2v_2}{l^3} + \frac{\phi_2}{l^2} \end{cases} \tag{2.35}$$

Now it is necessary to take the values of the C coefficients and substitute them back into the general Displacement Function, equation 2.30. By rearranging the obtained Displacement Function in terms of each d.o.f, the next equation is obtained:

$$\begin{aligned} v &= C_1 + C_2 \cdot x + C_3 \cdot x^2 + C_4 \cdot x^3 \\ &= v_1 + \phi_1 \cdot x + \left(\frac{-3v_1}{l^2} + \frac{-2\phi_1}{l} + \frac{3v_2}{l^2} + \frac{-\phi_2}{l} \right) \cdot x^2 + \left(\frac{2v_1}{l^3} + \frac{\phi_1}{l^2} + \frac{-2v_2}{l^3} + \frac{\phi_2}{l^2} \right) \cdot x^3 \\ &= v_1 + \phi_1 x + \frac{-3v_1x^2}{l^2} + \frac{-2\phi_1x^2}{l} + \frac{3v_2x^2}{l^2} + \frac{-\phi_2x^2}{l} + \frac{2v_1x^3}{l^3} + \frac{\phi_1x^3}{l^2} + \frac{2v_1}{l^3} + \frac{-2v_2}{l^3} + \frac{\phi_2}{l^2} \\ &= \left(1 - \frac{3x^2}{l^2} + \frac{2x^3}{l^3}\right) \cdot v_1 + \left(x + \frac{-2x^2}{l} + \frac{-x^3}{l^2}\right) \cdot \phi_1 + \left(\frac{3x^2}{l^2} + \frac{2x^3}{l^3}\right) \cdot v_2 + \left(\frac{-x^2}{l} + \frac{x^3}{l^2}\right) \cdot \phi_2 \end{aligned} \tag{2.36}$$

So, by isolating each d.o.f from the previous equation, it is possible to write it as:

$$v = N_1 \cdot v_1 + N_2 \cdot \phi_1 + N_3 \cdot v_2 + N_4 \cdot \phi_2 \tag{2.37}$$

or in matrix form:

$$v = [N] \cdot \{d\} \tag{2.38}$$

where each N_i is a shape function of the beam when the respective d.o.f. has a unit value and all the other d.o.f are fixed and therefore have a value of zero.

In Figure 7 are presented four graphics that represent the deformed beam with each individual d.o.f activated and the respective shape function.

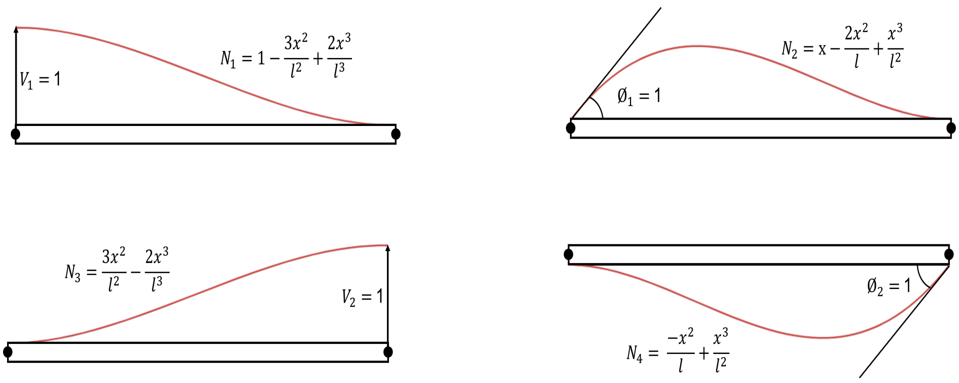

Figure 7: Deformed beam for each Shape function

2.5.2 Stiffness matrix

The stiffness matrix, denoted by $[k]$, defines how much each node in the element will displace for a set of forces and moments applied to the element. It is the key to solve the displacements at every node of the mesh. It consists in a square matrix, where the number of rows and columns will be the same as the number of d.o.f of the element that it represents (Cook et al., 2001).

For a beam element like the one presented in Figure 6, with 4 d.o.f, the stiffness matrix is:

$$[k] = \begin{bmatrix} k_{11} & k_{12} & k_{13} & k_{14} \\ k_{21} & k_{22} & k_{23} & k_{24} \\ k_{31} & k_{32} & k_{33} & k_{34} \\ k_{41} & k_{42} & k_{43} & k_{44} \end{bmatrix} \tag{2.39}$$

Since the FEM analyses each element individually, it will generate an individual stiffness matrix for each element, which will have the name of the local stiffness matrix. As refereed previously, the method will then compile all the individual stiffness matrices into a global one, known as the global stiffness matrix $[k]$. To a matrix like the one of Equation 2.39 it is applied the following general rule:

A column of $[k]$ is the vector of loads that must be applied to an element at its nodes to maintain a deformation state in which the corresponding nodal d.o.f has a unit value while all the other nodal d.o.f are zero (Cook et al., 2001).

To obtain the values of the stiffness matrix, it is required to resort to the Beam Theory, explored in Chapter 2.2.2.

Moments and Shear are related to the transverse displacement in the following way:

$$M(x) = EI \cdot \frac{d^2v}{dx^2} \quad \text{and} \quad V(x) = EI \cdot \frac{d^3v}{dx^3} \tag{2.40}$$

To get the System of a finite element $\{f\} = [k]\{d\}$ it is necessary to solve the displacement Equation 2.37 in order of moments and shear by the relations presented above. For example, in order to get the moment in node 1, M_1, it is necessary to do a double derivative of the Displacement function presented in Equation 2.37 with unit value for ϕ_1 and all other d.o.f fixed, and therefore, with the value of zero. In this case, it is used the Beam Theory sign convention, which states that a bending moment is considered positive if it causes concavity upward and a shear force that moves the left side of the section upward or the right side of the section downward is considered as positive.

For the displacements vector $[v_1 = 1; \quad \phi_1 = 0; \quad v_2 = 0; \quad \phi_2 = 0]$:

$$F_1 = V(x=0) = EI \cdot \frac{d^3v}{dx^3} = \frac{EI}{l^3} \cdot (12 \cdot v_1 + 6l \cdot \phi_1 - 12l \cdot v_2 + 6l \cdot \phi_2) \tag{2.41}$$

For the displacements vector $[v_1 = 0; \quad \phi_1 = 1; \quad v_2 = 0; \quad \phi_2 = 0]$:

$$M_1 = -M(x=0) = -EI \cdot \frac{d^2v}{dx^2} = \frac{EI}{l^3} \cdot \left(6l \cdot v_1 + 4l^2 \cdot \phi_1 - 6l \cdot v_2 + 2l^2 \cdot \phi_2\right) \tag{2.42}$$

For the displacements vector $[v_1 = 0; \quad \phi_1 = 0; \quad v_2 = 1; \quad \phi_2 = 0]$:

$$F_2 = -V(x=l) = -EI \cdot \frac{d^3v}{dx^3} = \frac{EI}{l^3} \cdot (-12 \cdot v_1 - 6l \cdot \phi_1 + 12l \cdot v_2 - 6l \cdot \phi_2) \tag{2.43}$$

For the displacements vector $[v_1 = 0; \quad \phi_1 = 0; \quad v_2 = 0; \quad \phi_2 = 1]$:

$$M_2 = M(x=l) = EI \cdot \frac{d^2v}{dx^2} = \frac{EI}{l^3} \cdot \left(6l \cdot v_1 + 2l^2 \cdot \phi_1 - 6l \cdot v_2 - 4l^2 \cdot \phi_2\right) \tag{2.44}$$

By taking the four previous equations and writing them in matrix form, the following system is obtained:

$$\{f\} = [k]\{d\} \quad \Leftrightarrow \quad \begin{Bmatrix} F_1 \\ M_1 \\ F_2 \\ M_2 \end{Bmatrix} = \frac{EI}{l^3} \cdot \begin{bmatrix} 12 & 6l & -12 & 6l \\ 6l & 4l & -6l & 2l^2 \\ -12 & -6l & 12 & -6l \\ 6l & 2l^2 & -6l & -4l \end{bmatrix} = \begin{Bmatrix} v_1 \\ \phi_1 \\ v_2 \\ \phi_2 \end{Bmatrix} \tag{2.45}$$

The matrix $[k]$ in the system above represents the local stiffness matrix of a beam element.

2.6 Frame Structural System

A frame is a structural system composed of interconnected beams and columns that form a rigid structure capable of withstanding external loads and pressures. These structures are distinguished by the use of elements like beams and columns to transmit loads from the elements above to those below, such as from a building's roof to its foundations.

In engineering and architecture, frames are extensively used to design and evaluate the behaviour of buildings and other structures. One of the primary benefits of frame models is their ease of formulation and analysis. In other words, engineers can model and study the behaviour, stability, and strength of a complex structure by breaking it down into basic elements such as beams and columns. This is an accessible and effective way to design and analyse the behaviour of buildings and other structures. Furthermore, the simplicity of analysing a Frame model is a very important feature in practical engineering, where the design created by one company must be verified by others. Frame models are also very simple to build, making them a popular choice for constructions with regular geometric patterns, such as residential buildings, bridges, or skyscrapers. As a result, building procedures become more efficient and cost-effective. Another benefit of frame models is their adaptability. Engineers may quickly change the shape and attributes of the model's elements to test multiple design concepts and scenarios, resulting in optimal design solutions. Summing up, their simplicity, ease of construction, and flexibility make them a favored option for a wide range of applications, resulting in more efficient and cost-effective construction processes.

2.6.1 Design approach

As mentioned, concrete frames are simple structures, therefore, their design principles are based on the general structural theories of concrete design. The process of designing a Frame system consists in the drawing of its elements, namely, concrete beams and columns. The design of concrete structures typically follows the principles of mechanics and statics, which deal with bodies at rest and equilibrium, despite being subjected to forces. Equilibrium is considered to occur when all the forces sum to zero.

Engineers often begin the design process of reinforced concrete frames by calculating suitable dimensions for columns and beams to meet drift restrictions, and then calculate the needed steel reinforcement to ensure strength and ductility criteria are fulfilled. To validate the design, it is often compared to similar projects completed previously and code's rules. This procedure is adequate for the majority of structural design applications (Arroyo et al., 2018).

The process starts with a structural analysis, which involves determining the internal forces, specifically axial, shear, and bending, that act on the elements of a structure. This information is then applied to designing the elements with the capability to resist these forces. It entails the calculation of forces and stresses within a structure as well as the determination of the structure's deformation and stability (Nawy, 2009). Then the limit state design is applied, which usually includes load design methods and load factors based on statistical data used to account for uncertainties in the design process (AISC, 2016). Limit State Design (LSD) considers the strength and serviceability limit states of the structure (Fintel, 2011). The aim is to design the reinforced concrete components with a sufficient level of safety so that they will not experience failure when subjected to imposed loads. The design process entails determining the structural load-carrying capacity and evaluating various limit states, such as collapse, buckling, fatigue, deflection, cracking, and durability, as prescribed by Eurocode (Eurocode, 2010).

It is important to mention that the design of structures requires a comprehensive understanding of the behaviour of materials. This examines the structure under external loads and provides insight into the relationship between force, stress, and strain in the structure's elements, as well as the response of different materials to loads (Nawy, 2009). In the case of reinforced concrete frames, the performance of the concrete and steel used will significantly impact the overall performance of the structure. Additionally, factors such as casting, curing, and jointing during construction are critical for ensuring the quality and performance of concrete structures (Reynolds, Steedman, 1987).

The design process of Frames can be represented by the following scheme:

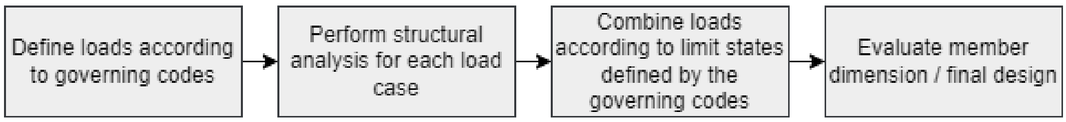

Figure 8: Limit State Design framework

2.6.2 BEAM DESIGN

The present section comprises the formulation for the design of a rectangular, doubly reinforced beam cross-section for ULS, subjected to bending. The partial factors considered for the ultimate limit state are $\gamma_c = 1,5$ for concrete and $\gamma_s = 1,15$ for the reinforcement steel, values taken from Eurocode, table 2.1N.

To determine the Design value of concrete compressive strength, the following equation is used:

$$f_{cd} = a_{cc} \cdot \frac{f_{ck}}{\gamma_c} \tag{2.46}$$

where f_{ck} is taken from the table 3.1 of EC, depending of the class of concrete used, and a_{cc} is the coefficient that accounts for the long term effects in the compression resistance of Concrete. This value should vary between 0.8 and 1, according to each country's National Annex. For the purpose of this work, this value will be considered 0,85.

Next, it is calculated the Design strength of reinforcement:

$$f_{yd} = \frac{f_{yk}}{\gamma_s} \tag{2.47}$$

where f_{yk} is the yield strength of the steel, with a value varying according to the type of steel selected. For exemple, for steel 500A, $f_{yk} = 500$ MPa.

Using the value of the moment applied to the section, and according to the Design Table ($\mu - \upsilon$ interaction diagrams) for rectangular cross-sections, with respect to ω (or μ_s):

$$\mu = \frac{M_{Ed}}{b \cdot d^2 \cdot f_{cd}} \tag{2.48}$$

After obtaining μ, it is necessary to interpolate from the tables a value for ω. Next, from the chosen d_2/d from the tables, the values of the upper and lower reinforcement are obtained by the following formulas:

$$A_{s1} = \frac{1}{f_{yd}} \cdot (\omega_1 \cdot b \cdot d \cdot f_{cd}) \tag{2.49}$$

$$A_{s2} = \frac{f_{cd}}{f_{yd}} \cdot (\omega_2 \cdot b \cdot d) \tag{2.50}$$

In case the beam is subjected to shear, the formulation to calculate shear reinforcement is presented next. The partial factors considered for ultimate limit states are $\gamma_c = 1,5$ for concrete and $\gamma_s = 1,15$ for reinforcing steel.

Determination of the Design value of concrete compressing strength:

$$f_{cd} = a_{cc} \cdot \frac{f_{ck}}{\gamma_c} \tag{2.51}$$

where a_{cc} is according to the National Annex of the country in analysis. For the purpose of this work, this value will be considered 0,85.

Determination of the Design yield strength of reinforcement:

$$f_{yd} = \frac{f_{yk}}{\gamma_s} \tag{2.52}$$

The design load for the cross-section: V_{Ed}

Design with respect to EN 1992-1-1:2004:

$$z = 0.9 \cdot d \tag{2.53}$$

$$1.0 \leq cot\theta \leq 2.5$$

$$A_{sw,requ}/s = V_{Ed}/(f_{ywd} \cdot z \cdot cot\theta) \tag{2.54}$$

2.6.3 Column design

The formulation for the design of a rectangular column cross-section for ULS, subjected for bending is presented next. The partial factors considered for ultimate limit states are $\gamma_c = 1,50$ for concrete and $\gamma_s = 1,15$ for reinforcing steel.

Determination of the Design value of concrete compressive strength:

$$f_{cd} = a_{cc} \cdot \frac{f_{ck}}{\gamma_c} \tag{2.55}$$

where a_{cc} is according to the country's National Annex in analysis. For the purpose of this work, this value will be considered 0,85.

Determination of the Design yield strength of reinforcement:

$$f_{yd} = \frac{f_{yk}}{\gamma_s} \tag{2.56}$$

Design loads for the cross-section are N_{Ed} and M_{Eds}. The next relation is established:

$$\frac{e_d}{h} = |\frac{M_{Ed}}{N_{Ed} \cdot h}| \tag{2.57}$$

If $e_d/h \leq 3.5$, then axial force is dominant, and so design with respect to $\mu - \upsilon$ interaction diagram is suggested.

Design with respect to interaction diagram for concrete C12/15 - C50/60, rectangular cross-section with double symetric reinforcement:

$$\mu_{Eds} = \frac{M_{Eds}}{b \cdot h^2 \cdot f_{cd}} \tag{2.58}$$

$$V_{Eds} = \frac{N_{Eds}}{b \cdot h \cdot f_{cd}} \tag{2.59}$$

From design chart for $d_1/h = 0.05/0.5 = 0.1$, ω_{tot}:

$$As,tot = \omega_{tot} \cdot \frac{b \cdot h}{f_{yd}/f_{cd}} [cm^2] \tag{2.60}$$

$$As1 = A_{s2} = \frac{As,tot}{2} [cm^2] \tag{2.61}$$

In case the beam is subjected to shear, the formulation to calculate shear reinforcement is the same as for the design of beams, already presented previously.

2.7 Shell Structural System

2.7.1 Design approach

Reinforced concrete Shell structures are a widely studied topic, with several researchers making different proposals on how to calculate the required reinforcement. Next are presented some of the most relevant theories. (ACI, ????) (Sofistik, 2020) (Reynolds, Steedman, 1999) are used as references.

2.7.1.1 Three-layer model

The three-layer model is a simplified approach that has been adopted by structural codes such as the CEB Model Code 1990. It is very similar to the sandwich model introduced in Eurocode 2. The model involves dividing the shell into three distinct layers: the top layer, the middle layer, and the bottom layer. The outer layers consist of reinforced concrete and provide resistance to the bending moments Mx, My, and Mxy, as well as the membrane forces Nx, Ny, and Nxy acting on the element. On the other hand, the inner layer is responsible for resisting the transverse shear Vx and Vy.

2.7.1.2 Baumann Method

The Baumann method is a formal approach for analysing and designing reinforced concrete shells based on the concept of "membrane action." This theory considers the shell as a thin plate that is primarily loaded in its plane and assumes that it behaves like a flexible membrane under the applied loads. The stresses in the shell are determined by the geometry of the shell and the loads applied to it.

In reinforced concrete surface structures, the main tensile stresses are absorbed by a network of reinforcing units, which may differ from the direction of the principal stresses. The design of this reinforcement network requires knowledge of the inner/internal force state, which is generally a statically indeterminate task.

To address this, this approach introduces the direction of the concrete compressive force stiffening the reinforcement mesh as indeterminate and determines it using the law of the minimum of deformation work. The size of the shear force to be absorbed by the concrete is determined in a similar manner. In addition to the stiffness of reinforcement and concrete, the stiffness of the interlocking and anchoring of the crack surfaces is also considered.

The Baumann method can be simplified as follows: the shell section is subjected to a moment and membrane stress. The moment is subsequently decomposed into a moment couple and then combined with the membrane forces. The result is two distinct panel forces, or disc forces, as illustrated in figure 9. These two membrane forces are then employed to calculate the design forces and required reinforcing, which will be placed in two perpendicular directions.

2.7.1.3 Capra-Maury Method

The Capra-Maury method is a semi-empirical approach that combines both theoretical and experimental techniques.

Similar to the Baumann method, this approach considers the reinforced concrete shell as a thin plate primarily loaded in its plane. However, it also incorporates the concept of the "transverse distribution of stresses", which refers to the variation of stresses across the thickness of the shell. To calculate the transverse distribution of stresses in the shell, this method employs a set of mathematical equations based on the geometry of the shell and the applied loads.

Furthermore, the analysis of the stresses in concrete and steel are calculated for all with a uni-axial iteration of the strain state every 5 degrees (36 directions in total).

2.7.1.4 Multi-layer method

The Multi-layer method is a technique employed to design and analyse reinforced concrete shells, which involves dividing the shell into multiple layers. This method is similar to the three-layer model, but provides a more detailed analysis by considering more than three layers.

The Multi-layer method uses a set of mathematical equations to calculate the stresses and deformations in each individual layer of the shell, and then evaluated the interaction between these layers to determine the overall behaviour of the shell. The method employs a combination of analytical and numerical techniques, such as finite element analysis, to model the shell and calculate the stresses and deformations.

This approach is particularly advantageous for shells with complex geometry or for shells that will be subjected to high loads

2.7.2 Baumann Formulation

SOFISTIK uses the Baumann Method for reinforcement calculation of plates and shells. Therefore, it is this calculation that is presented next.

The Baumann method can be described in the following simplified way. The shell section is subjected to moment and membrane forces. The moment is resolved into a moment couple and then combined with the membrane forces in order to give two pure panel (or one can say disc) forces as per the pictures below. These two membrane forces are then used to determine the design forces and required reinforcing.

It is assumed that there are two layers of reinforcement, that is a top layer and a bottom layer of reinforcement in the two principal directions.

Next is presented the verification of the lower reinforcement in the bottom panel (the bottom fibre of the shell element is in tension in this example).

The internal forces of the QUAD element necessary for the analysis are the following:

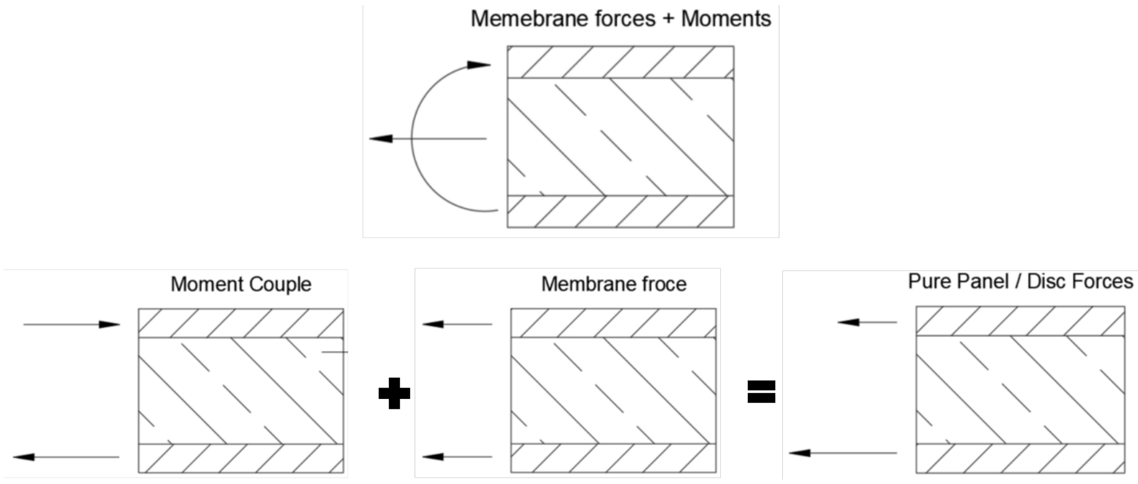

Figure 9: Forces in an elements according to the Baumann method (Eisenbau-Verbandes et al., 1972)

$$\begin{matrix} m_{xx} & m_{yy} & m_{xy} \\ n_{xx} & n_{yy} & n_{xy} \end{matrix} \tag{2.62}$$

where the moments are expressed in $\left[\frac{kn \cdot m}{m}\right]$ and the axial stresses in $\left[\frac{kn}{m}\right]$

From the available internal forces the principal bending moments can be assessed:

$$m_I = \frac{m_{xx}+m_{yy}}{2} + \frac{\sqrt{(m_{yy}-m_{xx})^2+4\cdot m_{xy}^2}}{2} \tag{2.63}$$

$$m_{II} = \frac{m_{xx}+m_{yy}}{2} - \frac{\sqrt{(m_{yy}-m_{xx})^2+4\cdot m_{xy}^2}}{2} \tag{2.64}$$

The angle between the principal bending moments:

$$\phi_m = \frac{atan(\frac{2\cdot m_{xy}}{m_{xx}+m_{yy}})}{2} \tag{2.65}$$

Similarly the principal normal forces can be assessed:

$$n_I = \frac{n_{xx}+n_{yy}}{2} + \frac{\sqrt{(n_{yy}-n_{xx})^2+4\cdot n_{xy}^2}}{2} \tag{2.66}$$

$$n_{II} = \frac{n_{xx}+n_{yy}}{2} - \frac{\sqrt{(n_{yy}-n_{xx})^2+4\cdot n_{xy}^2}}{2} \tag{2.67}$$

The angle between the principal normal forces:

$$\phi_n = \frac{atan(\frac{2 \cdot n_{xy}}{n_{xx}+n_{yy}})}{2} \tag{2.68}$$

This lever arm z is then used to calculate the virtual panel forces in direction of the element's local coordinate system on each side of the finite area element:

$$N_{xx} = \frac{n_{xx}}{2} + \frac{m_{xx}}{z_1} \quad \left[\frac{kN}{m}\right] \tag{2.69}$$

$$N_{yy} = \frac{n_{yy}}{2} + \frac{m_{yy}}{z_1} \quad \left[\frac{kN}{m}\right] \tag{2.70}$$

$$N_{xy} = \frac{n_{xy}}{2} + \frac{m_{xy}}{z_1} \quad \left[\frac{kN}{m}\right] \tag{2.71}$$

The next step is the transformation of the local panel forces into principal panel forces :

$$N_I = \frac{N_{xx}+N_{yy}}{2} + \frac{\sqrt{(N_{yy}-N_{xx})^2+4 \cdot N_{xy}^2}}{2} \quad \left[\frac{kN}{m}\right] \tag{2.72}$$

$$N_{II} = \frac{N_{xx}+N_{yy}}{2} - \frac{\sqrt{(N_{yy}-N_{xx})^2+4 \cdot N_{xy}^2}}{2} \quad \left[\frac{kN}{m}\right] \tag{2.73}$$

The angle between the principal panel forces:

$$\phi_N = \frac{atan(\frac{2 \cdot N_{xy}}{N_{xx}+N_{yy}})}{2} \tag{2.74}$$

The angle of the main reinforcement with the local x-axis of the quad is :

$$\varepsilon = 10 \quad [deg] \tag{2.75}$$

$$\alpha = |\phi_N - \varepsilon| \quad [deg] \tag{2.76}$$

Then the quotient of the principal panel membrane forces needs to be calculated:

$$q_N = \frac{N_{II}}{N_I} \tag{2.77}$$

It must be verified if this quotient is smaller or greather then the following expression:

$$(-tan(\alpha + \frac{\pi}{4})) \cdot tan(\alpha) \tag{2.78}$$

Since the quotient is greater, therefore the following expression must be used to calculate the tension force in the reinforcement in the principal reinforcement direction:

$$Z_I = N_I + \frac{N_I - N_{II}}{2} \cdot sin(2 \cdot \pi) \cdot (1 - tan(\alpha)) \quad \left[\frac{kN}{m}\right] \tag{2.79}$$

and in the cross reinforcement :

$$Z_I I = N_{II} + \frac{N_I - N_{II}}{2} \cdot sin(2 \cdot \pi) \cdot (1 - tan(\alpha)) \quad \left[\frac{kN}{m}\right] \tag{2.80}$$

The compression force in the concrete is equal:

$$D_C = (N_I - N_{II}) \cdot sin(2 \cdot \pi) \quad \left[\frac{kN}{m}\right] \tag{2.81}$$

also the equlibrium must be kept:

$$Z_I + Z_{II} - N_I - N_{II} \quad \left[\frac{kN}{m}\right] \tag{2.82}$$

Now, the necessary amount of reinforcement can be calculated easily if the steel stress of the rebars is given. In this example it is:

$$\sigma_{sd}$$

- which is the steel tensile stress divided by 1.15 => ex: 550 MPa / 1.15 = 480

The necessary amount of reinforcement in the principal reinforcement direction will be:

$$a_{sI} = \frac{Z_I}{\sigma_{sd}} \quad \left[\frac{cm^2}{m}\right] \tag{2.83}$$

The necessary amount of reinforcement in the cross reinforcement direction:

$$a_{sII} = \frac{Z_I I}{\sigma_{sd}} \quad \left[\frac{cm^2}{m}\right] \tag{2.84}$$

This lever arm is used to calculate the virtual panel forces in direction of the local element coordinate system on each side of the finite area element:

$$N_{xx} = \frac{n_{xx}}{2} - \frac{m_{xx}}{z_u} \quad \left[\frac{kN}{m}\right] \tag{2.85}$$

$$N_{yy} = \frac{n_{yy}}{2} - \frac{m_{yy}}{z_u} \quad \left[\frac{kN}{m}\right] \tag{2.86}$$

$$N_{xy} = \frac{n_{xy}}{2} - \frac{m_{xy}}{z_u} \quad \left[\frac{kN}{m}\right] \tag{2.87}$$

The next step is the transformation of the local panel forces into principal panel forces :

$$N_I = \frac{N_{xx} + N_{yy}}{2} + \frac{\sqrt{(N_{yy} - N_{xx})^2 + 4 \cdot N_{xy}^2}}{2} \quad \left[\frac{kN}{m}\right] \tag{2.88}$$

$$N_{II} = \frac{N_{xx} + N_{yy}}{2} - \frac{\sqrt{(N_{yy} - N_{xx})^2 + 4 \cdot N_{xy}^2}}{2} \quad \left[\frac{kN}{m}\right] \tag{2.89}$$

Let us calculate the design compression stress in the concrete:

$$f_{cd} = \frac{N_{II}}{x} \quad \left[\frac{N}{mm^2}\right] \tag{2.90}$$

Since it is smaller the the compression stress limit of the C 45 concrete :

$$f_{Rd} = \frac{f_{cd} \frac{N}{mm^2}}{1.5} \quad \left[\frac{N}{mm^2}\right] \tag{2.91}$$

3

Study Case

This chapter presents an introduction to the software used in the project, along with a description of the two scripts that were used to formulate the Frame and the Shell culvert models. The chapter will also provide an overview of the initial structure used to prepare the programs and verify that both were executing the same analysis. The aim of this chapter is to provide the reader with a better understanding of the software tools used in the project, as well as to highlight the importance of ensuring consistency and accuracy in the analysis of culvert structures.

3.1 SOFISTIK

To understand how the assignment was carried out, it is essential first to introduce the program used for the analysis, *SOFISTIK*, which is a software produced by *SOFISTIK AG*.

SOFISTIK is a commercial powerful FE-software that specializes in structural analysis. It allows the user to access the commands through a simple script language, allowing to make generalized templates in terms of scripts. This program does extensive and efficient structural analysis and offers accurate solutions, providing a comprehensive set of tools for analysis and design. Therefore, its popularity among engineering and consulting firms is growing. The software provides users with multiple analysis methods, including pre-defined options, graphic interfaces, and coding-based user interfaces, which allow for the analysis of complex and intricate problems. Additionally, *SOFISTIK* has a number of characteristics that make it a viable tool for a wide range of engineering applications. Comprehensive analytical capabilities for concrete, steel, and timber structures, as well as bridges and tunnels. Moreover, the program has dynamic and seismic analysis options, as well as non-linear analytical capabilities.

The software is composed of various modules, each performing different tasks. At the core of the *SOFISTIK* analysis program is the Central Data Base (CDB), which acts as a hub for all of the program's modules. This centralization allows for seamless integration between the different modules, making it easy for users to work with multiple programs at once. *SOFISTIK's* modules can be accessed through standard text files or graphical user interfaces, providing flexibility for users with different preferences. By utilizing the CDB, users can open multiple programs with different windows that can easily exchange information and access the same database. In addition to its various modules, each individual module comes with a comprehensive manual that provides theoretical background and detailed descriptions for all possible input and output from the module (Figure 10). This makes it easier for users to understand and utilize the full potential of each module within *SOFISTIK*.

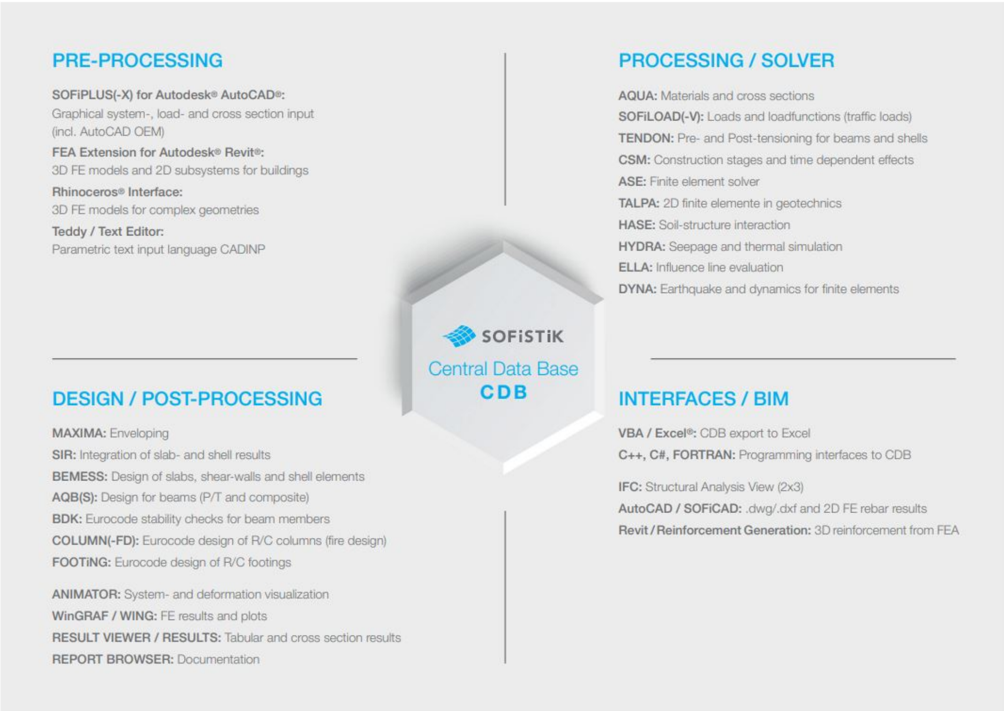

Figure 10: Different modules in SOFISTIK

SOFISTIK Structural Desktop (SSD) represents a uniform user interface for the total range of *SOFISTIK software*. It is the module that controls the complex interaction between all the modules and interfaces, from pre to post-processing. It is the work environment for the user to navigate between text input files and graphical interfaces. The entire project is organized within SSD. Figure 11 is an example of the SSD used in one of the models in this work.

The software is highly flexible in the sense that the user determines the preferred form of input, the modules to use, and the type of output provided by the program. The user is only restricted by minimal obligations in a sequence of analysis.

The user has the option to input data into the software through either graphical or text-based interfaces. For the graphical input, *SOFISTIK* provides *SOFIPLUS*, an AutoCAD-based system, which allows the user to define the geometry and load values of the structure in a CAD-environment. For text input, the program *"Teddy"* is used. This text editor can be accessed through the embedded

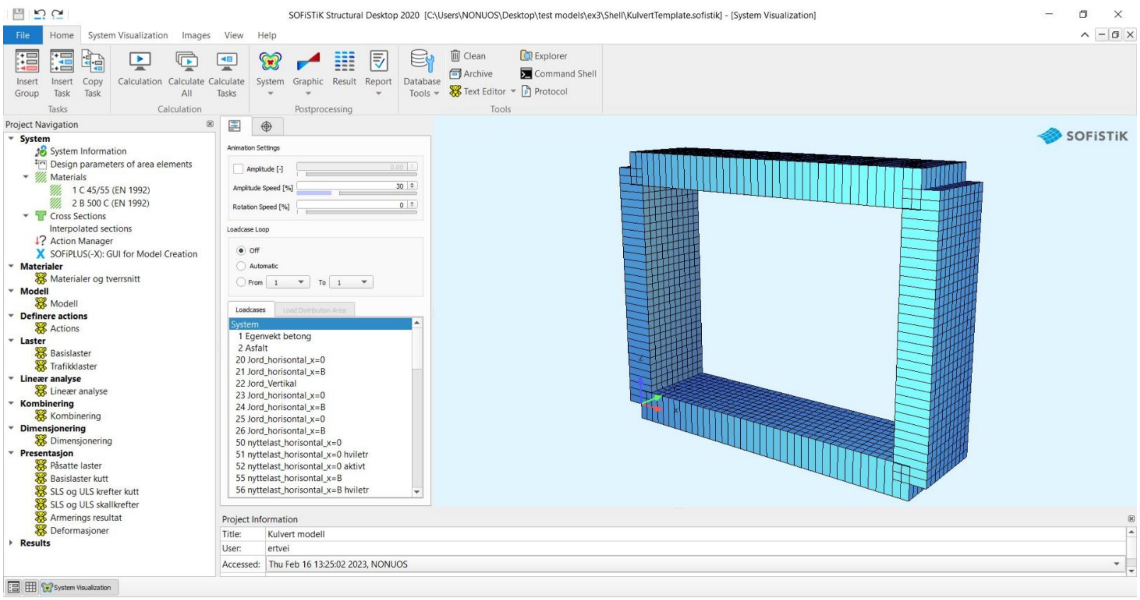

Figure 11: SOFISTIK Structural Desktop

version in the SSD or in the standalone application. It allows the user to perform tasks through programming code in *Teddy's* specific programming language, CADINP-command language. This is the most powerful, versatile, and direct method to use the software. Both the graphical and *Teddy* input tasks can be accessed and organized through the SSD.

In Figure 12 it is represented a simple scheme of the organisation and operating structure of the *SOFISTIK* software:

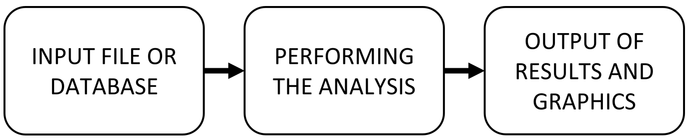

Figure 12: SOFISTIK Structure

As previously stated, the input files for the pre-processing can be obtained through *SOFIPLUS* or *Teddy*, or both. This stage corresponds to the modelling of the structure, in which the user introduces the software characteristics such as materials, cross-sections, geometries and loading. Furthermore, during this stage, the program *SOFIMESH* is used to generate the analysis system, the mesh for the FEA, for the structure under analysis. The total number and the type of elements are permanently defined here. However, the structure can be divided into groups, and the analysis can be performed on only one member of the structure.

The processing stage corresponds to the performance of the analysis. This analysis is conducted through the SSD, where the program reads the input provided by the user and executes the tasks. These tasks can include different analyses such as linear, non-linear, and thermal, among others.

The post-processing step corresponds to the design stage, where the program provides the results of the tasks requested by the user. The results can be in the form of graphics, figures, tables, etc.

Figure 13 represents the workflow of the analysis of the Frame model (on the left) and the Shell model (on the right). This diagram is commonly referred to as the *"task tree"*, where each task is presented and users can insert, delete and organize tasks intended for the analysis. The calculation status of each task is also shown in the task tree, with the corresponding Figure 14 denoting the possible status and its respective meaning.

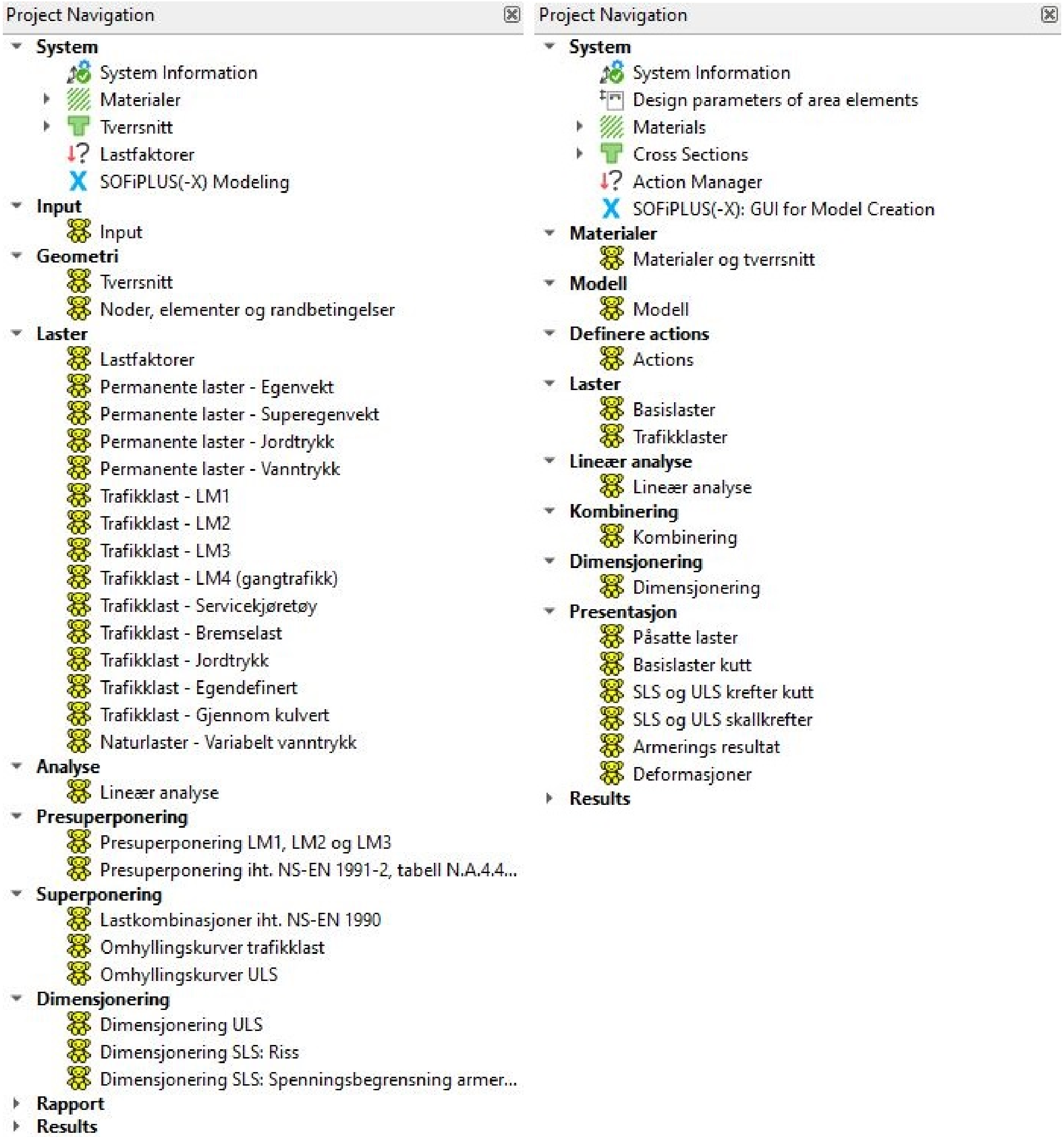

Figure 13: Workflow from the Frame model (left) and Shell model (right)

Icon overlay	Description
none or blank	input is written directly to CDB
	no calculation required
	error message → calculation required
	warning message → calculation required

Figure 14: Status of the task (AG, 2023)

3.2 Introduction to Scripts

This section provides an introduction to the two programs used for designing culverts.

For the design of a box culvert, engineers at *Sweco* can use two different models: a Frame model and a Shell model. Since the two programs were developed by different people, they present different formulations and have different functionalities. Therefore it is important to provide an overview of how both of them work.

3.2.1 Frame model

In the case of the program that performs the design of the culvert as a Frame, the tasks are written directly in the embedded version of *Teddy*.

The initial task, named "input" (Figure 13), is where the user provides the main characteristics of the culvert, such as the category of material chosen, diameter of the steel bars and the thickness of the concrete cover, as well as characteristics of the earth pressure, This task also comprises the possibility to select which load cases are going to be active in the model, between traffic loading, water pressure or by assigning the logical value of 1 or 0 to the respective variables. In this task, the variables are defined with the command *"STO"* which means that the corresponding value will be saved to the database, being valid for every task that comes afterwards and using that variable.

```
$--------------------------------------------------------------------------------------
sto#bkulv_i 3.6                 $ Indre bredde kulvert [m].
sto#hkulv_i 2.7                 $ Indre høyde kulvert  [m].
sto#hsaale 0.6                  $ Sålehøyde [m] Betydning kun hvis ktype = 3.
sto#hoverfylling_v 1            $ Høyde overfylling, venstre [m].
sto#hoverfylling_h 1            $ Høyde overfylling, høyre [m].
sto#hoppfylling 0               $ Masser over bunnplate [m]. Ingen betydning hvis ktype = 3.
$--------------------------------------------------------------------------------------

$ Generelle tverrsnittverdier
$--------------------------------------------------------------------------------------
sto#overdekning 75              $ Overdekning [mm].
sto#cc_avstand 0.15             $ Senteravstand minimumsarmering eller valgt senteravstand [m]
sto#betongkvalitet 45           $ B45 = 45 eller B35 = 35?
$--------------------------------------------------------------------------------------

$ Tverrsnitt vegg     parede
$--------------------------------------------------------------------------------------
sto#htverr_v_b 0.4              $ Tverrsnittshøyde vegg, bunn [m].
sto#htverr_v_m 0.4              $ Tverrsnittshøyde vegg, midt [m].
sto#htverr_v_t 0.4              $ Tverrsnittshøyde vegg, topp [m].
sto#d_min_armeringv 16          $ Beregningsmessig diamteter minimumsarmering eller valgt arme
sto#d_min_armering_bv 21        $ Byggemål diamteter minimumsarmering eller valgt armering i b
```

Figure 15: Input file in the Frame script

All the tasks that appear after the input file are written in function of the variables defined in the input page.

3.2.2 Shell model

On the other hand, in the case of designing the culvert as a Shell, a different approach is taken. An external softare was developed where the user provides information to a template (Figure 16), which then generates Teddy files. These files are saved in the same folder as the *SOFISTIK* file, and each task in the program is set to read the respective *Teddy* file.

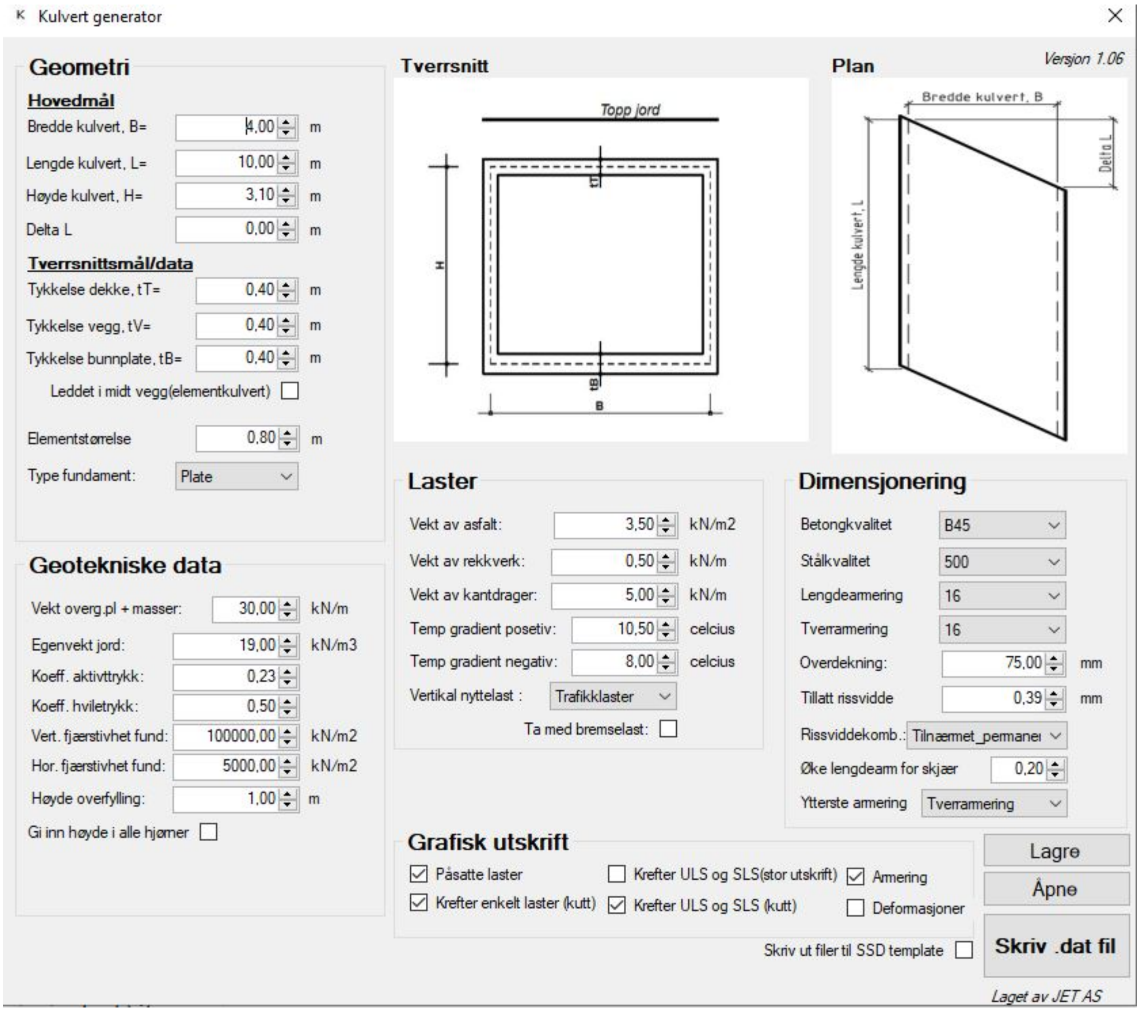

Figure 16: Template to generate Teddy files

While the template makes it easier for the user to generate a culvert, its characteristics are predefined in a generalized way. If the project requires more specific characteristics, it is necessary to edit the *Teddy* files as needed.

3.3 Models Setup

The initial programs that were provided to perform the work of this thesis have different formulations because they were developed by different people. Although both of them are used to design a concrete culvert, they differ in many aspects, from input to output.

To perform the comparative analysis, it was crucial to make sure that they were evaluating the same structure and producing the same outputs. To achieve this goal, the initial task was to create a reference geometrical model of the culvert which was used as the basis for both programs. Then, several trial-and-error attempts were made to adjust both models until they produced identical results.

This section has presented an explanation of the model used and the process for completing this task.

3.3.1 Material selection

The culvert in the analysis is made of reinforced concrete. Therefore, one of the initial steps was to select the appropriate material categories for both concrete and steel.

The *SOFISTIK* program provides a material database that offers a wide range of material types and classifications. Once these variables are defined, the program generates the corresponding properties in accordance with EC specifications. However, it is also possible to make manual modifications to these properties. Hence, it was necessary to guarantee that all of the properties would match to ensure consistency between the models being compared.

Firstly, the concrete category used was C45/55. The properties of this material are presented in the following tables:

Table 1: Concrete C45/55 Properties

Property	**Symbol**	**Value**	**Units**
Self weight	γ	25.0	kN/m3
Density	ρ	2400	kg/m3
Elastic Modulus	E	36283	N/mm2
Poisson ratio	μ	0.2	-
Shear modulus	G	15118	N/mm2
Compression Modulus	K	20157	N/mm2

Concrete C45/55 has the following strength values:

Table 2: Concrete C45/55 strength values

Property	Symbol	Value	Units
Effective strength	f_{cd}	38.25	MPa
Tensile strength	f_{ctm}	3.80	MPa
Lower fractile value of tensile strength	$f_{ctk,0.5}$	2.66	MPa
Fatigue strength	$f_{cd,fat}$	20.91	MPa
Design bond strength	f_{bd}	3.99	MPa
Mean strength	f_{cm}	53.0	MPa
Modules of Elasticity for service	E	38097	N/mm2
Design tensile strength	f_{td}	1.51	MPa

In terms of steel for the reinforcement, B500 steel was chosen with the following properties:

Table 3: Steel B500 Properties

Property	Symbol	Value	Units
Self weight	γ	78.5	kN/m3
Density	ρ	7850	kg/m3
Elastic Modulus	E	200000	N/mm2
Poisson ratio	μ	0.3	-
Shear modules	G	76923	N/mm2
Compression modules	K	166667	N/mm2

Steel B500 has the following strength values:

Table 4: Steel B500 strength values

Property	Symbol	Value	Units
Yield strength	f_y	500	MPa
Tensile strength	f_t	575	MPa
Compressive strength	f_{tc}	575	MPa
Compressive yield strength	f_{yc}	500	MPa
Ultimate strain	-	75.0	permil
Elastic limit	-	500.0	MPa

3.3.2 Structure Geometry

After selecting the appropriate materials, the next step is to define the geometry of the culvert. A homogeneous thickness of 0.4 meters was chosen for both the vertical and horizontal elements of the reference model.

In the Frame file, the thickness of the elements can vary. The user can input different thicknesses for the top, middle, and bottom of the walls, as well as for the edges and the middle of the top and bottom surfaces. However, in the Shell file, only a single thickness can be attributed to each element. So, for consistency, the same thickness was used for all elements in both programs.

The initial model was designed with a length of 1 meter for the culvert since the Frame program is configured to design the culvert with this specific length. In the civil engineering industry, it is usual for consultancy companies to calculate the structure by the meter of length and then extrapolate the results to the entire length of the structure. This approach assumes that the meter used as a reference is the most heavily loaded. Therefore, the amount of reinforcement used in the whole length will also be for this case, even in areas of the structure that may not require as much reinforcement.

This approach leads to excessive use of materials in the structure, as the reinforcement calculations are based on the assumption that the entire structure will experience the same maximum loading as the one-meter reference section, which may not be the case for the entire length of the structure. Nonetheless, it is justified to use this approach due to the significant reduction in workload for the designing team, whose work is to calculate a single portion of the structure, instead of several portions with different loading. Moreover, it is also beneficial for the construction team as they can use the same plant for the entire structure, reducing the possibility of misinterpretations of the project. This approach results in a reduction of time and labour costs for both the design and construction teams.

As already explained, since it was crucial to have both the Frame and the Shell model with the same geometries, the length of the Shell model was also set to one meter. Finally, it is important to mention that comparing a one-meter Frame model with a Shell culvert of the same length could lead to different behaviours due to the Shell effects. Figure 17 shows a schematic example of a culvert model.

Nonetheless, it will be demonstrated later that this will not be an issue.

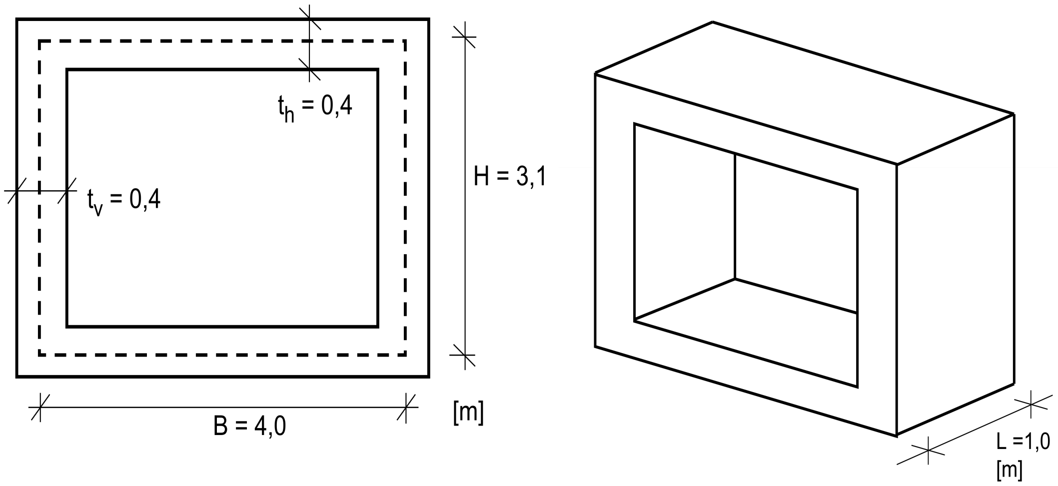

Figure 17: Cross-section (left) and perspective view (right) of the culvert model

As previously stated, the software used for the structural analysis allows for the division of the structure into groups, which is a common feature of most structural analysis software programs. The ability to divide the structure into groups can be beneficial as it enables a more efficient and targeted assessment of specific sections of the structure.

By splitting the structure into groups, it becomes easier to make specific changes to one group without affecting the others, such as altering the material properties or cross-sectional dimensions of one group without influencing the rest of the structure.

Furthermore, defining loads directly into a certain group can help in studying the behaviour of that group under specific loading conditions without taking the rest of the structure into account. Splitting the structure into groups can also simplify the analysis by reducing the number of components that need to be studied, thereby saving processing time and increasing the efficiency of the study. Figure 18 shows an example of the division into groups of Frame *Vs* Shell.

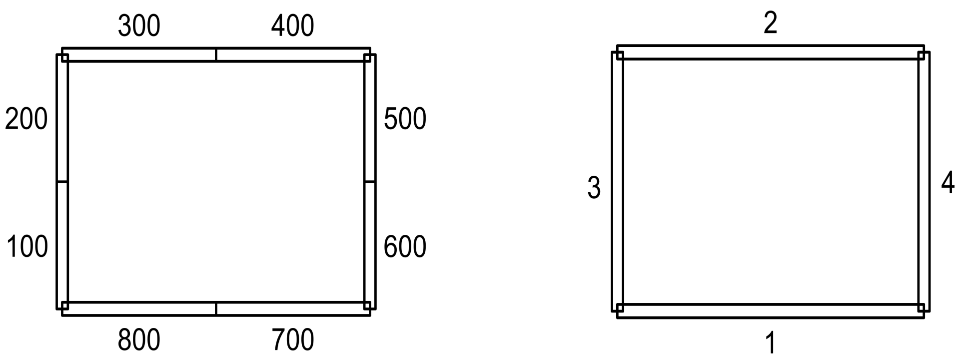

Figure 18: Division of the Frame (left) and the Shell (right) into groups

3.3.3 Mesh

SOFISTIK is a Finite Element Analysis software. An essential step in performing FEA is to deconstruct the structure into a mesh of small elements. The mesh generation is an automated process performed by the *SOFIMSH-C* module, which is responsible for generating the finite elements. This module analyses, processes and describes the entered information of the structural elements. Here, structural lines are defined by their endpoints and structural surfaces by a closed sequence of structural edges.

The description of the structural elements is followed by the creation of the actual finite elements, which will be quadrilateral elements.

First, a triangular mesh is generated for the entire model. These triangles will serve as the basis for building the quadrilateral elements. Figure 19 represents the process of transforming the triangular mesh into a quadrilateral mesh. The basic idea is to replace two triangular elements with four new quadrilateral elements. Taking as an example a square slab, the first step is to divide it into triangular elements. The size of these elements depends on whether they are automatically defined by the program, based on the size of the structure, or manually defined by the user. The disposition of the mesh is always generated by the module.Next, the pair of triangles is replaced by four quadrilateral elements. If there are any leftover triangular elements, they will be transformed into three quadrilateral elements. Once all the triangular elements are converted to quadrilaterals, a node relaxation process takes place to ensure a homogeneous, high-quality mesh with more consistent element sizes (as it is perceptible in the last phase of figure 19).

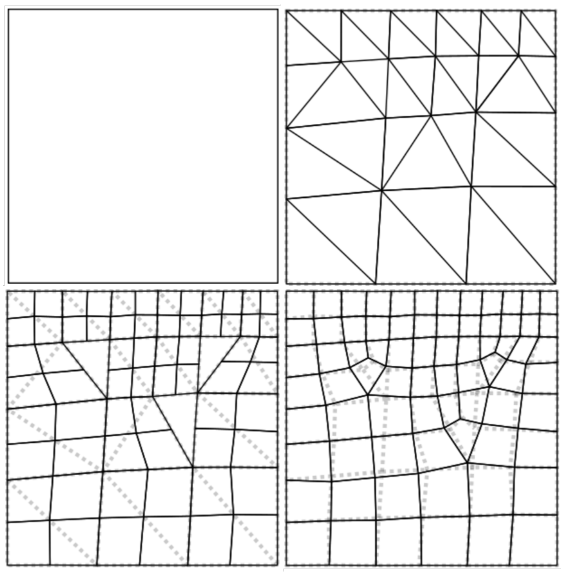

Figure 19: Mesh

It is worth mentioning that it is also possible to create a fully user-defined mesh with the module *SOFIMSH-A* in the text interface *Teddy*.

For both the Frame and Shell models, a mesh size of 10 centimeters was defined, which was generated automatically by *SOFIMSH-C*.

3.3.4 Loading applied to the culvert

In this section, an introduction to the loading applied to the culvert is presented.

The initial loading to consider is the self-weight, which is defined as the weight of the structure itself. In the case of a concrete structure, this comprises the weight of all of the concrete used in its construction, as well as any additional materials used, such as steel reinforcement. It is crucial to consider the self-weight of a structure during the design process, as it significantly affects its overall stability and load-bearing capacity. Engineers must account for the self-weight of the concrete when building a structure to ensure that it is strong enough to support itself and any additional loads that may be imposed on it.

Next, the earth pressure is considered. Given that the structure under analysis is a Culvert, which is an underground structure, it is essential to consider the soil-structure interaction. Earth pressure is the pressure exerted by soil or earth on a structure when they are in contact. Calculating earth pressure accurately is critical for constructing safe and strong structures that can resist pressures imposed by the surrounding soil. Earth pressure is classified into three types: active, passive, and at rest. Estimating earth pressure is an important step in the design of underground structures since it can impact the structure's stability and safety. Therefore, engineers need to carefully consider the soil conditions and other factors when determining the earth pressure for a particular project.

Furthermore, an additional loading that has to be considered is the weight of the embankment. When an underground structure is located beneath an embankment, the weight of the embankment can create substantial pressure on the structure. The pressure value increases with the height of the embankment. Engineers must carefully evaluate this additional load and build the structure accordingly to guarantee the security and cohesion of a subterranean project. When an underground structure, such as a culvert, is put beneath an embankment, the weight of the embankment can create additional loads on the structure. This is due to the weight of the embankment exerting increasing vertical pressure on the structure's top. During the design phase of the structure, it is essential to verify its ability to withstand additional stress.

Another load that was considered in the present analysis is traffic loading. As already established, the culvert under analysis has the purpose of allowing traffic to pass over it while creating a passage through it. Therefore, considering the action of traffic on the culvert is indispensable. The weight and frequency of vehicles moving over a structure can have a major influence on the integrity and safety of the structure. Design codes provide regulations on how to compute traffic loads for various types of structures and vehicles, as well as how to incorporate them into the design process.

Traffic loads correspond to the loading that results from road traffic, consisting of cars, lorries and special vehicles. Vertical and horizontal static and dynamic forces are generated by this loading.

As the traffic Load Models (LM) were calibrated and based on actual traffic data, they accurately reflect the real effects induced by traffic. These loads are calculated according to Eurocode 8 (NS-EN 1991-2:2003), plus Norway's National Annexe (NA: 2010), and these norms count for four types of load models:

- Load Model 1 (LM1): Concentrated and uniformly distributed loads;
- Load Model 2 (LM2): Single axel load applied on specific tyre contact areas;
- Load Model 3 (LM3): Special vehicles and can be considered on request;
- Load Model 4 (LM4): Crowd loading.

To simplify the analysis, a decision was made to consider solely the first two Load Models in the assessment. These LM are the most frequent and significant loads for the structure examination.

Regarding LM1, it accounts for the majority of traffic-induced consequences and is recommended for both global and local verification. According to EC 1991-2, "Traffic loads on bridges", LM1 is intended to cover flowing, congested or traffic jam situations with a high percentage of heavy lorries. It consists of the use of two partial systems:

1. Double axle concentrated loads (tandem system TS);
2. Uniform distributed load (UDL system).

Figure 20 illustrates the distribution of different loads on different lanes, with the respective spacing between tandem systems on different lanes and the dimensions and spacing between the tyre contact areas for this load model.

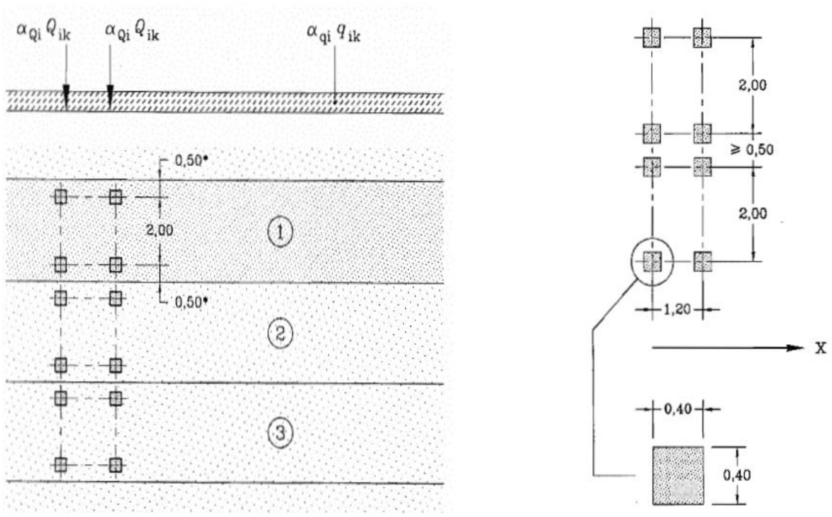

Figure 20: LM1 tandem distribution and tyre contact areas

Additionally, to each traffic lane is attributed a value for the axle system and for the UDL system, which are presented in Figure 21.

Location	**Tandem system *TS***	***UDL* system**
	Axle loads Q_{ik} (kN)	**AC1 q_{ik} (or q_{rk}) (kN/m^2) AC1**
Lane Number 1	300	9
Lane Number 2	200	2,5
Lane Number 3	100	2,5
Other lanes	0	2,5
Remaining area (q_{rk})	0	2,5

Figure 21: Intensity of loading according to lane

On the other hand, LM2 is composed of a single axle load of $\beta_Q \cdot Q\_ak$, with Q_{ak} = 400kN. It is applied on areas that correspond to the contact area of tyres. This load case accounts for the dynamic effects of the normal traffic on short structural members. Figure 22 represents the spacing between tyre contact areas and respective dimensions.

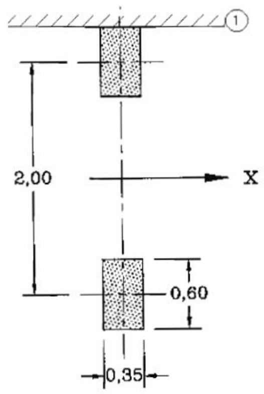

Figure 22: LM2 tyre contact area

3.3.5 Load Cases

This section is explained how each Load Case is defined within the program.

The initial programs for the Frame and Shell models had, by default, different sets of loads defined. Therefore, the initial task in this domain was to identify the corresponding load cases that were already defined and create a matching set of LCs between both scripts. However, there were some LCs that were present in both programs, but it was decided to remove them since their impact on the overall analysis wouldn't be significant. This allowed for shorter running times in the program.

- Concrete self-weight

The Load Case for the self-weight of the concrete is automatically generated using the input provided by the user, such as the concrete class, and uses the corresponding values of that material to calculate the self-weight loading.

To verify that the structure is behaving in the same way, the module *GRAPHIC* was used to plot a visual output of the results. Figure 23 shows the load configuration of the self-weight LC acting on the culvert and the corresponding displacements for both the Frame and the Shell models.

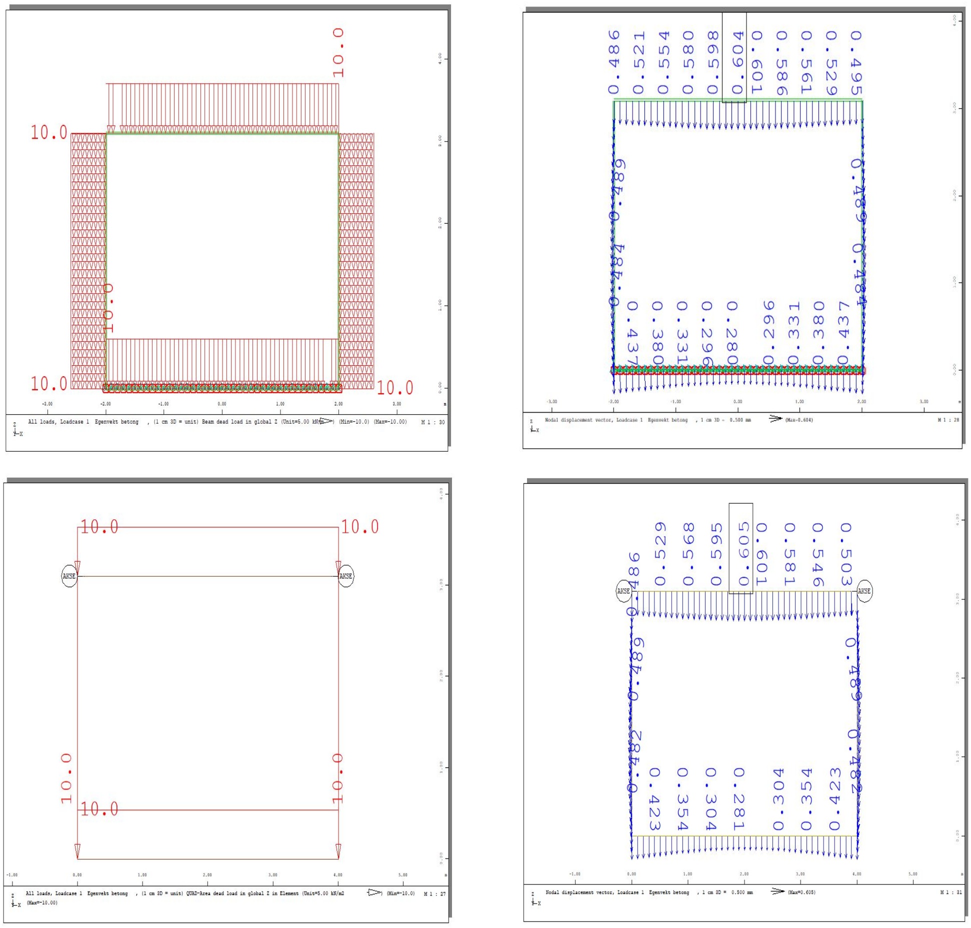

Figure 23: Self-weight load (left) and corresponding displacements (right) - Frame on top and Shell on the bottom

As it is possible to verify by the previous Figures, the displacements resulting from the application of the self-weight are the same in both models. This verification process was repeated for all the LCs and the results are displayed in Appendix A.

- Weight above the culvert

The term "weight above the culvert" is intended to refer to the loading that results from elements placed on the top of the culvert, such as the embankment and the asphalt.

In the initial model, a soil height of 1 meter with and volume weight of 19 kN/m3 was selected for the embankment.

Both programs defined this LC differently. While the Shell model had an individual load case for each element, the Frame model combined the calculation of both loading into the same task using the "superegenvekt" file.

However, the module used for the graphic output allowed to combine two LCs and display the respective displacement of the combination. This way, it was possible to confirm that the sum of displacements of the asphalt loading and the embankment loading in the Shell script corresponded to the "superegenvekt" LC in the Frame script.

- Earth pressure

The loading that results from the Earth's pressure is automatically generated by the program. It is comprised of two initial LC, each of them acting on one side of the culvert, corresponding to the at-rest pressure. Then, a set of four more LCs are defined that correspond to the active and passive pressure, which are a copy of the at-rest LCs with a multiplication factor of 0.5 for the passive and 0.25 for the active earth pressures.

- Traffic loads

The LCs corresponding to traffic loads were the most significant challenge.

In the template used to generate the *Teddy* files for the Shell script, there is an option for traffic loads that, if selected, creates a file with all the necessary loads to perform a complete analysis. However, it was not possible to create the *Teddy* file for a culvert with a length of only 1 meter. Therefore, the LCs had to be manually created.

Figure 24 presents an example of the code made for the loading scheme corresponding to LM1.

```
LC 81 Type 'None' TITL 'LM1 center'  $actual loading scheme
AREA ref QGRP 2 type pg P1 26.0417 X1 0.2 Y1 0.0 Z1 3.1  P2 26.0417 X2 0.2 Y2 0.7 Z2 3.1
                        P3 26.0417 X3 2.6 Y3 0.7 Z3 3.1  P4 26.0417 X4 2.6 Y4 0.0 Z4 3.1
AREA ref QGRP 2 type pg P1 26.0417 X1 0.2 Y1 0.3 Z1 3.1  P2 26.0417 X2 0.2 Y2 1.0 Z2 3.1
                        P3 26.0417 X3 2.6 Y3 1.0 Z3 3.1  P4 26.0417 X4 2.6 Y4 0.3 Z4 3.1
AREA ref QGRP 2 type pg P1 26.0417 X1 1.4 Y1 0.3 Z1 3.1  P2 26.0417 X2 1.4 Y2 1.0 Z2 3.1
                        P3 26.0417 X3 3.8 Y3 1.0 Z3 3.1  P4 26.0417 X4 3.8 Y4 0.3 Z4 3.1
AREA ref QGRP 2 type pg P1 26.0417 X1 1.4 Y1 0.0 Z1 3.1  P2 26.0417 X2 1.4 Y2 0.7 Z2 3.1
                        P3 26.0417 X3 3.8 Y3 0.7 Z3 3.1  P4 26.0417 X4 3.8 Y4 0.0 Z4 3.1
```

Figure 24: Code made for LM1

The loading was created according to the specifications of EC. Four loads of 150 kN were applied at the level of the surface of the embankment. Each load was applied along the surface corresponding to the tyre contact area (40x40). Then, the angle of dispersion of the load was defined as 45º according to EC. The intensity of the loading to be spread along the area of the culvert was:

$$150/(0.4+2*1)^2 = 26.0417$$

Each line "AREA" on the code represents the squared area loading of one tyre in the structure. The command "ref" attributes the loading to group 2, which corresponds to the top surface of the culvert. The term "type pg" indicates that the direction of the loading is the direction of gravity. P# is the value of the loading acting on that specific point, with "#" being one of the corners of the square. Lastly, the following X, Y and Z are the coordinates in space of that corner. These coordinates were calculated by hand taking into consideration the location of the tyre pressure and the dispersal ratio.

Nevertheless, after performing the analysis of the structure with this LC, it was concluded that the displacements of both models were not equal (Figure 25).

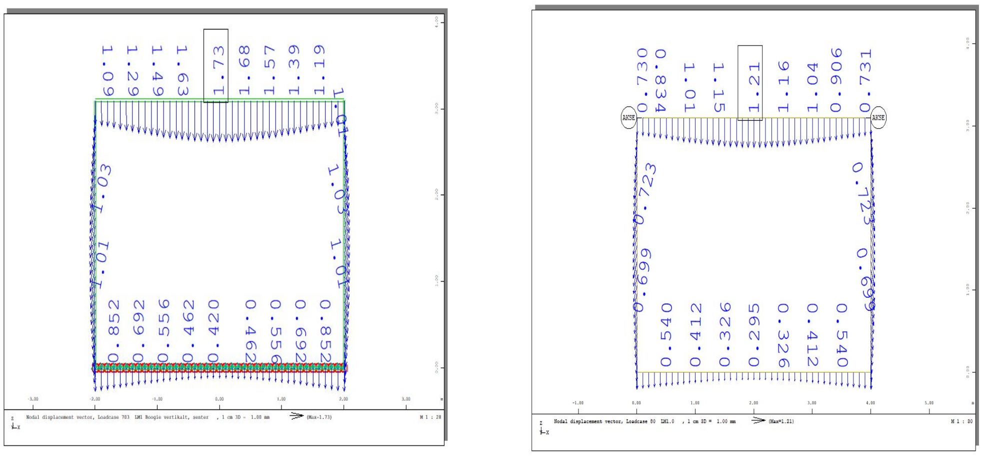

Figure 25: Displacement of the Frame model (left) and the Shell model (right)

The justification for this disparity relies on the fact that Frame models do not consider surface loading. In the Shell model, each tyre load has a designated area of action, but when two or more tyres overlap, the loads are superimposed. Consequently, the corners of the culvert experience a loading of 26kN, the middle of the edges 26*2 = 52 kN and the centre of the structure experience 26*4 = 104 kN.

On the other hand, since the Frame model is a planar model, the loading will only act in the centre of gravity of the elements. Therefore, it is assumed that the beam is subjected to two tyre loads of 52kN each. Consequently, the places of the structure that were loaded with only 26kN in the Shell would be, in the Frame, subjected to twice the load, resulting in increased displacement.

In order to validate this argument, assuring that the different behaviour is due to the different elements and not an error of the code, a different load case was created for the Shell model to mimic the Frame model's loading assumption (Figure 26).

```
LC 80 Type 'None' TITL 'LM1.0'  $for same displacement as in frame model
AREA ref QGRP 2 type pg P1 52.083333 X1 0.2 Y1 0.0 Z1 3.1  P2 52.083333 X2 0.2 Y2 1.0 Z2 3.1
                        P3 52.083333 X3 2.6 Y3 1.0 Z3 3.1  P4 52.083333 X4 2.6 Y4 0.0 Z4 3.1
AREA ref QGRP 2 type pg P1 52.083333 X1 1.4 Y1 0.0 Z1 3.1  P2 52.083333 X2 1.4 Y2 1.0 Z2 3.1
                        P3 52.083333 X3 3.8 Y3 1.0 Z3 3.1  P4 52.083333 X4 3.8 Y4 0.0 Z4 3.1
```

Figure 26: LM1 for the Shell with the same displacement as the Frame

The previous LC induced in the Shell model the displacement shown in Figure 27:

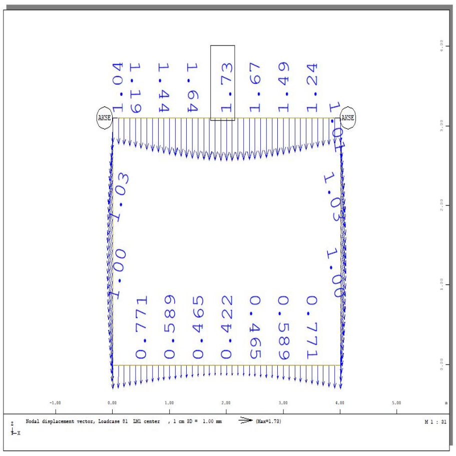

Figure 27: LM1 for the Shell with the same displacement as the Frame

With the previously presented process, one of the main differences in the behaviour of both models can be concluded. Frame and Shell models behave similarly when subjected to area loads that vary only along the x-axis. However, if the variation is along the y-axis, these models will react to the loads differently. In the case of the Frame, the load will be transformed into a uniform load along the y-axis, misrepresenting the real loading. Therefore, it is expected to obtain different outcomes for other LCs that present the same variations along the y-axis.

The same process was done for LM2, with two different LCs being created, one to obtain the real displacement and the other to replicate the displacement of the Frame model.

3.3.6 Partial safety coefficients

Table 5 presents the partial safety coefficients used for the respective LCs:

Table 5: Partial safety factors

Action	**Description**	**γ-u**	**γ-f**	**γ-a**	**Ψ_0**	**Ψ_1**	**Ψ_2**	**Ψ_1INF**
G_1	*Self-weight*	1.35	1.00	1.00	1.00	1.00	1.00	1.00
G_2	*Weight above culvert*	1.35	1.00	1.00	1.00	1.00	1.00	1.00
GR_1	*Traffic loads*	1.35	1.00	0.00	0.70	0.70	0.20	0.80
GR_2	*Earth pressure*	1.35	0.00	0.00	0.70	0.70	0.20	0.80

3.4 Reaction forces

In order to establish that the models are equivalent, meaning that they exhibit the same overall behaviour in response to the set of LC's defined, and in addition to ensuring matching displacements for the individual LC's, another verification must be carried out.

The applied loads result in reaction forces on the structure. If both structures have equal geometry and are subjected to the same set of loads, then the reaction forces for each individual load case should also be the same. Figure 28 presents the comparison between the reactions of Frame and Shell.

LC	LC-title	RX [kN]	RZ [kN]
1	Egenvekt betong	0.0	142.0
2	Superegenvekt	0.0	90.0
5	Jordtrykk høy-lav	-40.5	0.0
6	Jordtrykk lav-høy	40.5	0.0
701	LM1 Boogie vertikalt, venstre	0.0	250.0
702	LM1 Boogie vertikalt, høyre	0.0	250.0
703	LM1 Boogie vertikalt, senter	0.0	250.0
710	LM1 vertikalt, UDL	0.0	36.0
801	LM2 vertikalt, venstre	0.0	153.8
802	LM2 vertikalt, høyre	0.0	153.8
803	LM2 vertikalt, senter	0.0	153.8

	LC	LC-title	RZ [kN]	RX [kN]	RY [kN]
1	1	Egenvekt betong	142.0	0.0	0.0
2	2	Asfalt	14.0	0.0	0.0
5	22	Jord_Vertikal	76.0	0.0	0.0
6	23	Jord_horisontal_x=0	0.0	-40.5	0.0
7	24	Jord_horisontal_x=B	0.0	40.5	0.0
10	80	LM1.0	250.0	0.0	0.0
11	81	LM1 center	175.0	0.0	0.0
12	82	UDL LM1	36.0	0.0	0.0
13	83	LM2.0 center	153.8	0.0	0.0
14	84	LM2 center	123.1	0.0	0.0

Figure 28: Reactions from the Frame (left) and from the Shell (rigth)

Based on the Figure, taken from the *SOFSISTIK* software, it is possible to conclude that the reaction forces match and therefore it is possible to proceed the analysis.

4

Parametric Study and Discussion of Results

This chapter provides the parametric analysis conducted on the two culvert design models: Frame and shell.

Here, a parametric study is carried out to investigate the impact of various design parameters on the structural behaviour of the culvert and to gain a better understanding of the performance of the culvert under loading. This analysis entails changing geometrical design factors and comparing the outcomes of the two models to have a better idea of when using one design method over the other. The most advantageous model will then be chosen after comparing and evaluating the results from the two models.

4.1 Variation of culvert geometry

To perform the parametric analysis, three key parameters were selected: the length and width of the culvert and the height of the embankment. These variables were chosen over others as they were expected to have a significant influence on the structural behaviour of culverts.

The values of the dimensions used, expressed in meters, are presented below:

$$\text{Variation of Length} = \left\{1;2;4;8\right\}$$

$$\text{Variation of Width} = \left\{3;5;10\right\}$$

$$\text{Variation of Height} = \left\{1;3;5;10\right\}$$

As mentioned earlier, since the Frame model is set at a constant length of one meter, only the other parameters were altered, resulting in 12 variations of the Frame culvert. In the case of the Shell model, all three parameters were combined, leading to the creation of 48 models.

The collection of 60 parametric models constitutes a comprehensive dataset for the analysis of concrete culverts. It encompasses a wide range of design scenarios and offers valuable insights into culvert behaviour under different conditions.

4.2 CREATION OF THE MODELS

Instead of using a single model and modifying the design parameters, 60 distinct models were generated.

By employing multiple models, it is possible to analyse the structural behaviour of culverts under various design scenarios and compare the results. Furthermore, by establishing different models for each design parameter combination, the need to continually revise a single model is reduced, as is the possibility of mistakes or inconsistencies in the modelling process.

This method also enables the precise isolation and examination of the impacts of each design parameter on the structural behaviour of the culverts.

Therefore, to create the Frame models, the input file described in chapter 3 was duplicated, and the dimensions of the culvert were changed directly on the input page. For the Shell models, the template was used to generate the Teddy files that would define the whole structure. However, as explained previously, only some of them were used, in combination with the ones that had previously been altered.

Table 6 presents the models and respective naming systems:

Table 6: Name attribution for each model

Frame	Shell			
	Length = 1	Length = 2	Length = 4	Lenght = 8
L1W3H1	L1W3H1	L2W3H1	L4W3H1	L8W3H1
L1W3H3	L1W3H3	L2W3H3	L4W3H3	L8W3H3
L1W3H5	L1W3H5	L2W3H5	L4W3H5	L8 W3H5
L1W3H10	L1W3H10	L2W3H10	L4W3H10	L8W3H10
L1W5H1	L1W5H1	L2W5H1	L4W5H1	L8W5H1
L1W5H3	L1W5H3	L2W5H3	L4W5H3	L8W5H3
L1W5H5	L1W5H5	L2W5H5	L4W5H5	L8W5H5
L1W5H10	L1W5H10	L2W5H10	L4W5H10	L8W5H10
L1W10H1	L1W10H1	L2W10H1	L4W10H1	L8W10H
L1W10H3	L1W10H3	L2W10H3	L4W10H3	L8W10H3
L1W10H5	L1W10H5	L2W10H5	L4W10H5	L8W10H5
L1W10H10	L1W10H10	L2W10H10	L4W10H10	L8W10H10

4.3 Load Model loads

Precisely defining the traffic loads for all of the Shell models, despite being a time-consuming operation, was critical to ensure the analysis's validity. It was necessary to assure that both Frame and Shell would be subjected to the same traffic loading, so the models' structural behaviour was appropriately simulated and the comparison feasible.

The definition of the LCs referring to traffic loading involved manually configuring the LC for each traffic load, for each model. Given the number of different models, it was necessary to make this process more efficient, avoiding the need to calculate and input every value manually for the coordinates of the applied loads and respective intensity. Hence an excel sheet was used which will be presented in this section.

To accomplish this task, it was essential to establish a standardized system for the placement of traffic loads on the culvert surface, regardless of geometry. It was determined that the traffic lane would be positioned in the middle of the culvert's length to ensure consistency across all models.

To determine the position of the loads on the culvert surface, a reference point was required (Figure 30). For the centre LM loads, the geometrical centre of the culvert's surface, C, was selected as the reference point. This approach ensured that the analysis was performed with a consistent and standardized method across all models.

$$C = \left(\frac{Wc}{2}; \frac{Lc}{2}\right) \tag{4.1}$$

The methodology presented defines the coordinates of the tandem system for LM1. To calculate LM2, the same process was followed.

LM1 comprises four loads (F in Figure 30), each with a value of 150 kN, arranged in a square position with a spacing of 1.2 meters along the x-axis and 2 meters along the y-axis (Figure 29).

To obtain the coordinates for the application point of each load Q on the surface of the embankment, half of the spacing between loads were added or subtracted to their respective coordinate, starting from point C. The contact area of each tyre is given by $a \cdot b$, where in the case of LM1, it is 0.4 meters by 0.4 meters.

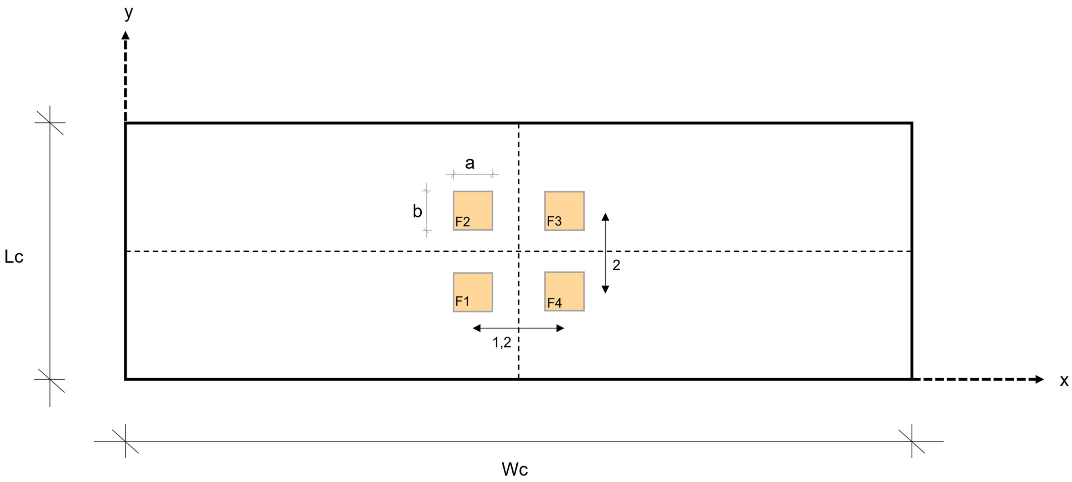

Figure 29: LM top view

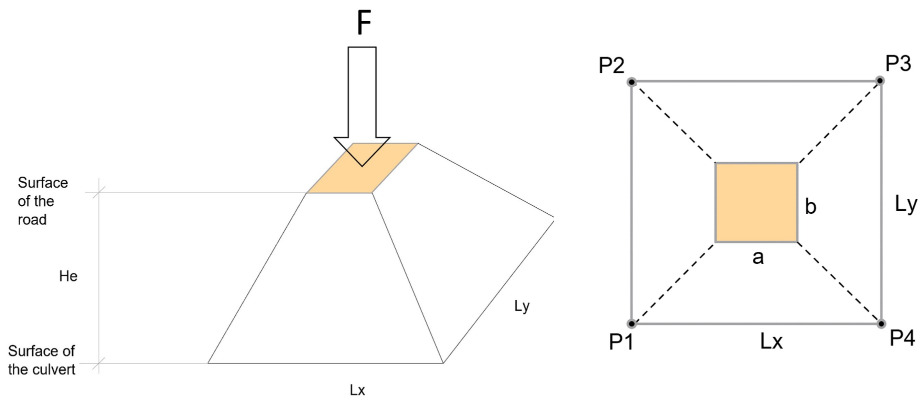

Figure 30: Spread ratio (left) and coordinates (rigth) of LM1

The spread ratio of the LM loads is 45º, therefore the load distribution over the surface of the culvert is calculated based on the embankment height (He) and the dimensions of the area load along the indexed axis (Lx and Ly):

$$Lx = 2 \cdot He + a \tag{4.2}$$

$$Ly = 2 \cdot He + b \tag{4.3}$$

Using the dimensions of Lx and Ly, the coordinates of the area load applied on the surface of the culvert (P1, P2, P3 and P4) could be determined. Furthermore, the intensity of the load at the level of the culvert is calculated by dividing F by the area $Lx \cdot Ly$ (Figure 53 and 32).

$$Q = \frac{150}{Lx \cdot Ly} \tag{4.4}$$

	INPUT
Lc	1
Wc	3
He	1
Hc	3.1

Center C	
x	y
1.5	0.5

LM1	
Q	150
a	0.4
b	0.4

		overlap
Lx	2.4	1.2
Ly	2.4	0.4
Q/m2	26.0417	

LM2	
Q	200
a	0.35
b	0.6

		overlap
Lx	2.35	
Ly	2.6	0.6
Q/m2	32.7332	

Figure 31: Input data

	LM1	P1		P2		P3		P4	
	1st L	x	y	x	y	x	y	x	y
Center	F1	-0.30	-1.70	-0.30	0.70	2.10	0.70	2.10	-1.70
	F2	-0.30	0.30	-0.30	2.70	2.10	2.70	2.10	0.30
	F3	0.90	0.30	0.90	2.70	3.30	2.70	3.30	0.30
	F4	0.90	-1.70	0.90	0.70	3.30	0.70	3.30	-1.70

Figure 32: Coordinates of LM1 central load

As previously mentioned, the traffic loading under analysis in this project consists of LM1 and LM2. In order to accurately model the loading of the culvert, it was necessary to apply these loads not only at the centre of the culvert but also at the edge. To ensure symmetry of loading, two extra LCs were created for each LM. One LC was placed on the left side and the other on the right side of the culvert, along the road. The purpose of adding these LCs was to replicate the passage of traffic on the road and evaluate the respective loading in the culvert. This extra loading would induce the maximum shear.

Once all the values for coordinates and intensities for the six LCs corresponding to LM1 and LM2 were obtained, the LC code for the Teddy file needed to be assembled. This code is the one already presented in Figure 24.

4.4 DESIGN LOAD COMBINATION

Structures are designed to meet strength and serviceability requirements. This means that they are designed for the critical (largest) load that can act on them, withstanding the critical (biggest) load that could affect them.

To meet these requirements, design load combinations take into account the possibility of simultaneous occurrence of different types of loads, such as dead loads, live loads, wind loads, earthquake loads, etc. These loads are multiplied by their corresponding load factors according to the design code to obtain the design loads.

The load factors are based on the probability of the occurrence of the respective loads, and they vary with the type of load and the intended level of safety.

Once these design loads are obtained, the designer can determine the required reinforcement for the structure. The reinforcement should be selected such that it can withstand the factored design loads without exceeding the allowable stresses or deflections. The designer then decides the appropriate reinforcement to achieve the desired safety and serviceability requirements.

SOFiSTiK has automated load combinations to allocate the maximum and minimum load for every single element of the structures. Load combinations can be defined through the graphical user interface or the text interface. The module *MAXIMA* is responsible for performing all the combinations and superpositions.

In the present work, the structures were checked and designed to withstand load combinations in the ultimate limit state (ULS) and the Service Limit State was not considered.

The Ultimate Limit State (ULS) is the moment at which a structure has reached its maximum capacity and can no longer carry the loads for which it was built. ULS is normally established by the structure's most critical failure mode. In a concrete column, for example, ULS may be defined by concrete crushing, steel reinforcement buckling, or column collapse caused by bending or shear.

It is essential to guarantee that ULS is not exceeded during the construction's design life. Engineers do this by multiplying the characteristic loads by a factor known as the factor of safety. This multiplier considers a variety of parameters, including the kind of structure, materials utilized, and appropriate design rules and standards.

In ULS, three combination sets are checked using the most unfavourable load case in design. These sets include EQU Global equilibrium, STR/GEO Capacity, and STR/GEO Safety towards soil failure.

The most common ULS load combinations are those with permanent or variable load effects. For critical design conditions, equations 6.10, 6.10a and 6.10b in EC0, equations 4.5, 4.6 and 4.7, respectively, offer alternative load effects that are computed and validated against the structure's capacity. Engineers can verify that the structure can sustain the maximum predicted load and avoid failure by comparing the load effects to the structure's capacity.

$$\sum_{j\geq 1} \gamma_{G,j} * G_{k,j} + \gamma_{Q,1} Q_{k,1} + \sum_{i>1} \gamma_{Q,i} \Psi_{0,i} Q_{k,i} \tag{4.5}$$

$$\sum_{j\geq 1} \gamma_{G,j} * G_{k,j} + \gamma_{Q,1} \Psi_{0,1} Q_{k,1} + \sum_{i>1} \gamma_{Q,i} \Psi_{0,i} Q_{k,i} \tag{4.6}$$

$$\sum_{j\geq 1} \xi_j \gamma_{G,j} * G_{k,j} + \gamma_{Q,1} Q_{k,1} + \sum_{i>1} \gamma_{Q,i} \Psi_{0,i} Q_{k,i} \tag{4.7}$$

4.5 Analysis framework

This section describes the process of analysing all the created models.

As established in chapter 3, Frame and Shell models behave similarly when subjected to area loads that vary only along the x-axis. However, if the variation is along the y-axis, these models will interpret the loads differently. In the case of the Frame, the load will be transformed into a uniform load along the y-axis, misrepresenting the real loading. Due to this, it was expected that, when performing the analysis of the culverts loaded by the whole set of LCs, the behaviour would be different, making the comparison of results difficult to perform.

To mitigate this deviation, and in order to have a reliable comparison term and ensure accurate results, two distinct scenarios were created.

Firstly, the culverts were solely subjected to the LCs corresponding to self-weight, active and passive earth pressure, and the weight of the embankment, which are uniformly distributed. This group of loads will now be referred to as SET1. This scenario allowed for the evaluation of the structural response to the basic loads that the culverts would experience over their lifetime.

In the second analysis, the traffic loads and the weight of the asphalt were added to the previous set of loads, called SET2. This scenario considered the more extreme conditions that the culverts might face during their operational life. By including these additional loads, which also act along the y-axis, the analysis provided a comprehensive evaluation of the structural response to different load cases.

4.6 Performance of the Analysis

Once all necessary load cases were assembled, a linear analysis of the structures subjected to both sets of loads was performed.

The main module of *SOFISTIK* is ASE or Advanced Solution Engine, which is responsible for conducting the Finite Element analysis. This tool performed the general static analysis of the

Finite Element structure and provided the solutions by calculating the effects of general loading on both types of structures.

To ensure a valid comparison between the models, it was crucial to compare the analysed variables in the same location of all structures. Therefore, the centre of the upper face of the culvert was chosen as the reference location.

The module WING provides a graphical representation of the Finite Element Structure. A new window allows the user to see the structure and get useful information for the analysis. This module was used to identify the specific Finite Element located at the defined position and retrieve the respective identification number.

According to the geometry of the culvert, the nodes presented in table 7 were determined to be located at the reference point, and therefore, these were the elements used for the comparison between models.

Table 7: Number of analysed element

	Frame	Shell			
		Length = 1	Length = 2	Length = 4	Length = 8
Width = 3	3000015	20122	20310	20620	21240
Width = 5	3000025	20255	20510	21020	22040
Width = 10	3000050	20505	21010	22020	24040

To display the results effectively, *SOFISTIK* provides RESULT, a Graphical and Tabular Finite Element Post-processing module, which presents several different types of data about the structure and numerical results of the calculation. Through a new window, the user can select which information to display and the module creates the respective table containing the desired information. Furthermore, it is possible to select certain parts of the structure and display only the information regarding the selected portion. This feature was used to search for the element through the identification number and to visualize the results of the calculation in that element.

To perform the comparison between both models, the values of bending moments and amount of lower reinforcement were collected and compiled in the following tables.

Table 8: value of maximum moments [mm] - SET1

	Frame	Shell			
		Length = 1	Length = 2	Length = 4	Length = 8
W3H1	26.78	26.73	26.47	26.36	26.62
W3H3	61.51	61.30	60.70	60.46	61.09
W3H5	96.24	95.87	94.93	94.57	95.55
W3H10	183.06	182.30	180.51	179.83	181.71
W5H1	69.18	69.06	68.50	68.01	68.30
W5H3	158.23	157.87	156.58	155.46	156.15
W5H5	247.27	246.69	244.65	242.91	244.00
W5H10	469.88	468.72	464.83	461.54	463.62
W10H1	224.00	223.64	222.34	220.26	219.62
W10H3	516.43	515.56	512.56	507.75	506.29
W10H5	808.86	807.48	802.77	795.23	792.97
W10H10	1539.94	1537.29	1528.30	1513.96	1509.65

Table 9: Reinforcement - SET1

	Frame	Shell			
		Length = 1	Length = 2	Length = 4	Length = 8
W3H1	13.40	1.76	1.74	1.77	1.80
W3H3	13.40	1.78	4.07	4.06	4.13
W3H5	13.40	6.43	6.36	6.35	6.46
W3H10	13.40	12.49	12.34	12.29	12.46
W5H1	13.40	4.77	4.73	4.72	4.77
W5H3	13.40	11.09	11.00	10.89	10.99
W5H5	16.25	17.69	17.54	17.37	17.52
W5H10	39.77	36.53	36.11	35.71	36.03
W10H1	13.72	15.68	15.58	15.42	15.38
W10H3	47.16	41.29	40.95	40.41	40.25
W10H5	78.06	81.63	79.88	78.84	78.53
W10H10	165.92	167.62	166.56	164.91	164.42

Table 10: value of maximum moment [kNm/m] - SET2

	Frame	Shell			
		Length = 1	Length = 2	Length = 4	Length = 8
W3H1	123.14	30.26	29.97	29.85	30.15
W3H3	81.87	64.84	64.21	63.95	64.61
W3H5	110.13	99.41	98.44	98.05	99.08
W3H10	194.03	185.84	184.01	183.31	185.23
W5H1	265.43	77.50	76.87	76.32	76.64
W5H3	206.70	166.31	164.95	163.77	164.49
W5H5	280.35	255.13	253.02	251.22	252.34
W5H10	496.01	477.16	473.20	469.84	471.97
W10H1	675.76	250.68	249.22	246.88	246.17
W10H3	663.51	542.60	539.43	534.37	532.84
W10H5	914.66	834.52	829.65	821.86	819.52
W10H10	1623.58	1564.33	1555.18	1540.58	1536.20

Table 11: Lower Reinforcement - SET2

	Frame	Shell			
		Length = 1	Length = 2	Length = 4	Length = 8
W3H1	13.40	2.01	1.99	2.02	2.05
W3H3	13.40	4.33	4.32	4.31	4.38
W3H5	13.40	6.69	6.61	6.60	6.71
W3H10	13.40	12.76	12.61	12.56	12.73
W5H1	18.43	5.37	5.33	5.31	5.36
W5H3	13.40	11.72	11.62	11.51	11.61
W5H5	19.75	18.35	18.19	18.02	18.18
W5H10	42.68	37.46	37.03	36.61	36.94
W10H1	62.92	17.72	17.61	17.43	17.37
W10H3	61.09	44.37	43.99	43.40	43.23
W10H5	90.62	84.18	83.51	82.45	82.14
W10H10	176.11	170.67	169.59	167.92	167.42

Another important result to analyse was the nodal displacement at the reference location. To obtain this displacement, it was necessary to identify the node corresponding to the element already identified in each geometry and retrieve its respective displacement value. To achieve this, the identification number of the nodes needed to be obtained first. Once again the module WING was used to visualize the Finite Element structure and identify the element and respective node located at the defined position. The following table presents the identification numbers of the nodes by geometry.

Table 12: Number of analysed node

	Frame	Shell			
		Length = 1	Length = 2	Length = 4	Length = 8
Width = 3	4	1415	1600	1970	2710
Width = 5	4	1585	1870	2440	3580
Width = 10	4	2010	2545	3615	5755

Once these numbers were obtained, it was possible to use the RESULT module to display corresponding displacement value for the identified node.

Table 13: value of maximum displacement [mm] - SET1

	Frame	Shell			
		Length = 1	Length = 2	Length = 4	Length = 8
W3H1	1.055	1.05	1.05	1.05	1.05
W3H3	1.836	1.83	1.83	1.82	1.82
W3H5	2.616	2.61	2.60	2.59	2.59
W3H10	4.567	4.56	4.54	4.52	4.52
W5H1	2.047	2.05	2.03	2.01	2.00
W5H3	4.135	4.12	4.09	4.04	4.02
W5H5	6.223	6.21	6.16	6.08	6.05
W5H10	11.444	11.41	11.32	11.17	11.11
W10H1	11.789	11.79	11.67	11.51	11.33
W10H3	26.549	26.54	26.27	25.90	25.48
W10H5	41.309	41.19	40.88	40.30	39.64
W10H10	78.209	78.18	77.39	76.28	75.03

Table 14: value of maximum displacement [mm] - SET2

	Frame	Shell			
		Length = 1	Length = 2	Length = 4	Length = 8
W3H1	2.81	1.13	1.13	1.12	1.12
W3H3	2.27	1.91	1.90	1.89	1.89
W3H5	2.91	2.69	2.68	2.66	2.66
W3H10	4.80	4.56	4.61	4.59	4.59
W5H1	5.85	2.24	2.23	2.20	2.19
W5H3	5.27	4.32	4.29	4.24	4.21
W5H5	7.00	6.40	6.35	6.27	6.24
W5H10	12.06	11.61	11.51	11.36	11.30
W10H1	30.33	13.13	13.03	12.85	12.64
W10H3	33.70	27.85	27.63	27.24	26.80
W10H5	46.66	42.56	42.24	41.64	40.95
W10H10	82.45	79.36	78.74	77.62	76.34

4.7 Validation of results

To ensure an accurate solution when using FEM software like *SOFISTIK*, it is advised to validate the results manually, by hand calculation.

This section is presents the comparison between the value obtained by *SOFISTIK* and the values obtained with the use of the formulas presented in chapter 2. The moments used are the ones provided by the program.

Table 15: Number of analysed node

	Frame	**Shell**
Moment used [kN/m]	675.76	30.26
Reinforcement[cm^2/m]:	lower	lower
SOFISTIK	62.92	2.01
Hand Calculation	62.04	2.1147

The previous tables show that the difference between the results provided by *SOFISTIK* and the results obtained with the formulas provided is minimal. Therefore, it is safe to conclude that the software provides reliable results. The used formulas to validate these results are exposed in Appendix C.

4.8 Comparison of Results

In this section, a graphical comparison of the results and respective analyses are presented.

Image 33 demonstrates the relation between the height of the embankment and the required reinforcement for the Frame model and the different lengths of the Shell model, resultant from the second analysis, with all loads, for a width of 3 meters.

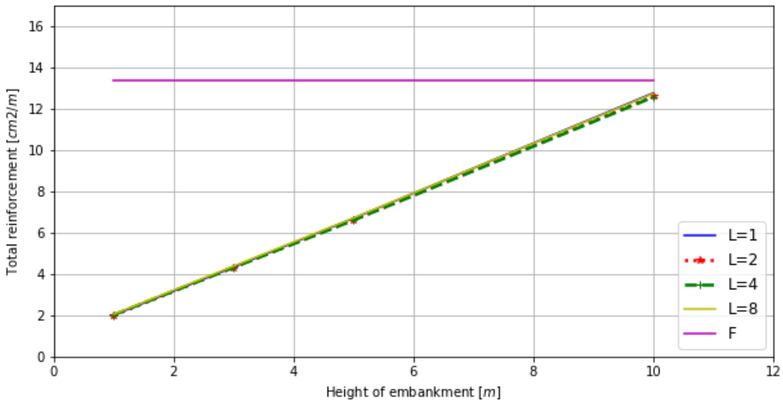

Figure 33: Different modules in SOFISTIK

As can be observed from the image above, the Frame model presents a constant value of reinforcement. This is due to the formulation of the Frame script, which is designed to output the minimum allowable reinforcement as specified by the EC. In contrast, the Shell script provides the actual value of reinforcement obtained from the calculation, which is lower than the minimum allowable value specified by EC.

Therefore, it can be stated that for short-width culverts, there is no advantage of one model over the other in terms of the amount of reinforcement required. This is because the amount of reinforcement if defined by the EC and is the same for both models regardless of which one is selected. Hence, the Frame model has an advantage due to its simpler formulation and verification, requiring less work and resources compared to the Shell model.

Next is presented the same relation, but for the models with a width of 5 and 10 meters, respectively (Figure 34).

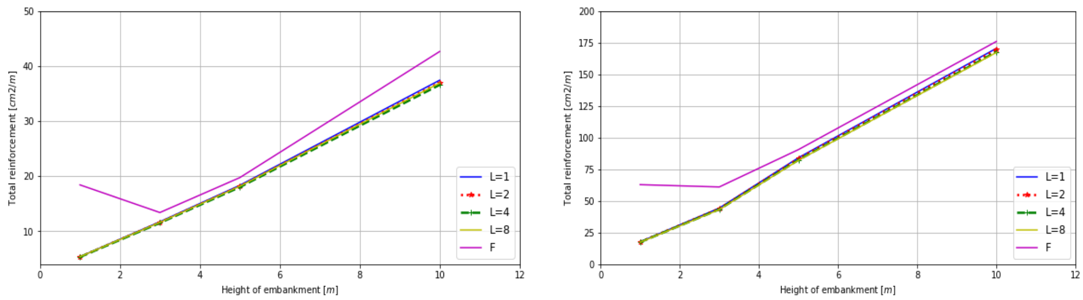

Figure 34: Relation between height of embankment and Reinforcement required for W=5 (left) and W=10 (right)

In the case of a 1-meter embankment, the Frame model requires a significantly higher amount of reinforcement than the Shell model to support the same conditions. This discrepancy can be attributed to the assumptions made by the planar model, which treats loads as uniform along the y-axis, disregarding any variation. In the specific case of this study, this is reflected in the response of both models to LM loading. In lower embankments, the distance between the surface of the culvert and the road is smaller, resulting in more concentrated effects of the LM loads. This leads to a greater difference in intensity between the areas loaded by one tyre and those loaded by two or four. Additionally, the tyre pressure varies along the y-axis, contributing to a larger discrepancy between the two models. Therefore, for lower embankments, the Shell model performs significantly better, allowing for a reduction of the reinforcement for the same loading conditions. As the height of the embankment increases, the discrepancy between both models decreases. This is because the spread ratio of the LM loads induces an increase of the span of the loading in the surface of the culvert, therefore reducing the differences in the response of both models to the loading.

Next, the effect of increasing the height of the embankment will be analysed.

The following graphic displays a comparative analysis of the displacement induced in the culvert. This comparison is made between different widths of both the Frame and Shell models, considering only SET1.

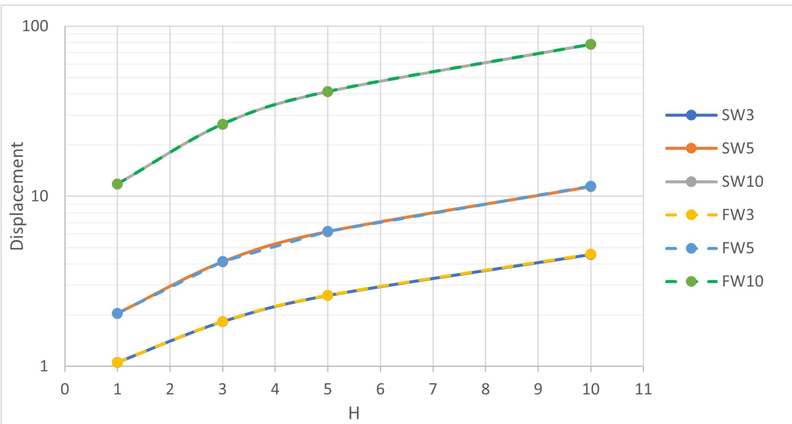

Figure 35: Displacement in the function of embankment height

The second graphic corresponds to the same set of structures but is subjected to the loading from SET2.

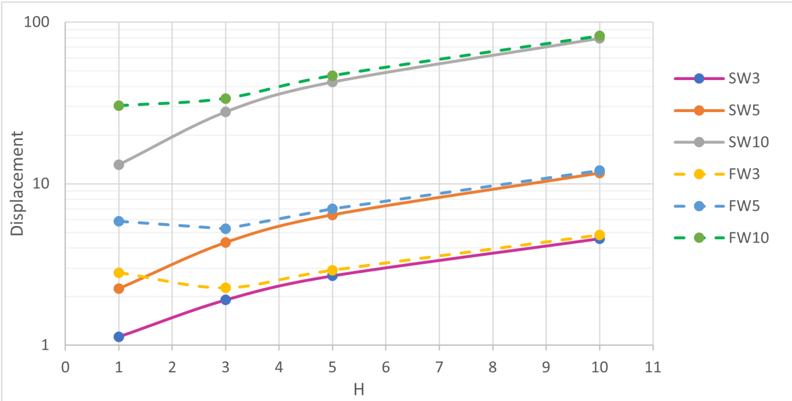

Figure 36: Displacement in the function of embankment height

From the previous graphics it is possible to conclude that, without the traffic loading, the response of the Frame and Shell model is very similar. On the other hand, for SET2, the displacement differs. For lower embankments, the difference between the two models behaviour is significant. As this height increases, it is possible to see an approximation of the values of the displacement.

This evolution strengthens the previously established conclusion that, for lower embankments, the assumption made by the Frame model will lead to worse performance of the structure. It is also noticed that the variation of width doesn't impact this behaviour, as the evolution remains the same, from width to width.

In conclusion, it is possible to affirm that each model has its own benefits for different scenarios. The Shell model represents a better choice for lower embankments. As the height value increases, the Frame model becomes the better choice because it reflects the same behaviour of the shell model and is significantly more simple to design and replicate.

5

Conclusions and Future Work

5.1 MAIN CONCLUSIONS

The primary goal of this project was to ascertain the conditions under which each type of culvert, frame or shell, should be employed. Both models possess unique advantages and disadvantages, making them ideal for specific scenarios. This study aimed to investigate these factors and provide a reference model of future decision-making for engineers and consultants associated with *Sweco* company. During the course of this project's development, an extensive investigation of the theme under consideration was conducted.

The project commences with a comprehensive study of the fundamental concepts associated with the construction structure under examination. Firstly, the concept of a culvert is defined, along with a detailed analysis of its inherent advantages and disadvantages. Subsequently, the finite element analysis technique, which is the numerical method utilized by the software employed for the structural calculations of these structures, is explained. In addition, the element units used for the analysis that took place during the project are described in detail. Finally, the two structural systems used to model the structure object of study, a Frame model and a Shell model, are introduced, accompanied by their respective and corresponding theories. Finally, the design process of the frame and shell structure is explicitly presented, providing a thorough understanding of the analysis and design of the culverts.

Following the literature review, the study case is thoroughly described. The scripts of both culvert models are introduced in the *SOFISTIK* software, which was utilized throughout the entire analysis process. The models were prepared by selecting factors such as the material and type of structure for the object under examination to assume. To perform the analysis, the mesh and load cases were defined, ensuring that the forces applied to both structures were equivalent for the analysis to be considered valid. These steps were taken to ensure that a rigorous and accurate analysis could be conducted, providing reliable results for the culvert design process.

Then, a parametric analysis was carried out. Initially, three variables that were expected to influence the structural behaviour of the designed culverts were selected: length, width, and height. The various combinations of these variables resulted in a total of 60 models to be analysed, with the Load Model loads being defined with precision. To ensure that the analysis was properly prepared, two possible scenarios were constructed, and subsequently, the analysis was conducted. Through a detailed comparison of the results, contrasting the various models, it was concluded that, when the culverts were subjected to uniform loads, the results were very similar between the shell and frame models. On the other hand, when the loads became more irregular, the behaviour started to differ.

The results of the parametric analysis only came to reinforce this conclusion. In the first analysis, when LM loads are not present, both models perform in a very similar way. In contrast, when LM loads are included, the variation along the y-axis induces very different behaviours in both models. It is important to mention that the previous statements are applicable to low embankment. In this case, there is a clear advantage in using a Shell model, because it will provide more accurate results, yielding lower bending moment and, consequently, lower displacements and less reinforcement.

The analysis conducted suggests that the assumptions made in the Frame model may not always be accurate. The model considers that the external loading acts along the center of gravity of the element (along the x-axis). If a variation occurs along that line, then the model assumes the loading correctly. Frame and Shell models behave similarly when subjected to area loads that vary only along the x-axis. However, if there is a variation in the loading along the y axis, the Frame will assume the higher value as the loading applied to the whole y dimension. The Shell model, on the other hand, can accurately account for variations in loading in both directions.

The parametric analysis carried out in this study supports this conclusion. Without LM loads, both models perform similarly, but with the inclusion of LM loads, the Shell model outperforms the Frame model. This is particularly observed for low embankments, where the difference in behaviour between the two models is more pronounced.

As a result of this analysis, it is recommended to use the Shell model for designing culverts in situations where low embankments are used and the loading may not be uniform along the x and y axes. Therefore, more accurate outcomes are produced, along with lower bending moment, and consequently, lower displacements and less reinforcement.

As the height of the embankment increases, the difference in behaviour between the Frame and Shell models becomes less clear. This is due to the fact that the effect of LM loads becomes less concentrated and more evenly distributed. Consequently, the assumption of different loading patterns, which is used to attribute an advantage to the Shell model, becomes less significant.

Concluding, while the results from the analysis alone do not provide a clear preference for either model, for a scenario where the embankment height is higher, the simplicity of the Frame model formulation makes it a more favorable option.

These findings have significant practical implications, as they provide valuable insights into the most appropriate culvert model to be selected based on the nature of the loads they are expected to withstand. The results of the parametric analysis serve as a reference for future culvert design processes, enabling engineers to make informed decisions concerning the most appropriate culvert model for a given project.

5.2 Future work perspectives

The future perspectives for this project aim to expand, complement, and enhance the conducted analysis.

Having examined the present findings, a potential future initiative could further investigate the behaviour of the frame and shell models, specifically the behaviour of elements from both models located on the edge of the structure, analysing the shear force and the respective reinforcement.

On the other hand, adding new loads to the built models may provide a more complete picture of their behaviour. The inclusion of additional loads would aid in the creation of a more realistic scenario that more closely resembles actual situations. The study would be able to better represent real-world situations and hence offer a more realistic assessment of the model's strength. A more precise model analysis would result in more reliable design suggestions, which would assist to assure the safety of the structure and people who use it.

Additionally, incorporating the structure's dynamic performance would enhance and deepen the analysis, making it more relevant and precise for the many simulated scenarios. The study would be able to offer a more accurate assessment of the structure's behaviour in real-life situations, which are essentially dynamic in nature, if the dynamic performance of the structure was taken into consideration. This would allow for the detection of possible concerns such as resonant vibrations, excessive deformations, or strains, as well as the determination of acceptable solutions. Moreover, dynamic analysis can give insights into the structure's reaction to external loads and other dynamic events, like as earthquakes, which can have a substantial impact on its behaviour.

Therefore, by considering the dynamic performance of the structure, the analysis would be more comprehensive, accurate, and suitable for a wide range of scenarios, providing valuable information for optimizing the design and ensuring the safety and reliability of the structure.

Bibliography

ACI . ????

AG SOFiSTiK. Sofistik FEA 2023 - Calculation Status. 2023.

AISC . Load and Resistance Factor Design (LRFD) Specification for Structural Steel Buildings. 2016.

Arroyo Orlando, Liel Abbie B, Gutiérrez Sergio, Liel Abbie. A Design Method for Reinforced Concrete Frame Buildings based on Pondered Virtual Work. 2018.

Awwad E, Mabsout M, Sadek S, Tarhini K. Finite Element Analysis of Concrete Box Culverts. 2000.

Balkham Matt., Fosbeary Chris, Kitchen Amanda, Rickard , Charlie . Culvert design and operation guide. 2010. 342.

Bathe Klaus-Jürgen. Finite Element Method. 2008.

Bauchau O. A., Craig J. I. Structural Analysis. 2009.

Carrera Erasmo, Giunta Gaetano. Refined Beam Theories based on a Unified Formulation // International Journal of Applied Mechanics. 3 2010. 2. 117–143.

Cook Robert D., Malkus David S., Plesha Michaek E., Witt Robert J. Concepts and applications of finite element analysis. 2001.

Cook Robert D., Young Warren C. Advanced Mechanics of Materials. 1998. second.

Craveiro Marina Vendl, Bittencourt Túlio Nogueira, Bella João Carlos Della. Design and verification of reinforced concrete shell elements // Revista IBRACON de Estruturas e Materiais. 2021. 14.

Eisenbau-Verbandes Deutsche, (Germany) Hafenbautechnische Gesellschaft, Beton-Vereins Deutsche, Bautechnik VDI-Gesellschaft, Bauingenieurwesen Deutsche Gesellschaft für. Der Bauingenieur. 1972.

Eurocode . European Committee for Standardization. (2010). Eurocode 0: Basis of structural design (EN 1990:2010). 2010.

Faroudja Meziani, Amar Kahil, Aghiles Nekmouche, Said Boukais. Modelling of reinforced concrete RC frame using a simplified approach. 2017.

Fintel Michael. Concrete Structures. 2011.

Gupta Ajaya K. Membrane Reinforcement in Concrete Shells: a review. 1984. 63–75.

Kattimani Komal S, Shreedhar R. Parametric studies of box culverts. 2013. 58–65.

Liu Z., Teng J.G. Mechanics of materials. 2002.

Moore I. D. Buried pipes and culverts. 2001.

Murty A. V.Krishna. Toward a consistent beam theory // AIAA Journal. 1984. 22. 811–816.

Nawy Edward G. Reinforced Concrete: a fundamental approach. 2009.

Parke Gerard, Hewson Nigel. The Manual of Bridge Engineering. 2022.

Patel Roshan, Jamle Sagar. Analysis and Design of Box Culvert: A Manual Approach // International Journal of Advanced Engineering Research and Science. 2019. 6. 286–291.

Patel Roshan, Jamle Sagar, Scholar M Tech. Analysis and Design of Box Culvert: A Review // International Journal for Research in Engineering Application Management (IJREAM). 2019. 05. 1.

Reynolds Charles E, Steedman James C. Reinforced Concrete Designer's Handbook. 1987.

Reynolds Charles E., Steedman James C. Reinforced concrete designers handbook. 1999.

Roylance David. Finite Element Analysis. 2001.

Segerlind Larry J. Applied Finite Element Analysis. 1984.

In-Situ Load Testing of Corrugated Steel Pipe-Arch Culverts. // . 2008.

Skibeli Marte. Concrete Plates Designed with FEM. 2017.

Sofistik Manual. Design of Plates and Shells | SOFISTIK. 2020.

Szabó Barna, Babuska Ivo. Finite Element Analysis: Method, Verification and Validation. 2021.

Timoshenko , Woinowsky-Krieger . Theory of plates and shells. 1989.

Wang C.M., Reddy J.N., Lee K.H. [6]Theories of Plate Bending // Shear Deformable Beams and Plates. 1 2000. 89–109.

A

Displacements for individual LCs

Self-weight Load

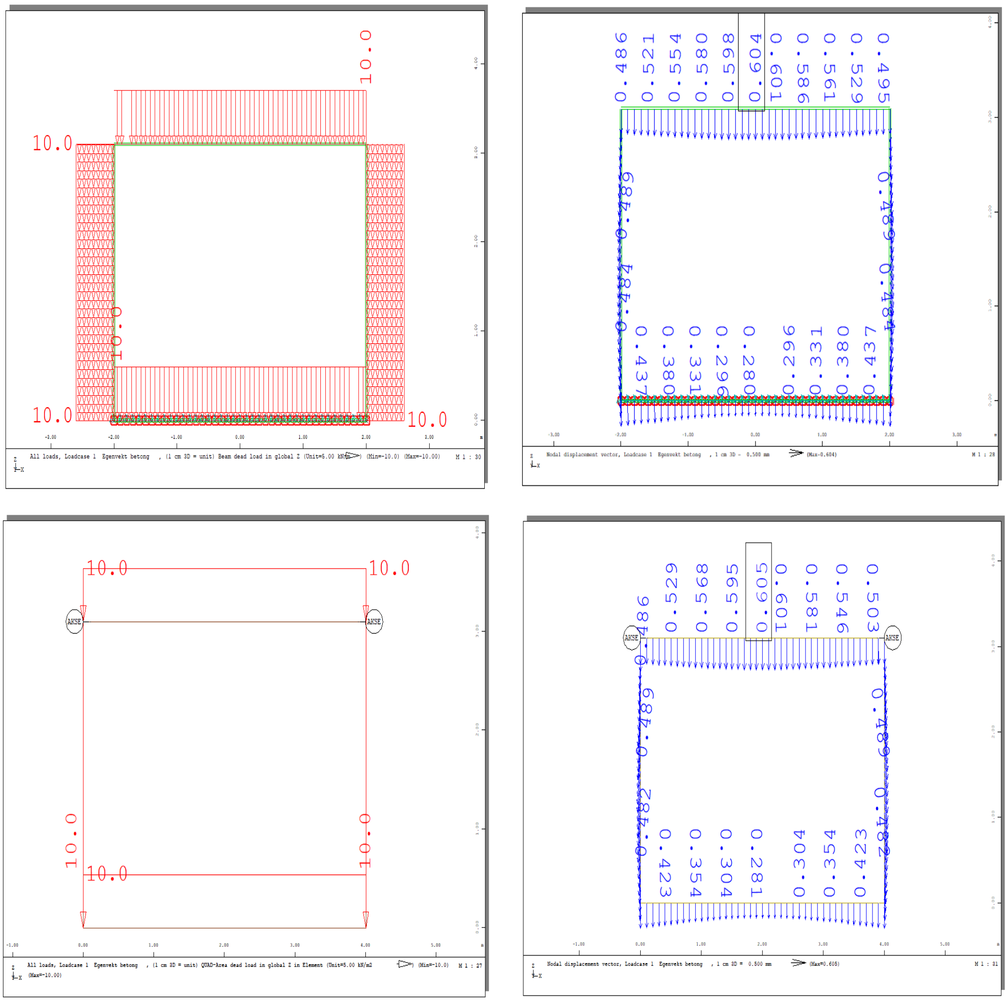

Figure 37: Self-wheight load (left) and corresponding displacements (right) - Frame on top, and Shell on the bottom

Asphalt load

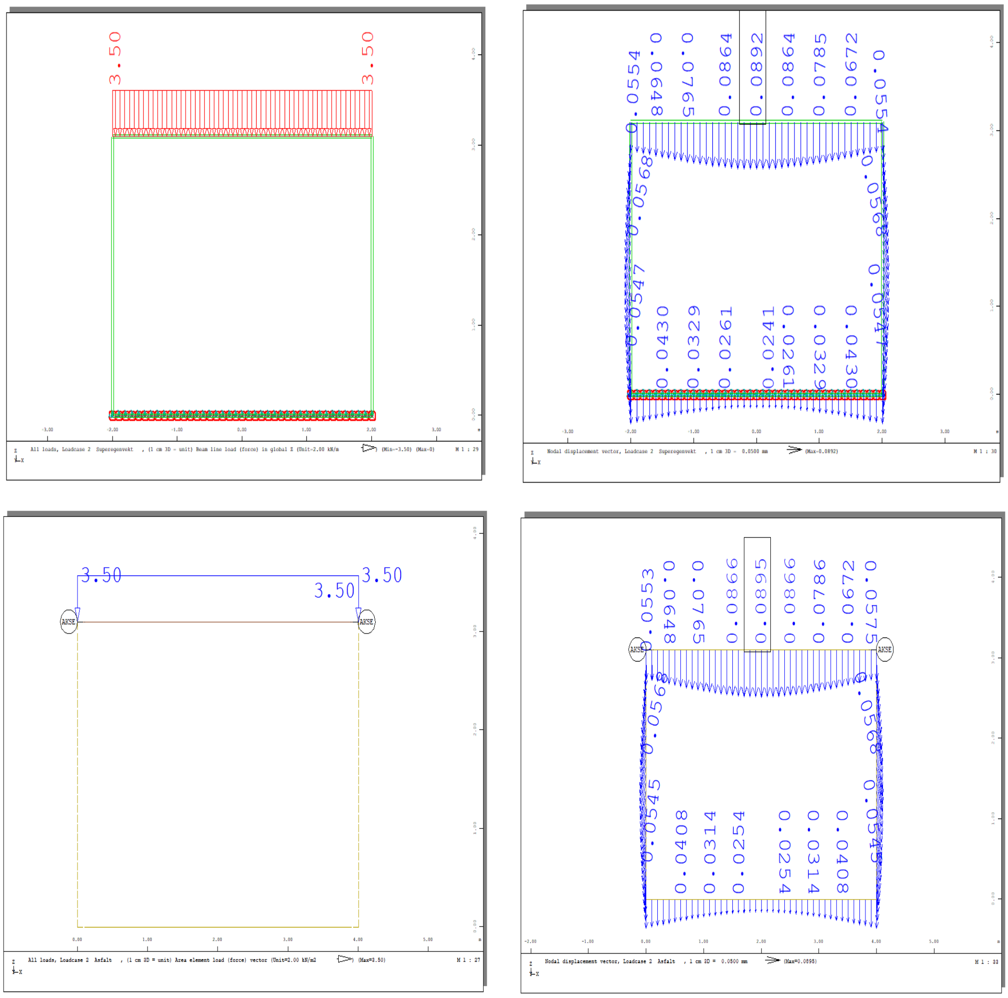

Figure 38: Asphalt load (left) and corresponding displacements (right) - Frame on top, and Shell on the bottom

Embankment load

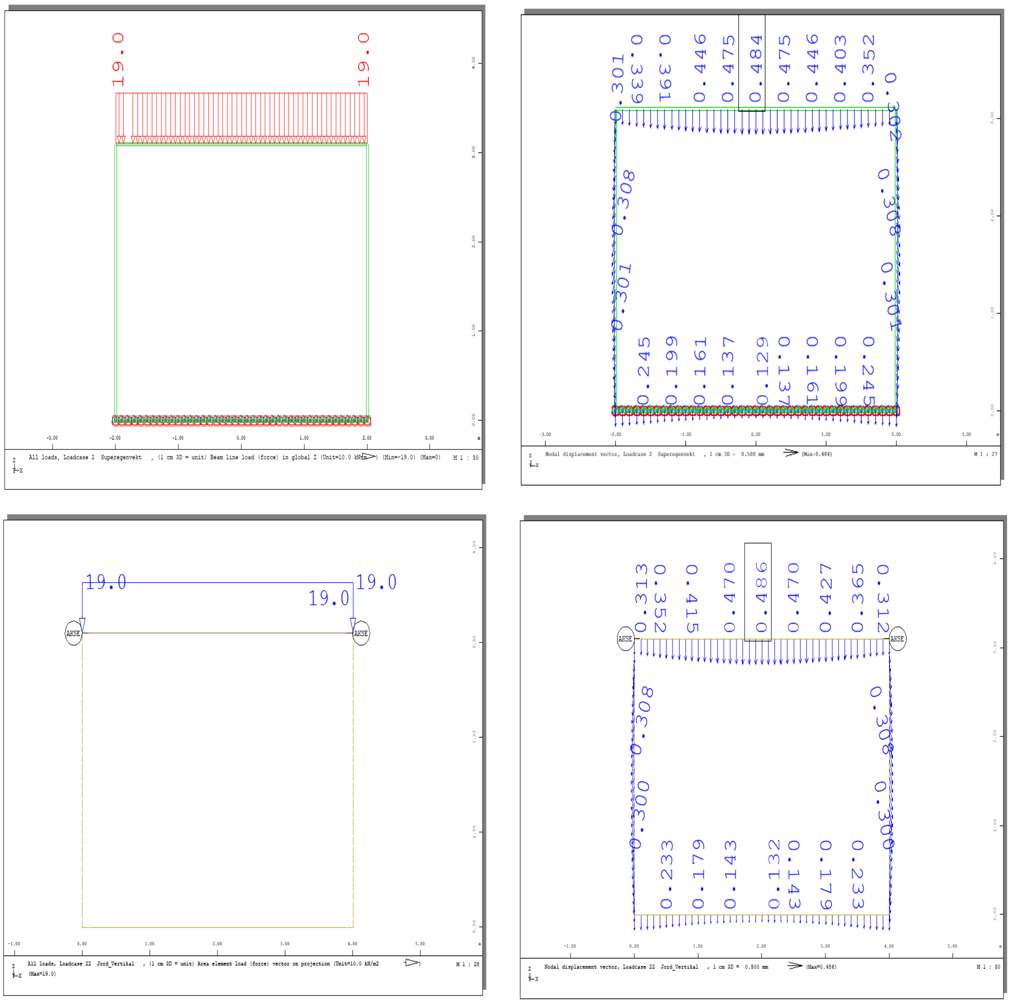

Figure 39: Embankment load (left) and corresponding displacements (right) - Frame on top, and Shell on the bottom

Active and Passive loads

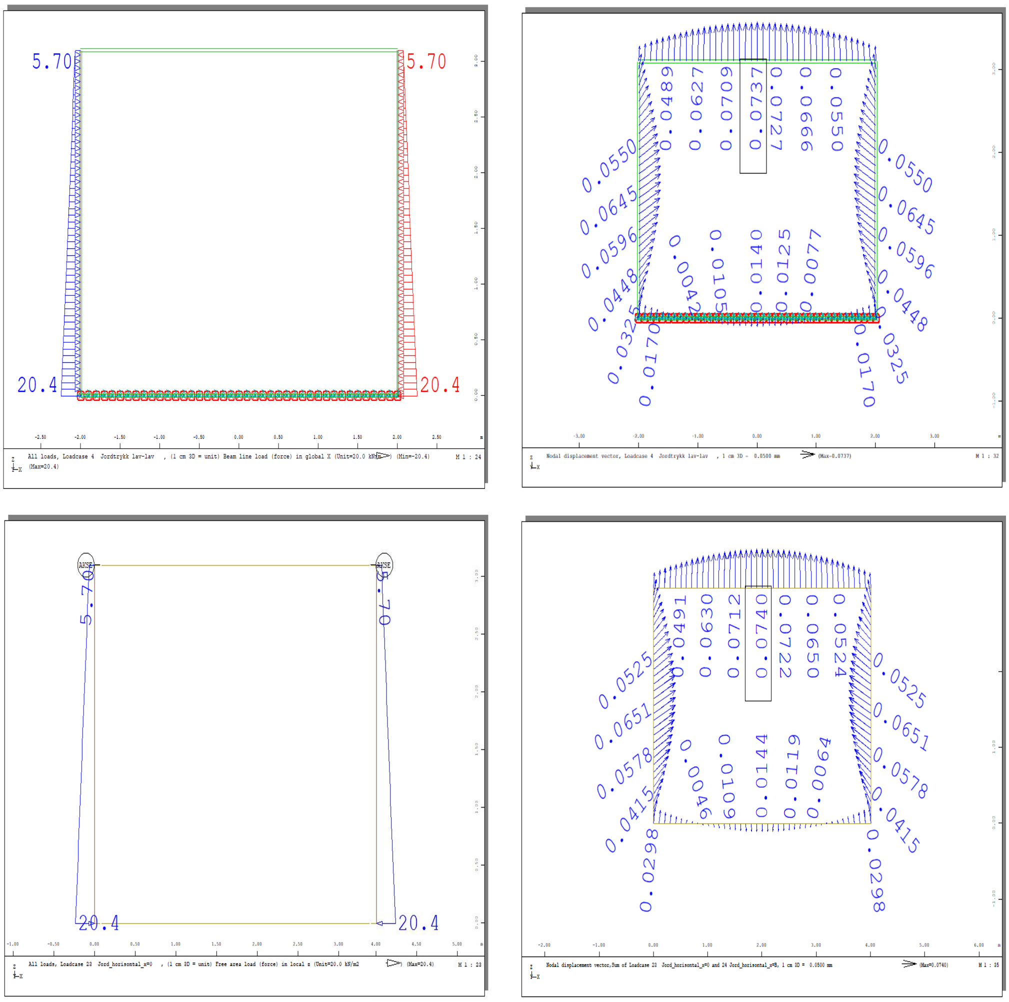

Figure 40: Active load (left) and corresponding displacements (right) - Frame on top, and Shell on the bottom

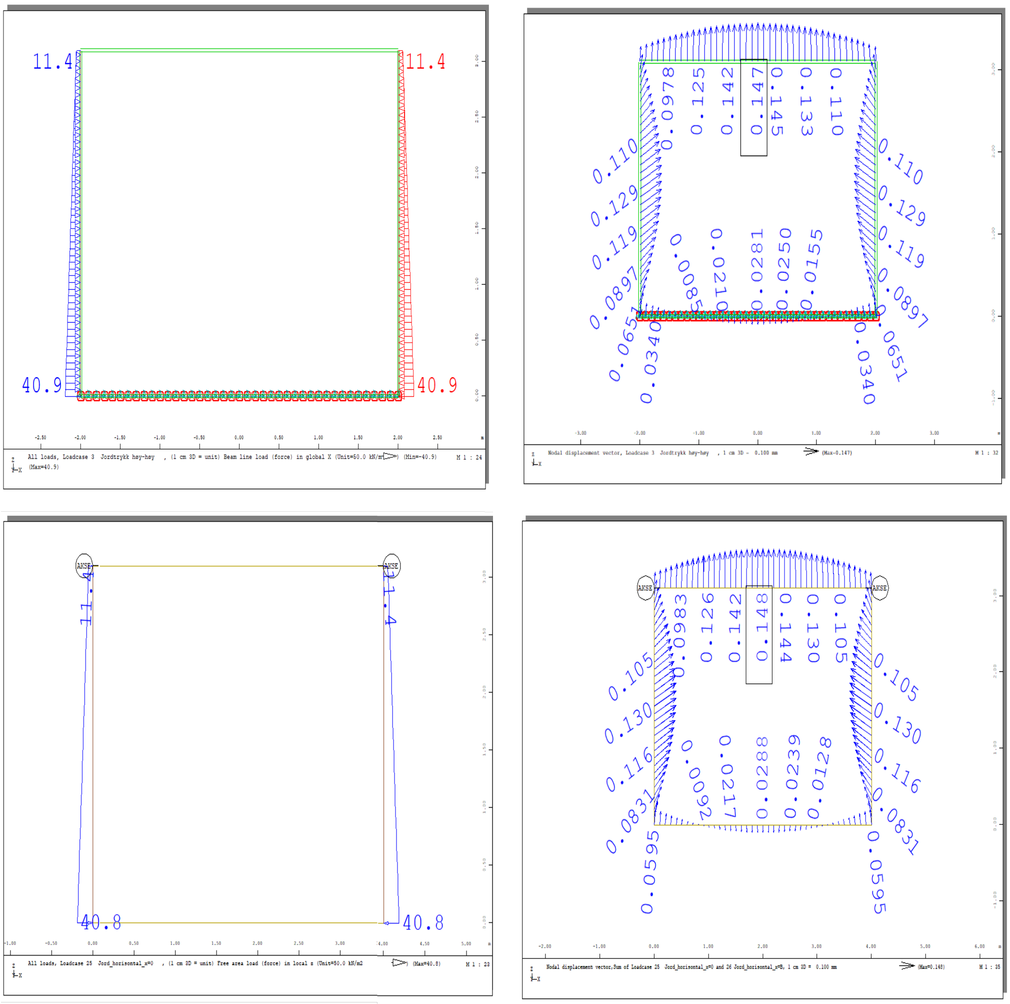

Figure 41: Passive load (left) and corresponding displacements (right) - Frame on top, and Shell on the bottom

Load Model 1 (LM1)

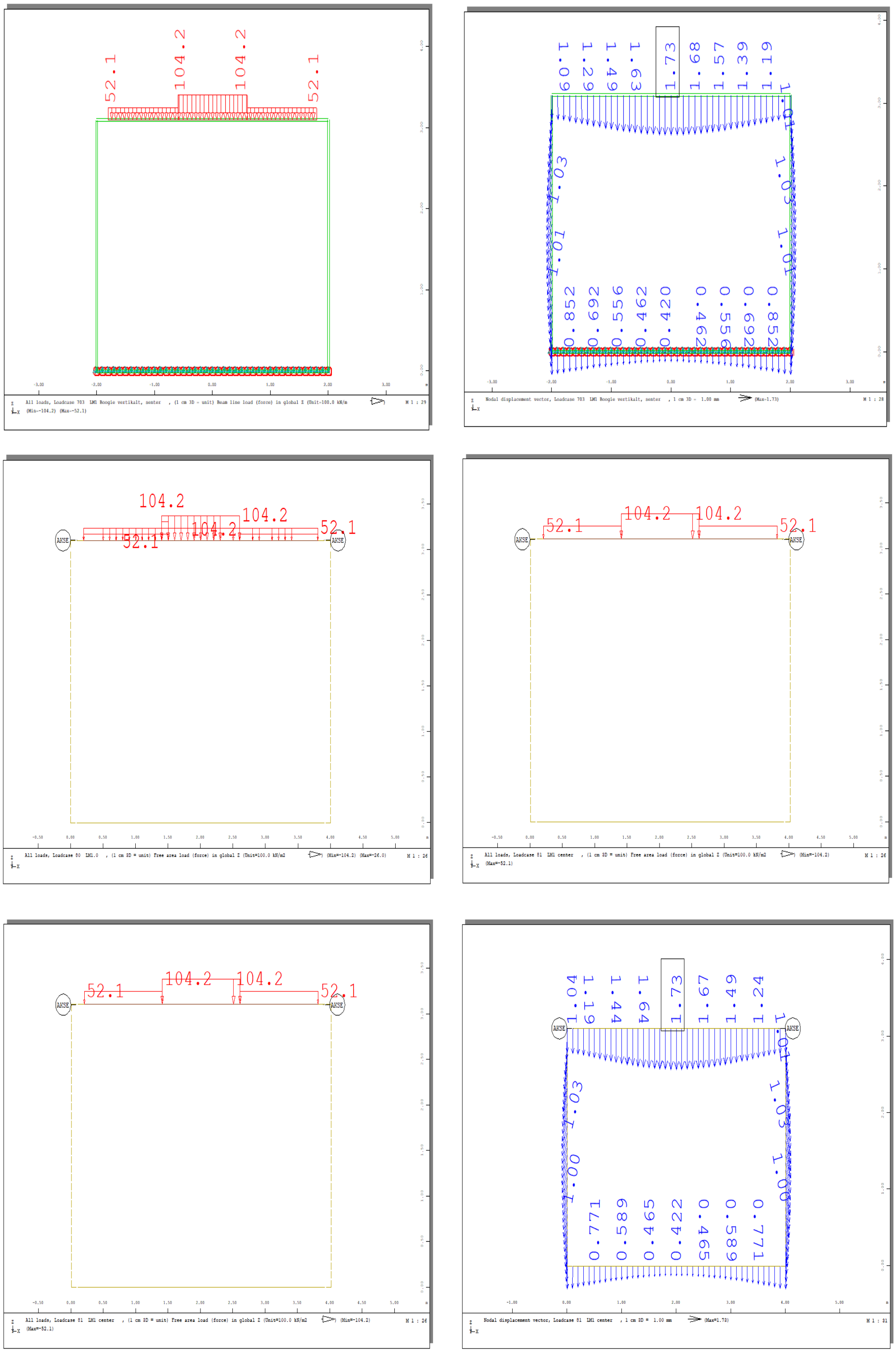

Figure 42: Load Model 1 (left) and corresponding displacements (right) - Frame on top first row; Shell real load on middle row; and Shell equivalent load on the bottom row

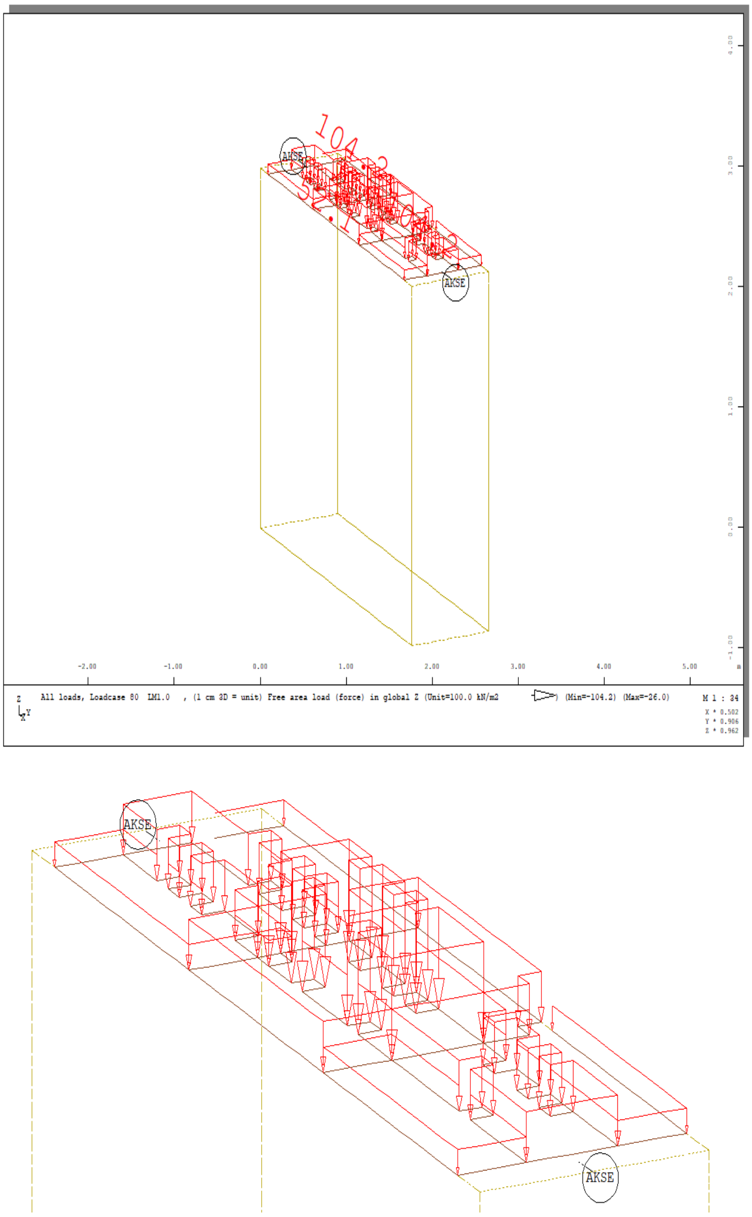

Figure 43: Real Load Model 1 in perspective

Load Model 1 Uniform Distributed Load (UDL)

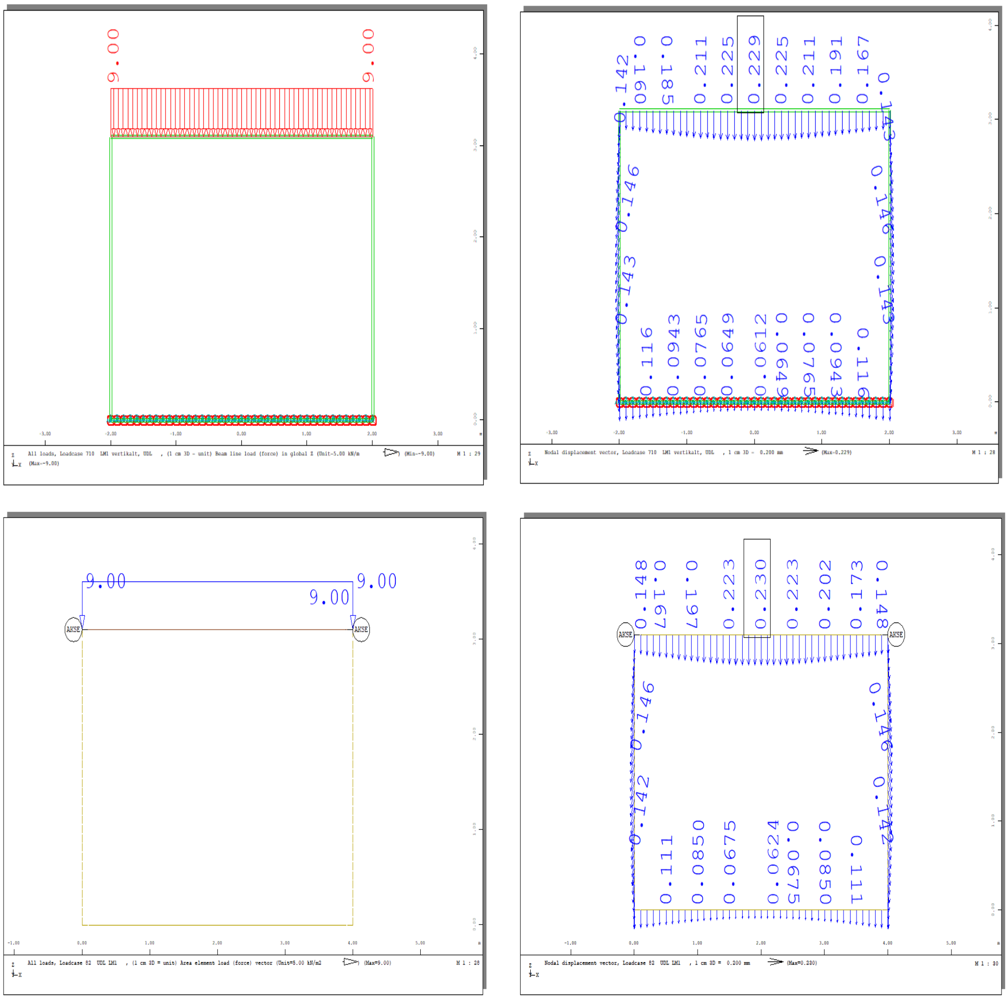

Figure 44: Uniform Distribuited load (left) and corresponding displacements (right) - Frame on top, and Shell on the bottom

Load Model 2 (LM2)

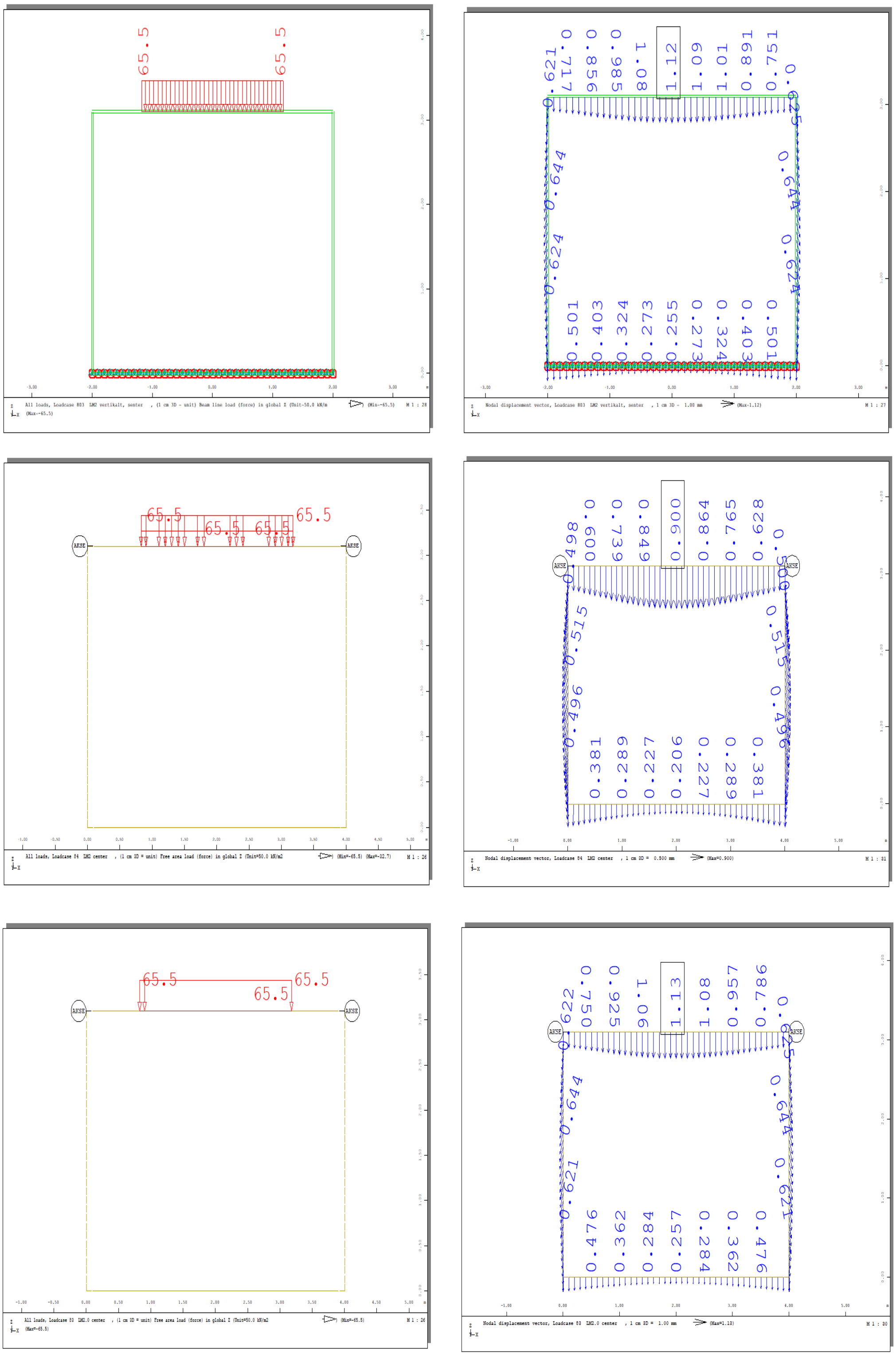

Figure 45: Load Model 2 (left) and corresponding displacements (right) - Frame on top first row; Shell real load on middle row; and Shell equivalent load on the bottom row

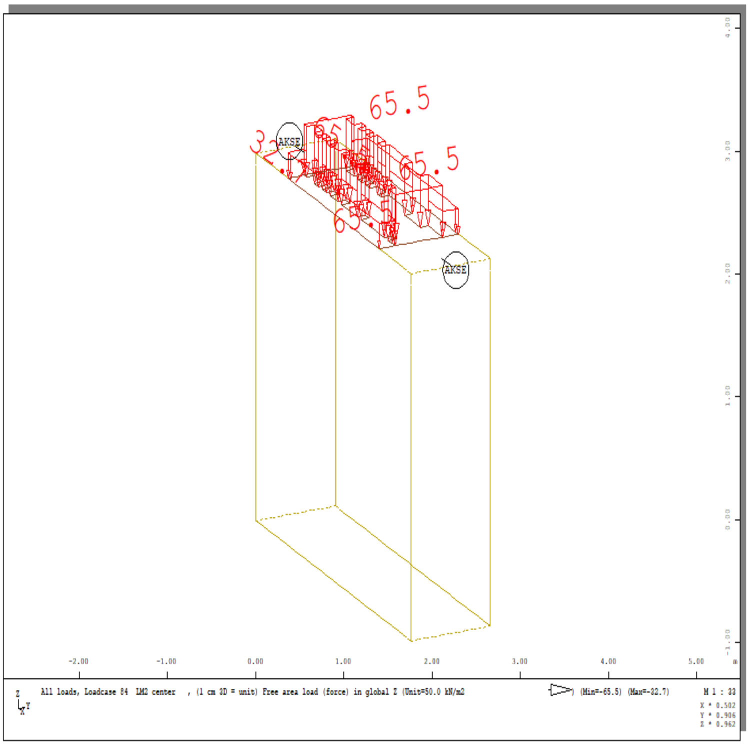

Figure 46: Real Load Model 2 in perspective

B

LM loads - coordinates calculation

	INPUT
Lc	1
Wc	3
He	1
Hc	3.1

Center C	
x	y
1.5	0.5

LM1	
Q	150
a	0.4
b	0.4

		overlap
Lx	2.4	1.2
Ly	2.4	0.4
Q/m2	26.0417	

LM2	
Q	200
a	0.35
b	0.6

		overlap
Lx	2.35	
Ly	2.6	0.6
Q/m2	32.7332	

Figure 47: Input Data

	LM1	P1		P2		P3		P4	
Center	1st L	x	y	x	y	x	y	x	y
	F1	-0.30	-1.70	-0.30	0.70	2.10	0.70	2.10	-1.70
	F2	-0.30	0.30	-0.30	2.70	2.10	2.70	2.10	0.30
	F3	0.90	0.30	0.90	2.70	3.30	2.70	3.30	0.30
	F4	0.90	-1.70	0.90	0.70	3.30	0.70	3.30	-1.70

Figure 48: Coordinates of LM1 central load

Left	LM1	P1		P2		P3		P4	
	1st L	x	y	x	y	x	y	x	y
	F1	0.00	-1.70	0.00	0.70	2.40	0.70	2.40	-1.70
	F2	0.00	0.30	0.00	2.70	2.40	2.70	2.40	0.30
	F3	1.20	0.30	1.20	2.70	3.60	2.70	3.60	0.30
	F4	1.20	-1.70	1.20	0.70	3.60	0.70	3.60	-1.70

Figure 49: Coordinates of LM1 left load

Right	LM1	P1		P2		P3		P4	
	1st L	x	y	x	y	x	y	x	y
	F1	-0.60	-1.70	-0.60	0.70	1.80	0.70	1.80	-1.70
	F2	-0.60	0.30	-0.60	2.70	1.80	2.70	1.80	0.30
	F3	0.60	0.30	0.60	2.70	3.00	2.70	3.00	0.30
	F4	0.60	-1.70	0.60	0.70	3.00	0.70	3.00	-1.70

Figure 50: Coordinates of LM1 right load

Center	LM2	P1		P2		P3		P4	
		x	y	x	y	x	y	x	y
	F1	0.33	-1.80	0.33	0.80	2.68	0.80	2.68	-1.80
	F2	0.33	0.20	0.33	2.80	2.68	2.80	2.68	0.20

Figure 51: Coordinates of LM2 central load

Left	LM2	P1		P2		P3		P4	
		x	y	x	y	x	y	x	y
	F1	0.00	-1.80	0.00	0.80	2.35	0.80	2.35	-1.80
	F2	0.00	0.20	0.00	2.80	2.35	2.80	2.35	0.20

Figure 52: Coordinates of LM2 left load

Right	LM2	P1		P2		P3		P4	
		x	y	x	y	x	y	x	y
	F1	0.65	-1.80	0.65	0.80	3.00	0.80	3.00	-1.80
	F2	0.65	0.20	0.65	2.80	3.00	2.80	3.00	0.20

Figure 53: Coordinates of LM2 right load

C

Validation of Results

C.1 DESIGN PROCESS OF A FRAME MODEL

Beam Design

Design of a rectangular, doubly reinforced Cross-section for Bending design of a doubly reinforced section for ULS, subjected to pure flexure, like a beam. The partial factors considered for the ultimate limit state are $\gamma_c = 1,5$ for concrete and $\gamma_s = 1,15$ for the reinforcement steel, values taken from Eurocode, table 2.1N.

1) Determination of the Design value of concrete compressive strength:

$$f_{cd} = a_{cc} \cdot \frac{f_{ck}}{\gamma_c} = 0,85 \cdot \frac{45}{1.5} = 25.5 \quad MPa \tag{C.1}$$

where $f_{ck} = 45MPa$ is taken from the table 3.1 of EC and $a_{cc} = 0.85$ according to the National Annex.

2) Determination of the Design strength of reinforcement:

$$f_{yd} = \frac{f_{yk}}{\gamma_s} = \frac{500}{1.15} = 435 \quad MPa \tag{C.2}$$

where f_{yk} = 500 MPa

3) Calculation of the necessary reinforcement:

The moment applied is M_{Ed} = 678.76 $kN \cdot m$, the cross section considered has b = 1m and h = 0.4m for dimensions, being d = 0.9*d = 0.36m.

$$\mu = \frac{M_{Ed}}{b \cdot d^2 \cdot f_{cd}} = \frac{678.76}{1 \cdot 0.36^2 \cdot 25.5} = 0.259 \tag{C.3}$$

With μ and A/A'=0.23 it is necessary to interpolate from the tables and obtain a value for ω =0.294. The values of the upper and lower reinforcement are obtained:

$$A_{s1} = \frac{1}{f_{yd}} \cdot (\omega_1 \cdot b \cdot d \cdot f_{cd}) = \frac{1}{435} \cdot (0.294 \cdot 1 \cdot 0.36 \cdot 25.5) = 62.04 \quad \left[\frac{cm^2}{m}\right] \tag{C.4}$$

A/A' = 0.2 :

C.2 Design process of a Shell model

For the Shell model the following moments and axial stresses were considered:

$$\begin{aligned} m_{xx} = 30,26 \quad m_{yy} = 0,85 \quad m_{xy} = -0,01 \\ n_{xx} = -11,77 \quad n_{yy} = -0,02 \quad n_{xy} = 0 \end{aligned} \tag{C.5}$$

, where the moments are expressed in $\left[\frac{kn \cdot m}{m}\right]$ and the axial stresses in $\left[\frac{kn}{m}\right]$.

1) From the internal forces the principal bending moments were assessed:

$$\begin{aligned} m_I &= \frac{m_{xx} + m_{yy}}{2} + \frac{\sqrt{(m_{yy} - m_{xx})^2 + 4 \cdot m_{xy}^2}}{2} = \\ &= \frac{30,26 + 0,85}{2} + \frac{\sqrt{(0,85 - 30,26)^2 + 4 \cdot (-0,01)^2}}{2} = \\ &= 30,26 \left[\frac{kn \cdot m}{m}\right] \end{aligned} \tag{C.6}$$

$$\begin{aligned} m_{II} &= \frac{m_{xx} + m_{yy}}{2} - \frac{\sqrt{(m_{yy} - m_{xx})^2 + 4 \cdot m_{xy}^2}}{2} = \\ &= \frac{30,26 + 0,85}{2} - \frac{\sqrt{(0,85 - 30,26)^2 + 4 \cdot (-0,01)^2}}{2} = \\ &= 0.85 \left[\frac{kn \cdot m}{m}\right] \end{aligned} \tag{C.7}$$

And the angle between the principal bending moments is:

$$\phi_m = \frac{atan(\frac{2 \cdot m_{xy}}{m_{xx} + m_{yy}})}{2} = \frac{atan(\frac{2 \cdot (-0.01)}{30.26 + 0.85})}{2} = -0.0195 \quad [deg] \tag{C.8}$$

2) Similarly the principal normal forces can be assessed:

$$\begin{aligned} n_I &= \frac{n_{xx} + n_{yy}}{2} + \frac{\sqrt{(n_{yy} - n_{xx})^2 + 4 \cdot n_{xy}^2}}{2} = \\ &= \frac{-11.77 + (-0.02)}{2} + \frac{\sqrt{-0.02 - (-11.77))^2 + 4 \cdot 0^2}}{2} = \\ &= -0.02 \left[\frac{kn}{m}\right] \end{aligned} \tag{C.9}$$

$$
\begin{aligned}
n_{II} &= \frac{n_{xx}+n_{yy}}{2} - \frac{\sqrt{(n_{yy}-n_{xx})^2+4\cdot n_{xy}^2}}{2} \\
&= \frac{-11.77+(-0.02)}{2} - \frac{\sqrt{(-0.02-(-11.77))^2+4\cdot 0^2}}{2} \\
&= -11.77 \left[\frac{kn}{m}\right]
\end{aligned} \tag{C.10}
$$

And the angle between the principal normal forces:

$$
\phi_n = \frac{atan(\frac{2\cdot n_{xy}}{n_{xx}+n_{yy}})}{2} = \frac{atan(\frac{2\cdot 0}{-11.77+(-0.02)})}{2} = 0 \quad [deg] \tag{C.11}
$$

3) This lever arm z = 0.306 is then used to calculate the virtual panel forces in direction of the element's local coordinate system on each side of the finite area element:

$$
N_{xx} = \frac{n_{xx}}{2} + \frac{m_{xx}}{z_1} = \frac{-11.77}{2} + \frac{30.26}{0.306} = 93.0039 \quad \left[\frac{kN}{m}\right] \tag{C.12}
$$

$$
N_{yy} = \frac{n_{yy}}{2} + \frac{m_{yy}}{z_1} = \frac{-0.02}{2} + \frac{0.85}{0.306} = 2.7678 \quad \left[\frac{kN}{m}\right] \tag{C.13}
$$

$$
N_{xy} = \frac{n_{xy}}{2} + \frac{m_{xy}}{z_1} = \frac{0}{2} + \frac{-0.01}{0.306} = -0.0327 \quad \left[\frac{kN}{m}\right] \tag{C.14}
$$

4) Transformation of the local panel forces into principal panel forces :

$$
\begin{aligned}
N_I &= \frac{N_{xx}+N_{yy}}{2} + \frac{\sqrt{(N_{yy}-N_{xx})^2+4\cdot N_{xy}^2}}{2} = \\
&= \frac{93.0039+2.7678}{2} + \frac{\sqrt{(2.7678-93.0039)^2+4\cdot(-0.0327)^2}}{2} = \\
&= 93.0039 \quad \left[\frac{kN}{m}\right]
\end{aligned} \tag{C.15}
$$

$$
\begin{aligned}
N_{II} &= \frac{N_{xx}+N_{yy}}{2} - \frac{\sqrt{(N_{yy}-N_{xx})^2+4\cdot N_{xy}^2}}{2} = \\
&= \frac{93.0039+2.7678}{2} - \frac{\sqrt{(2.7678-93.0039)^2+4\cdot(-0.0327)^2}}{2} = \\
&= 2.7678 \quad \left[\frac{kN}{m}\right]
\end{aligned} \tag{C.16}
$$

The angle between the principal panel forces:

$$
\phi_N = \frac{atan(\frac{2\cdot N_{xy}}{N_{xx}+N_{yy}})}{2} = \frac{atan(\frac{2\cdot(-0.0327)}{93.0039+2.7678})}{2} = -0.0208 \quad [deg] \tag{C.17}
$$

And the angle of the main reinforcement with the local x-axis of the quad is :

$$\varepsilon = 10 \quad [deg] \tag{C.18}$$

$$\alpha = |\phi_N - \varepsilon| = |-0.0208 - 10| = 10.0207 \quad [deg] \tag{C.19}$$

5) Calculation of the principal panel membrane forces:

$$q_N = \frac{N_{II}}{N_I} = \frac{2.7678}{93.0039} = 0.0298 \quad [] \tag{C.20}$$

Quotient verification:

$$(-tan(\alpha + \frac{\pi}{4})) \cdot tan(\alpha) = (-tan(10,0208 + \frac{\pi}{4})) \cdot tan(10,0208) = -0,2525 \tag{C.21}$$

- Since the quotient q_N is greater, the tension force in the principal reinforcement direction is calculated by:

$$\begin{aligned} Z_I &= N_I + \frac{N_I - N_{II}}{2} \cdot sin(2 \cdot \pi) \cdot (1 - tan(\alpha)) = 111 \frac{kN}{m} = \\ &= 93.0039 + \frac{93.0039 - 2.7678}{2} \cdot sin(2 \cdot \pi) \cdot (1 - tan(10.0208)) = \\ &= 105.734 \quad \left[\frac{kN}{m}\right] \end{aligned} \tag{C.22}$$

and in the cross reinforcement :

$$\begin{aligned} Z_{II} &= N_{II} + \frac{N_I - N_{II}}{2} \cdot sin(2 \cdot \pi) \cdot (1 - tan(\alpha)) = 111 \frac{kN}{m} \\ &= 2.7678 + \frac{93.0039 - 2.7678}{2} \cdot sin(2 \cdot \pi) \cdot (1 - tan(10.0208)) = \\ &= 20.9619 \quad \left[\frac{kN}{m}\right] \end{aligned} \tag{C.23}$$

7) The compression force in the concrete is equal:

$$\begin{aligned} D_C &= (N_I - N_{II}) \cdot sin(2 \cdot \pi) = \\ &= (93.0039 - 2.7678) \cdot sin(2 \cdot \pi) = 30.924 \quad \left[\frac{kN}{m}\right] \end{aligned} \tag{C.24}$$

also the equlibrium must be kept:

$$Z_I + Z_{II} - N_I - N_{II} = 105.734 + 20.9619 - 93.0039 - 2.7678 = 30.924 \quad \left[\frac{kN}{m}\right] O.K \tag{C.25}$$

6) Calculation of the necessary amount of reinforcement:

$$\sigma_{sd} = \sigma_{sf} \cdot \gamma_s = 575 \cdot 1.15 = 550[MPa]$$

- In the principal reinforcement direction:

$$a_{sI} = \frac{Z_I}{\sigma_{sd}}[\frac{cm^2}{m}] = \frac{105.734}{500 * 10} = 2.1147 \quad \left[\frac{cm^2}{m}\right] \tag{C.26}$$

- In the cross reinforcement direction:

$$a_{sII} = \frac{Z_I I}{\sigma_{sd}}[\frac{cm^2}{m}] = \frac{20.9619}{500 * 10} = 0.4192 \quad \left[\frac{cm^2}{m}\right] \tag{C.27}$$